

Accelerated Online Risk-Averse Policy Evaluation in POMDPs with Theoretical Guarantees and Novel CVaR Bounds

YAACOV PARIENTE, Technion - Israel Institute of Technology, Israel

VADIM INDELMAN, Technion - Israel Institute of Technology, Israel

Risk-averse decision-making under uncertainty in partially observable domains represents a central challenge in artificial intelligence and is essential for developing reliable autonomous agents. The formal framework for such problems is typically the partially observable Markov decision process (POMDP), where risk sensitivity is introduced through a risk measure applied to the value function. Among these, the Conditional Value-at-Risk (CVaR) has emerged as a particularly significant criterion. However, solving POMDPs is computationally intractable in general, and approximate solution methods rely on computationally expensive simulations of possible future agent trajectories.

This work introduces a theoretical framework for accelerating the evaluation of CVaR value functions in POMDPs while providing formal performance guarantees. As the mathematical foundation, we derive new bounds on the CVaR of a random variable X using an auxiliary random variable Y , under assumptions relating their respective cumulative distribution and density functions; these bounds yield interpretable concentration inequalities and converge as the distributional discrepancy vanishes. Building on this foundation, we establish upper and lower bounds on the CVaR value function computable from a simplified belief-MDP, accommodating general simplifications of the transition dynamics—including reduced-complexity observation and transition models. We develop estimators for computing these bounds during online policy evaluation within a particle-belief MDP framework and provide probabilistic performance guarantees. These bounds are employed for computational acceleration via action elimination: actions whose bounds indicate suboptimality under the simplified model are safely discarded while ensuring consistency with the original POMDP.

Empirical evaluation across multiple POMDP domains confirms that the bounds reliably separate safe from dangerous policies while achieving substantial computational speedups under the simplified model.

1 Introduction

Autonomous agents have emerged as a cornerstone of modern intelligent systems, with applications spanning healthcare, disaster response, education, industrial automation, and decentralized systems. From autonomous aerial vehicles coordinating firefighting efforts to multi-agent systems executing complex financial transactions, these agents are designed to perceive, reason, and act without continuous human oversight. However, ensuring that such systems behave safely and reliably in uncertain and partially observable environments remains a central challenge. In these settings, risk-aware decision-making frameworks, particularly those grounded in partially observable Markov decision processes (POMDPs), provide a principled foundation for modeling uncertainty and enforcing safety through explicit risk-sensitive optimization Ahmadi et al. 2023; Hou, Yeoh, and Varakantham 2016; Marecki and Varakantham 2010.

Exact solution methods for POMDPs become computationally intractable when the state, observation, and action spaces are large Papadimitriou and Tsitsiklis 1987a. To address this fundamental limitation, approximate planning algorithms utilize forward search trees constructed via simulation of future agent trajectories Silver and Veness 2010; Sunberg and Kochenderfer 2018. The sampling procedure is guided by the underlying reward function, which provides evaluative feedback for action selection. This approach enables practical online planning in partially observable domains by trading off solution optimality for computational tractability.

Risk-averse decision-making frameworks in the literature encompass three primary approaches: distributionally robust optimization, which hedges against distributional uncertainty Xu and Mannor 2010; chance-constrained programming, which enforces probabilistic feasibility constraints Assis Santana, Thiébaux, and Williams 2016; Moss et al. 2024b; and risk metric integration, wherein a risk measure—such as Conditional Value-at-Risk (CVaR)—is incorporated

directly into the value function Chow et al. 2015. Risk metric integration is particularly appealing when the risk measure is coherent, as coherent risk measures satisfy fundamental axioms—monotonicity, translation invariance, positive homogeneity, and subadditivity—that ensure rational and consistent behavior under aggregation and scaling of uncertain returns. These properties are especially important in sequential decision-making, where returns accumulate over time and diversification across stochastic outcomes should not be penalized. Moreover, coherence guarantees convexity of the resulting objective, enabling tractable optimization and facilitating theoretical analysis. Among coherent risk measures, CVaR has emerged as a widely adopted choice due to its explicit focus on tail risk and its compatibility with robust and distributional formulations. In the latter framework, CVaR is computed over the cumulative return, defined as the sum of stage-wise costs across the planning horizon. Chance-constrained and CVaR-based formulations reflect different perspectives on risk in sequential decision problems.

Chance constraints enforce probabilistic restrictions on state visitation, thereby preventing the agent from entering undesirable regions of the state space. Conversely, CVaR optimization targets the tail risk of the cumulative return, prioritizing mitigation of poor reward realizations. These objectives are complementary rather than interchangeable. Consider, for instance, an online algorithmic trading problem wherein the environment reward is defined as the percentage portfolio gain relative to the preceding portfolio value, and the state is characterized by current asset prices. In this setting, CVaR optimization of returns directly addresses the trader’s primary objective—managing downside risk in cumulative gains—whereas formulating the problem as a chance constraint on state space would be less natural and potentially misaligned with the risk management goal. Another example arises in sequential decision-making problems with multiple objectives, such as a navigating robot that must account for fuel availability, obstacles, and related operational constraints. In such settings, optimizing the cumulative reward provides a principled means of jointly accommodating all constraints.

Current state-of-the-art POMDP planning algorithms remain computationally demanding, as they rely on extensive sampling from the original POMDP dynamics. To mitigate this issue, the simplification approach replaces the true POMDP dynamics with a computationally tractable surrogate model, which is then employed during planning while still admitting performance guarantees relative to the original dynamics. Simplification techniques for expectation-based value functions are already available Barenboim and Indelman 2023; Lev-Yehudi, Barenboim, and Indelman 2024; Zhitnikov, Sztyglic, and Indelman 2025 and have been shown to accelerate POMDP planning. However, risk-averse simplification has remained largely unexamined; the only existing contribution in this direction employs a non-coherent risk measure Zhitnikov and Indelman 2022, which offers weaker justification for risk-averse decision making Majumdar and Pavone 2020.

We begin by establishing the mathematical foundations of this work, deriving several CVaR bounds for a random variable X using an auxiliary random variable Y , under assumptions relating their respective CDFs and PDFs. Although not all of these theoretical results are employed in our practical applications, they form a foundational framework that we expect will support future research on simplification. Building on these foundations, we analyze the relationship between the original value function—defined as the CVaR of the return—and its simplified belief transition-model counterpart. In particular, we establish lower and upper bounds on the original value function in terms of the simplified value function and provide corresponding performance guarantees. We then develop estimators for computing these bounds during online planning and derive performance guarantees for these estimators as well. The primary contributions of this work are as follows:

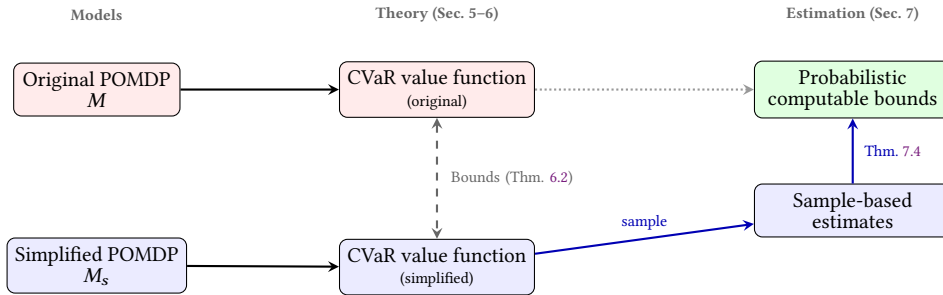


Fig. 1. Overview of the proposed framework. The original POMDP yields the original CVaR value function. The simplified POMDP M_s admits a simplified value function, related to the original via Theorem 6.2. In practice, the simplified value function and distributional discrepancy are estimated from sample trajectories, yielding probabilistic computable bounds on the original value function (Theorem 7.4).

- Derivation of bounds on the CVaR of a random variable X given another random variable Y . These bounds enable the approximation of $\text{CVaR}_\alpha(X)$ when direct access to X is limited. They also yield interpretable concentration inequalities that characterize the CVaR of X through the CVaR of Y under an adjusted confidence level, and we establish convergence of these bounds as the distributional discrepancy vanishes.
- Derivation of lower and upper bounds on the theoretical value function in risk-averse POMDPs expressed through the action-value function from a simplified belief-MDP transition model, with corresponding bounds for simplified observation models.
- Estimators for evaluating the simplified bounds during online planning, with probabilistic performance guarantees on the deviation between the theoretical action-value function and its estimated bounds computed using simplified belief-MDP and observation models within a particle-belief MDP framework.
- Application of the derived bounds to computational acceleration via action elimination, in which actions whose bounds indicate suboptimality are safely discarded, and empirical demonstration of substantial speedups with negligible degradation in policy performance across multiple POMDP domains.

An overview of the proposed framework is depicted in Figure 1. The remainder of this paper is organized as follows. Section 2 reviews related work. Section 3 introduces the necessary preliminaries on POMDPs, particle belief MDPs, and CVaR estimation. Section 4 formulates the problem of bounding the risk-averse value function under a simplified belief-transition model. Section 5 derives the foundational CVaR bounds using auxiliary random variables. Section 6 establishes value function bounds for the static CVaR value function under general and observation-model simplifications. Section 7 develops online estimators for computing these bounds during planning and provides corresponding performance guarantees. Section 8 discusses the limitations of the framework. Section 9 presents the experimental evaluation across multiple POMDP domains. Section 10 concludes the paper. Proofs and additional experimental details are provided in the appendix.

2 Related Work

Conditional Value at Risk (CVaR) Rockafellar, Uryasev, et al. 2000 is a principled and extensively studied risk measure with broad applicability across domains involving uncertainty. A central property of CVaR is its dual representation Artzner et al. 1999, which allows it to be interpreted as the expected loss in the worst-case tail of a cost distribution

Chow et al. 2015. Unlike Value at Risk (VaR), which identifies only the quantile threshold of extreme losses at a chosen confidence level, CVaR quantifies both the probability and the magnitude of such losses, yielding a more comprehensive assessment of risk. This property makes CVaR especially relevant in safety-critical decision-making contexts, where both the occurrence and severity of adverse outcomes are significant. Moreover, CVaR satisfies the axioms of coherent risk measures—such as subadditivity and positive homogeneity—ensuring consistent and rational aggregation of risk across time and decision stages Artzner et al. 1999. Practical estimators of CVaR are supported by concentration inequalities and deviation guarantees from the true risk value Brown 2007; Thomas and Learned-Miller 2019, further reinforcing its reliability in applied decision-making problems.

Risk can be incorporated into planning under uncertainty through multiple paradigms, including chance constraints Ono et al. 2015, exponential utility functions Koenig and Simmons 1994, distributionally robust optimization Cubuktepe et al. 2021; Osogami 2015; Xu and Mannor 2010, and quantile regression methods Dabney et al. 2018. Among these, distributionally robust formulations are particularly aligned with CVaR optimization, as both emphasize resilience to rare but high-impact events Chow et al. 2015. Risk measures map random cost variables to real-valued evaluations and are expected to satisfy fundamental axioms to ensure interpretability and consistency Majumdar and Pavone 2020. Coherent risk measures, by satisfying these axioms, provide a principled foundation for incorporating CVaR into sequential decision-making. General coherent risk formulations have been employed as optimization objectives in POMDPs, constrained MDPs, and shortest-path problems Ahmadi et al. 2020, 2021a,b; Dixit, Ahmadi, and Burdick 2023, where CVaR arises as a key special case. Specifically, Chow et al. 2015 introduced the CVaR-MDP framework, defining the value function as the CVaR of the return and deriving a value-iteration-based solution with formal error guarantees.

Simplification techniques for POMDPs aim to reduce computational complexity while retaining performance guarantees, thereby facilitating real-time deployment of POMDP-based policies in practical systems Papadimitriou and Tsitsiklis 1987b. Simplification refers to replacing one or more POMDP components with computationally tractable approximations while providing formal performance guarantees that ensure decision quality with respect to the original model. For instance, Lev-Yehudi, Barenboim, and Indelman 2024 examined simplification of the observation model by introducing a less expensive surrogate while establishing finite-sample convergence bounds. Similarly, Barenboim and Indelman 2026 studied simplification of the state and observation spaces, providing deterministic performance guarantees and integrating them into state-of-the-art solvers. Furthermore, Zhitnikov and Indelman 2022 examined the simplification of belief-dependent rewards and provided deterministic guarantees under the Value at Risk (VaR) criterion. However, VaR is not a coherent risk measure and therefore lacks several essential properties for principled risk-averse decision making. More broadly, the simplification of risk-averse planning remains largely unexplored, with Zhitnikov and Indelman 2022 being the only prior work in this direction. To the best of our knowledge, no prior work has addressed the problem of bounding the CVaR of a random variable using an auxiliary random variable with a known distributional discrepancy, which constitutes a key contribution of this work.

3 Preliminaries

3.1 Partially Observable Markov Decision Process

A finite-horizon Partially Observable Markov Decision Process (POMDP) is formally defined as the tuple (X, A, Z, T, O, c, b_0) , where X , A , and Z denote the state, action, and observation spaces, respectively. The transition model $T(x_{t+1} | x_t, a_t) \triangleq P(x_{t+1} | x_t, a_t)$ specifies the conditional probability of transitioning from state x_t to x_{t+1} given action a_t , while the

observation model $O(z_t | x_t) \triangleq P(z_t | x_t)$ defines the likelihood of observing z_t when the system is in state x_t . The belief space B is the set of all probability distributions over X , and the stage-wise cost function is given by $c : B \times A \rightarrow \mathbb{R}$.

At each time step t , the agent maintains a belief $b_t \in B$, representing the posterior distribution over the latent state conditioned on the history of observations and actions. The history is denoted by $H_t = \{z_{1:t}, a_{0:t-1}, b_0\}$, and the belief update is defined as $b_t(x_t) \triangleq P(x_t | H_t)$ for each $x_t \in X$. A policy $\pi_t : B \rightarrow A$ is a measurable mapping that prescribes the action $a_t = \pi_t(b_t)$ based on the current belief state. The immediate expected cost under belief b_t and action a_t is

$$c(b_t, a_t) \triangleq \mathbb{E}_{x \sim b_t} [c_x(x, a_t)], \quad (1)$$

where $c_x(x, a_t)$ denotes the state-dependent cost, bounded as $R_{\min} \leq c_x(x, a_t) \leq R_{\max}$.

The cumulative cost, or *return*, over a finite horizon $T \in \mathbb{N}$ is given by

$$R_{t:T} \triangleq \sum_{\tau=t}^T c(b_\tau, a_\tau), \quad (2)$$

which serves as the performance criterion starting at time t . The value function associated with policy π and initial belief b_k is

$$V^\pi(b_k) \triangleq \mathbb{E}[R_{k:T} | b_k, \pi] = \sum_{t=k}^T \mathbb{E}[c(b_t, a_t) | b_k, \pi], \quad (3)$$

and the corresponding action-value function is

$$Q^\pi(b_k, a_k) \triangleq \mathbb{E}_{z_{k+1}} [c(b_k, a_k) + V^\pi(b_{k+1}) | b_k, a_k]. \quad (4)$$

A POMDP can equivalently be formulated as a fully observable *belief-MDP* (BMDP), in which the belief b_t serves as the state variable and is a sufficient statistic for the interaction history. In this formulation, the dynamics are governed by a belief transition kernel induced by the latent state-transition and observation models. Formally, the belief-MDP associated with a POMDP M is defined as

$$M_B \triangleq (\mathcal{B}, A, \tau, \rho, \gamma), \quad (5)$$

where $\mathcal{B} \triangleq \Delta(X)$ denotes the space of probability distributions over the latent state space X , A is the action space, τ denotes the belief-transition kernel, ρ is the expected cost, and γ is the discount factor. Given the state-transition and observation models, the belief-transition model of the belief-MDP is given by

$$P(b_{t+1} | b_t, a_t) = \int_{x_t \in X} \int_{x_{t+1} \in X} \int_{z_{t+1} \in Z} P(x_{t+1} | x_t, a_t) P(z_{t+1} | x_{t+1}) b_t(x_t) dx_t dx_{t+1} dz_{t+1}. \quad (6)$$

This BMDP formulation is exact but generally intractable, since the belief space \mathcal{B} is infinite-dimensional, motivating approximate representations such as particle belief MDPs.

3.2 Particle Belief MDP

In order to estimate the theoretical action-value function, we consider a particle belief MDP (PB-MDP) setting. Formally, denote by $M_P \triangleq (\Sigma, A, \tau, \rho, \gamma)$ the PB-MDP that is defined with respect to the POMDP M Lim et al. 2023 and $N_p \in \mathbb{N}$, where

- $\Sigma \triangleq \{\bar{b} : \bar{b} = \{(x_i, w_i)\}_{i=1}^{N_p}, x_i \in X, \forall i, w_i \geq 0, \exists i \text{ such that } w_i > 0\}$ is the state space over the particle beliefs.
- A is the action space as defined in the POMDP M .
- $\tau(\bar{b}_{t+1} | \bar{b}_t, a)$ is the belief transition probability, for $a \in A, \bar{b} \in \Sigma$.

- $\rho(\bar{b}, a) \triangleq \frac{\sum_{j=1}^{N_p} w_j c(x_j, a)}{\sum_{j=1}^{N_p} w_j}$ is the belief-dependent cost.
- γ as defined in the POMDP M .

This belief estimator maintains a finite set of state particles that serve as an approximation to the theoretical belief, which, in principle, may involve an infinite number of states.

3.3 Conditional Value-at-Risk

Let X be a random variable defined on a probability space (Ω, \mathcal{F}, P) , where \mathcal{F} is the σ -algebra, and $P : \mathcal{F} \rightarrow [0, 1]$ is a probability measure. Assume further that $\mathbb{E}[|X|] < \infty$. We denote the cumulative distribution function (CDF) of the random variable X by $F_X(x) = P(X \leq x)$. The value at risk at confidence level $\alpha \in (0, 1)$ is the $1 - \alpha$ quantile of X , i.e.,

$$\text{VaR}_\alpha(X) \triangleq \inf\{x \in \mathbb{R} : F_X(x) > 1 - \alpha\} \quad (7)$$

For simplicity we denote $q_\alpha^X = \text{VaR}_\alpha(X)$ or $q_\alpha^F = \text{VaR}_\alpha(X)$. The conditional value at risk (CVaR) at confidence level α is defined as Rockafellar, Uryasev, et al. 2000

$$\text{CVaR}_\alpha(X) \triangleq \inf_{w \in \mathbb{R}} \left\{ w + \frac{1}{\alpha} \mathbb{E}[(X - w)^+] \mid w \in \mathbb{R} \right\}, \quad (8)$$

where $(x)^+ = \max(x, 0)$. For a smooth F , it holds that Pflug 2000

$$\text{CVaR}_\alpha(X) = \mathbb{E}[X \mid X > \text{VaR}_\alpha(X)] = \frac{1}{\alpha} \int_{1-\alpha}^1 F^{-1}(v) dv. \quad (9)$$

Let $X_i \stackrel{\text{iid}}{\sim} F$ for $i \in \{1, \dots, n\}$. Denote by

$$\hat{C}_\alpha(X) \triangleq \hat{C}_\alpha(\{X_i\}_{i=1}^n) \triangleq \inf_{x \in \mathbb{R}} \left\{ x + \frac{1}{n\alpha} \sum_{i=1}^n (X_i - x)^+ \right\} \quad (10)$$

the estimate of $\text{CVaR}_\alpha(X)$ Brown 2007. Theorem 3.1, that bounds the deviation of the estimated CVaR and the true CVaR, was proved in Brown 2007.

THEOREM 3.1. *If $\text{supp}(X) \subseteq [a, b]$ and X has a continuous distribution function, then for any $\delta \in (0, 1)$,*

$$P\left(\text{CVaR}_\alpha(X) - \hat{C}_\alpha(X) > (b - a) \sqrt{\frac{5 \ln(3/\delta)}{\alpha n}}\right) \leq \delta, \quad (11)$$

$$P\left(\text{CVaR}_\alpha(X) - \hat{C}_\alpha(X) < -\frac{(b - a)}{\alpha} \sqrt{\frac{\ln(1/\delta)}{2n}}\right) \leq \delta. \quad (12)$$

The estimator in (10) can be expressed as

$$\hat{C}_\alpha(X) = X^{(n)} - \frac{1}{\alpha} \sum_{i=1}^{n-1} (X^{(i)} - X^{(i-1)}) \left(\frac{i}{n} - (1 - \alpha) \right)^+, \quad (13)$$

where $X^{(i)}$ is the i th order statistic of X_1, \dots, X_n in ascending order Thomas and Learned-Miller 2019. The results presented in Theorems 3.2 and 3.3, following the work of Thomas and Learned-Miller 2019, yield tighter bounds on the CVaR compared to those established by Brown 2007.

THEOREM 3.2. *If X_1, \dots, X_n are independent and identically distributed random variables and $\Pr(X_1 \leq b) = 1$ for some finite b , then for any $\delta \in (0, 0.5]$,*

$$\Pr\left(\text{CVaR}_\alpha(X_1) \leq Z_{n+1} - \frac{1}{\alpha} \sum_{i=1}^n (Z_{i+1} - Z_i) \left(\frac{i}{n} - \sqrt{\frac{\ln(1/\delta)}{2n}} - (1-\alpha) \right)^+\right) \geq 1 - \delta, \quad (14)$$

where Z_1, \dots, Z_n are the order statistics (i.e., X_1, \dots, X_n sorted in ascending order), $Z_{n+1} = b$, and $x^+ \triangleq \max\{0, x\}$ for all $x \in \mathbb{R}$.

THEOREM 3.3. *If X_1, \dots, X_n are independent and identically distributed random variables and $\Pr(X_1 \geq a) = 1$ for some finite a , then for any $\delta \in (0, 0.5]$,*

$$\Pr\left(\text{CVaR}_\alpha(X_1) \geq Z_n - \frac{1}{\alpha} \sum_{i=0}^{n-1} (Z_{i+1} - Z_i) \left(\min\left\{1, \frac{i}{n} + \sqrt{\frac{\ln(1/\delta)}{2n}}\right\} - (1-\alpha) \right)^+\right) \geq 1 - \delta, \quad (15)$$

where Z_1, \dots, Z_n are the order statistics (i.e., X_1, \dots, X_n sorted in ascending order), $Z_0 = a$, and $x^+ \triangleq \max\{0, x\}$ for all $x \in \mathbb{R}$.

Notably, Theorems 3.2 and 3.3 require only one-sided boundedness of the support and do not assume continuity of the distribution function, in contrast to Theorem 3.1, which requires both two-sided boundedness and a continuous distribution. The restriction to $\delta \in (0, 0.5]$ is mild in practice, as it corresponds to confidence levels of at least 50%.

4 Problem Formulation

In this work, we adopt a risk-averse formulation in which, instead of optimizing the expected return as in (3) and (4), the value function is defined as the CVaR of the return. Let $\alpha \in (0, 1)$, and denote the original POMDP by M . The value and action-value functions at time k are defined by

$$V_M^\pi(b_k, \alpha) \triangleq \text{CVaR}_\alpha^P \left[\sum_{t=k}^T c(b_t, \pi(b_t)) \mid b_k, \pi \right], \quad (16)$$

$$Q_M^\pi(b_k, a_k, \alpha) \triangleq \text{CVaR}_\alpha^P \left[c(b_k, a_k) + \sum_{t=k+1}^T c(b_t, \pi(b_t)) \mid b_k, \pi \right]. \quad (17)$$

Figure 3a illustrates the difference between the standard expected value function and the CVaR value function.

We consider cases in which the belief-MDP transition model is simplified for computational tractability. Let Ω_B be the sample space of the belief random variable and let $\Omega \triangleq \Omega_B^{T-k+1}$ denote the corresponding product space, endowed with a σ -algebra \mathcal{F} . We define two probability measures $P, P_s : \mathcal{F} \rightarrow [0, 1]$ on the measurable space (Ω, \mathcal{F}) , corresponding to the original and simplified belief models, respectively. The CDF of $R_{k:T}$ under the original model is

$$P(R_{k:T} \leq l \mid b_k, \pi) = \int_{b_{k+1:T} \in B^{T-k}} P(R_{k:T} \leq l \mid b_{k:T}, \pi) \prod_{i=k+1}^T P(b_i \mid b_{i-1}, \pi) db_{k+1:T}, \quad (18)$$

and the simplified CDF of $R_{k:T}$ is defined using only the simplified belief transition model:

$$P_s(R_{k:T} \leq l \mid b_k, \pi) = \int_{b_{k+1:T} \in B^{T-k}} P(R_{k:T} \leq l \mid b_{k:T}, \pi) \prod_{i=k+1}^T P_s(b_i \mid b_{i-1}, \pi) db_{k+1:T}. \quad (19)$$

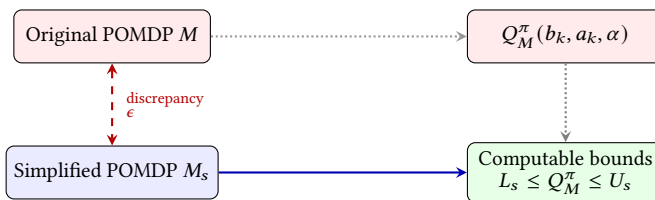


Fig. 2. Conceptual overview. Direct evaluation of Q_M^π under the original model M is computationally expensive. Instead, the simplified model M_s is used to compute bounds on Q_M^π , where the bound quality is governed by the distributional discrepancy ϵ between their belief transition models.

The belief-MDP transition model is defined using the state transition and observation models. Hence, simplification of the belief-MDP transition model is general enough to include simplifications of state and observation models simultaneously.

Denote the simplified POMDP by M_s . The value and action-value functions corresponding to M_s are denoted by $V_{M_s}^\pi(b_k, \alpha)$ and $Q_{M_s}^\pi(b_k, a_k, \alpha)$, respectively. These definitions are identical to those in (16) and (17), except that the return distribution is defined with respect to the simplified belief transition model P_s .

While the simplified model P_s is computationally tractable, directly using $Q_{M_s}^\pi(b_k, a_k, \alpha)$ as a surrogate for $Q_M^\pi(b_k, a_k, \alpha)$ may lead to incorrect risk assessments, since the return distributions under P and P_s differ. Our objective is to establish lower and upper bounds, denoted by L_s and U_s , such that $L_s \leq Q_M^\pi(b_k, a_k, \alpha) \leq U_s$, depending solely on quantities computable from the simplified model (19); this conceptual approach is summarized in Figure 2. These bounds provide formal guarantees on the true value function, enabling reliable action selection during online planning. As illustrated in Figure 3, the key quantity governing these bounds is ϵ , an upper bound on the discrepancy between the CDFs of the return under P and P_s . Bounding this CDF discrepancy allows us to bound the difference in CVaR, as established in subsequent sections.

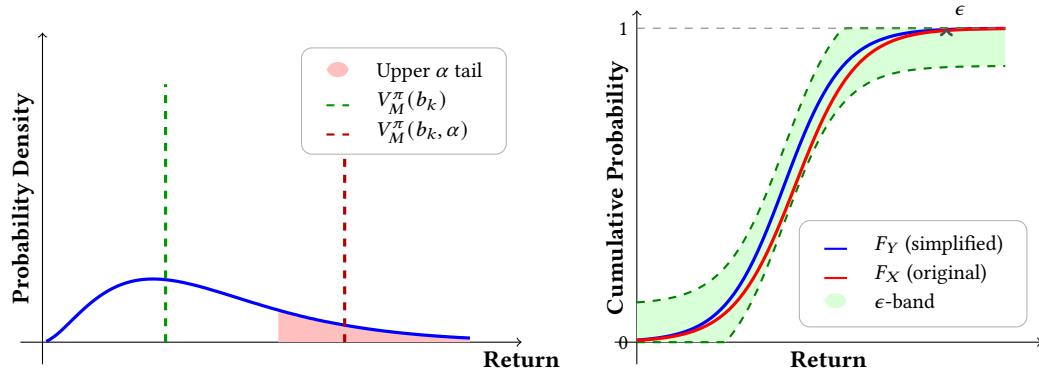
5 CVaR Bounds

In the previous section, we introduced a simplified belief-transition model with distribution P_s as a computationally tractable approximation of the original belief-transition model P . This approximation induces two corresponding random variables: X , representing the return under the original model P , and Y , representing the return under the simplified model P_s . While direct evaluation of risk-sensitive criteria for X is often computationally infeasible, sampling and analysis of Y can be carried out efficiently.

The goal of this section is to characterize how $\text{CVaR}_\alpha(X)$ can be bounded and estimated using information derived from Y . To this end, we first establish distributional bounds that relate X and Y , and then derive finite-sample guarantees that allow these bounds to be estimated from data. Together, these results provide a principled framework for bounding the CVaR of the true return using samples generated from the simplified model.

5.1 Theoretical CVaR Bounds

In this section, we establish bounds for the CVaR of the random variable X by leveraging an auxiliary random variable Y . Two forms of distributional relationships between their respective CDFs are considered: a uniform bound and a non-uniform bound, as illustrated in Figure 4a and Figure 4b. These results provide the theoretical basis for



(a) Comparison of expected value $V_M^\pi(b_k)$ and CVaR value $V_M^\pi(b_k, \alpha)$. The shaded region represents the worst α fraction of outcomes.

(b) CDF discrepancy between original (F_X) and simplified (F_Y) models. The ϵ -band bounds the discrepancy, enabling CVaR bounds.

Fig. 3. Problem formulation illustrations. (a) The CVaR value function focuses on the tail of the return distribution, unlike the expected value. (b) The simplified model P_s yields a computable CDF F_Y , while the original CDF F_X is intractable. When $|F_X(r) - F_Y(r)| \leq \epsilon$, bounds on $\text{CVaR}_\alpha(X)$ can be derived from Y .

subsequent sections, in which the derived bounds are applied to estimate the CVaR of random variables that are either computationally intractable or prohibitively expensive to sample directly.

Theorem 5.1 bounds $\text{CVaR}_\alpha(X)$ in terms of $\text{CVaR}_\alpha(Y)$ under the sole condition that the cumulative distribution functions of X and Y differ by at most a known uniform bound. This representation enhances the interpretability of the bound and constitutes a novel aspect of the result, made possible by framing the bounding problem in terms of distributional discrepancies. In the next section, we demonstrate that the bounds established in Thomas and Learned-Miller 2019 (theorems 3.2 and 3.3) arise as a special case of Theorem 5.1, thereby providing an interpretation for existing CVaR bounds that are otherwise difficult to interpret.

THEOREM 5.1. *Let X and Y be random variables and $\epsilon \in [0, 1]$.*

(1) **Upper Bound:** *assume that $P(X \leq b_X) = 1, P(Y \leq b_Y) = 1$ and $\forall z \in \mathbb{R}, F_Y(z) - F_X(z) \leq \epsilon$, then*

(a) *If $\alpha > \epsilon$,*

$$\text{CVaR}_\alpha(X) \leq \frac{\epsilon}{\alpha} \max(b_X, b_Y) + (1 - \frac{\epsilon}{\alpha}) \text{CVaR}_{\alpha-\epsilon}(Y). \quad (20)$$

(b) *If $\alpha \leq \epsilon$, then $\text{CVaR}_\alpha(X) \leq \max(b_X, b_Y)$.*

(2) **Lower Bound:** *If $P(X \geq a_X) = 1, P(Y \geq a_Y) = 1$ and $\forall z \in \mathbb{R}, F_X(z) - F_Y(z) \leq \epsilon$, then*

(a) *If $\alpha + \epsilon \leq 1$,*

$$\text{CVaR}_\alpha(X) \geq (1 + \frac{\epsilon}{\alpha}) \text{CVaR}_{\alpha+\epsilon}(Y) - \frac{\epsilon}{\alpha} \text{CVaR}_\epsilon(Y) \quad (21)$$

(b) *If $\alpha + \epsilon > 1$ and $a_{\min} = \min(a_X, a_Y)$,*

$$\text{CVaR}_\alpha(X) \geq \frac{1}{\alpha} (\mathbb{E}[Y] - \epsilon \text{CVaR}_\epsilon(Y) + (\alpha + \epsilon - 1)a_{\min}) \quad (22)$$

PROOF. The proof is available in Appendix A.1. □

The parameter ϵ quantifies the discrepancy between the random variables X and Y , and is defined as a uniform bound on the difference between their cumulative distribution functions. By construction, ϵ takes values in the interval

$[0, 1]$. In the limiting case where $\epsilon = 1$, Y provides no information about X . In this setting, the bounds provided by Theorem 5.1 reduce to trivial bounds on $\text{CVaR}_\alpha(X)$ involving the essential supremum of both X and Y , rendering them ineffective for practical use. When $\epsilon = 0$, the cumulative distribution functions of X and Y are identical, and thus the bound becomes exact, yielding $\text{CVaR}_\alpha(X) = \text{CVaR}_\alpha(Y)$.

THEOREM 5.2. *Under the definitions of X , Y , ϵ , and α specified in Theorem 5.1, the lower and upper bounds established therein converge to $\text{CVaR}_\alpha(X)$ as $\epsilon \rightarrow 0$.*

PROOF. The proof is available in Appendix A.2. □

For both the upper and lower bounds to be informative, Theorem 5.1 shows that $\alpha > \epsilon$ and $\alpha + \epsilon \leq 1$ must hold, thereby specifying the required relation between the distributional discrepancy ϵ and the CVaR confidence level α . Under these conditions, the bounding problem reduces to (20) and (21). For $\alpha > \epsilon$, the upper bound on $\text{CVaR}_\alpha(X)$ is a weighted average of the CVaR of Y at a confidence level shifted by the distributional discrepancy ϵ and the maximum of the supports of X and Y , where the weights are proportional to the amount of distributional discrepancy. For $\alpha + \epsilon \leq 1$, the bound in (21) satisfies

$$\text{CVaR}_\alpha(X) \geq \text{CVaR}_{\alpha+\epsilon}(Y) + \frac{\epsilon}{\alpha} (\text{CVaR}_{\alpha+\epsilon}(Y) - \text{CVaR}_\epsilon(Y)). \tag{23}$$

The lower bound corresponds to the CVaR of Y evaluated at a confidence level adjusted by the distributional discrepancy ϵ , augmented by a correction term that is proportional to the distributional discrepancy.

Theorem 5.1 assumes that the parameter ϵ provides an upper bound on the pointwise difference between the cumulative distribution functions F_X and F_Y . As illustrated in Figure 4a, this bound is particularly conservative in the vicinity of $x = -1$, where the actual discrepancy between F_X and F_Y is significantly smaller than the global bound ϵ . Ideally, a tighter bound on $F_X(x)$ would allow for variation with respect to x , rather than relying on a uniform constant. Specifically, one seeks a pointwise bound of the form $F_X(x) \leq F_Y(x) + g(x)$ for some non-negative function g , as illustrated in Figure 4b. In this paper, we defer the study of specific choices of the function g to future work, and instead provide general assumptions under which a feasible tighter bound can be established using such a function.

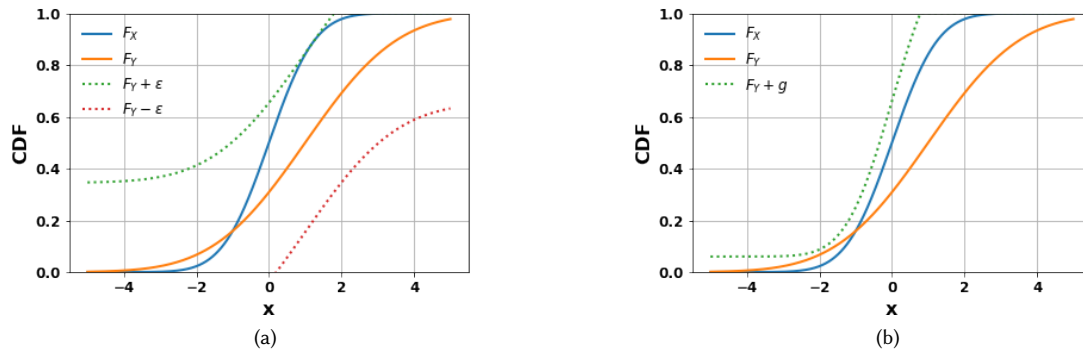


Fig. 4. Illustrations of bounds on $F_X(x)$. (a) Bounds from Theorem 5.1. (b) Bounds from Theorem 5.3, where g depends on x and yields a tighter result than $F_Y(x) + \epsilon$.

THEOREM 5.3. (*Tighter CVaR Lower Bound*) Let $\alpha \in (0, 1)$, X and Y be random variables. Define the random variable Y^L such that $F_{Y^L}(y) \triangleq \min(1, F_Y(y) + g(y))$ for $g : \mathbb{R} \rightarrow [0, \infty)$. Assume $\lim_{x \rightarrow -\infty} g(x) = 0$, g is continuous from the right and monotonic increasing. If $\forall x \in \mathbb{R}, F_X(x) \leq F_Y(x) + g(x)$, then F_{Y^L} is a CDF and $\text{CVaR}_\alpha(Y^L) \leq \text{CVaR}_\alpha(X)$.

PROOF. The proof is available in Appendix A.4. □

Theorem 5.3 defines a random variable Y^L , constructed from Y and the function g , such that the distributional discrepancy between Y^L and X is determined explicitly by g rather than being uniformly bounded as in Theorem 5.1. In addition, it offers a criterion for determining whether a given function g can be used to derive a lower bound on the CVaR. This bound extends the lower bound established in Theorem 5.1, which is obtained when $g(x)$ is constant and equal to ϵ for all $x \in \mathbb{R}$. Intuitively, F_{Y^L} is the largest valid CDF that remains within the pointwise discrepancy band $[F_Y(y), F_Y(y) + g(y)]$; since $F_X \leq F_{Y^L}$ by construction, monotonicity of CVaR yields the lower bound. Figure 4(c) illustrates this tighter construction.

Note that in Theorem 5.3, the function g is assumed to be non-decreasing and right-continuous. If one assumes only that $|F_X(x) - F_Y(x)| \leq g(x)$ for some function $g : \mathbb{R} \rightarrow [0, \infty)$, which is not necessarily monotonic or continuous, then the most general form of the CVaR bounds is given by

$$\text{CVaR}_\alpha(X) = \frac{1}{\alpha} \int_{1-\alpha}^1 \inf\{z \in \mathbb{R} : F_X(z) \geq \tau\} d\tau \geq \frac{1}{\alpha} \int_{1-\alpha}^1 \inf\{z \in \mathbb{R} : F_Y(z) + g(z) \geq \tau\} d\tau, \quad (24)$$

$$\text{CVaR}_\alpha(X) = \frac{1}{\alpha} \int_{1-\alpha}^1 \inf\{z \in \mathbb{R} : F_X(z) \geq \tau\} d\tau \leq \frac{1}{\alpha} \int_{1-\alpha}^1 \inf\{z \in \mathbb{R} : F_Y(z) - g(z) \geq \tau\} d\tau. \quad (25)$$

Another option is to specify the distributional discrepancy through the density functions underlying the cumulative distribution functions. Let f_x and f_y be the probability density functions of X and Y , respectively, and let $h : \mathbb{R} \rightarrow [0, \infty)$ describe the pointwise discrepancy between them. Theorem 5.4 specifies conditions on the function h under which a lower bound for the CVaR of X can be obtained. A key advantage is that this bound takes the form of the CVaR of a random variable, enabling its estimation with performance guarantees via CVaR concentration bounds given in Theorems 3.1, 3.3, 3.2 and Theorem 5.5.

THEOREM 5.4. Let $\alpha \in (0, 1)$, X and Y be random variables. Define $h : \mathbb{R} \rightarrow [0, \infty)$ to be a continuous function, $g(z) \triangleq \int_{-\infty}^z h(x) dx$ and Y^L to be a random variable such that $F_{Y^L}(y) \triangleq \min(1, F_Y(y) + g(y))$. If $\lim_{z \rightarrow -\infty} g(z) = 0$ and $\forall x \in \mathbb{R}, f_x(x) \leq f_y(x) + h(x)$, then F_{Y^L} is a CDF and $\text{CVaR}_\alpha(Y^L) \leq \text{CVaR}_\alpha(X)$.

PROOF. The proof is available in Appendix A.5. □

Theorem 5.4 is obtained as a corollary of Theorem 5.3 by defining a function g , as illustrated in Figure 4b, in terms of the function h . This construction demonstrates that the function g in Theorem 5.3 can be generated from a broad class of density discrepancy functions.

5.2 Concentration Inequalities

In this section, we derive concentration inequalities for $\text{CVaR}_\alpha(X)$ based on samples drawn from an auxiliary random variable Y . A notable special case of these inequalities arises when Y is taken to follow the empirical cumulative distribution function (ECDF) of X .

Let $X_1, \dots, X_n \stackrel{i.i.d.}{\sim} F_X$, where F_X is the CDF of a random variable X . The ECDF based on these samples is defined by $\hat{F}_X(x) = \frac{1}{n} \sum_{i=1}^n 1_{X_i \leq x}$, for $x \in \mathbb{R}$. Let $E_{\hat{F}_X}[X]$ denote the expectation with respect to \hat{F}_X , and let $C_\alpha^{\hat{F}_X}$ denote the CVaR computed under the empirical distribution \hat{F}_X .

THEOREM 5.5. *Let X be a random variable, $\alpha \in (0, 1]$, $\delta \in (0, 0.5)$, $\epsilon = \sqrt{\ln(1/\delta)/(2n)}$. Let $X_1, \dots, X_n \stackrel{iid}{\sim} F_X$ be random variables that define the ECDF \hat{F}_X .*

- (1) **Upper Bound:** *If $P(X \leq b) = 1$, then*
 - (a) *If $\alpha > \epsilon$ then $P(\text{CVaR}_\alpha(X) \leq (1 - \frac{\epsilon}{\alpha})C_{\alpha-\epsilon}^{\hat{F}_X} + \frac{\epsilon}{\alpha}b) > 1 - \delta$.*
 - (b) *If $\alpha \leq \epsilon$ then $\text{CVaR}_\alpha(X) \leq b$*
- (2) **Lower Bound:** *If $P(X \geq a) = 1$, then*
 - (a) *If $\alpha + \epsilon < 1$, then $P(\text{CVaR}_\alpha(X) \geq (1 + \frac{\epsilon}{\alpha})C_{\alpha+\epsilon}^{\hat{F}_X} - \frac{\epsilon}{\alpha}C_\epsilon^{\hat{F}_X}) > 1 - \delta$.*
 - (b) *If $\alpha + \epsilon \geq 1$, then $P(\text{CVaR}_\alpha(X) \geq \frac{1}{\alpha}[(\alpha + \epsilon - 1)a + E_{\hat{F}_X}[X] - \epsilon C_\epsilon^{\hat{F}_X}]) > 1 - \delta$.*

PROOF. The proof is available in Appendix A.3. □

Theorem 5.5 provides concentration inequalities for $\text{CVaR}_\alpha(X)$ in a form that enables the user to specify a desired bound consistency level δ , which determines the probability that the bound holds. This result follows as a corollary of Theorem 5.1, in which the auxiliary random variable Y is instantiated as the ECDF of X , whereas X denotes the underlying true random variable, which is inaccessible in practice. The distributional discrepancy required by Theorem 5.1, denoted by ϵ , is controlled in Theorem 5.5 via the Dvoretzky–Kiefer–Wolfowitz (DKW) inequality Dvoretzky, Kiefer, and Wolfowitz 1956. The DKW inequality ensures that the supremum distance between the true CDF and the ECDF converges to zero at a rate of order $1/\sqrt{n}$ as the number of samples n increases. Corollary 5.6 establishes the asymptotic convergence of the bounds given in Theorem 5.5 as the sample size tends to infinity.

COROLLARY 5.6. *Let X be a random variable, $\alpha \in (0, 1]$, $\delta \in (0, 0.5)$, $\epsilon = \sqrt{\ln(1/\delta)/(2n)}$, $a \in \mathbb{R}$, $b \in \mathbb{R}$. Let $X_1, \dots, X_n \stackrel{iid}{\sim} F_X$ be random variables that define the ECDF \hat{F}_X . Denote by $U(n)$ and $L(n)$ the upper and lower bounds respectively from Theorem 5.5, where n is the number of samples, then*

- (1) *If $P(X \leq b) = 1$, then $\lim_{n \rightarrow \infty} U(n) \stackrel{a.s.}{=} \text{CVaR}_\alpha(X)$.*
- (2) *If $P(X \geq a) = 1$, then $\lim_{n \rightarrow \infty} L(n) \stackrel{a.s.}{=} \text{CVaR}_\alpha(X)$.*

where a.s. denotes almost sure convergence.

PROOF. The proof is available in Appendix A.6. □

The concentration bounds established by Thomas and Learned-Miller 2019 coincide with those given in Theorem 5.5, rendering the results of Thomas and Learned-Miller 2019 a special case of Theorem 5.5. This equivalence arises because both Theorem 5.5 and Thomas and Learned-Miller 2019 derive concentration bounds for $\text{CVaR}_\alpha(X)$ by constructing an alternative CDF that stochastically dominates the true distribution F_X , employing the DKW inequality to control the discrepancy. The principal distinction between the two results lies in the formulation of the CVaR bound: Thomas and Learned-Miller 2019 express the bound through a sum of reweighted order statistics (theorems 3.2 and 3.3), resulting in a more intricate form, whereas Theorem 5.5 presents a more interpretable bound in terms of CVaR. The interpretability of these bounds constitutes a contribution of this paper.

Theorem 5.7 provides concentration inequalities for the theoretical $\text{CVaR}_\alpha(X)$ based on samples drawn from an auxiliary random variable Y , assuming only a bound on the distributional discrepancy between X and Y .

THEOREM 5.7. *Let X and Y be random variables, $\epsilon \in [0, 1]$, $\delta \in (0, 0.5)$, and $\eta = \sqrt{\ln(1/\delta)/(2n)}$, $\epsilon' = \min(\epsilon + \eta, 1)$. Let Y_1, \dots, Y_n be independent and identically distributed samples from F_Y , and denote by \hat{F}_Y the associated empirical cumulative distribution function.*

- (1) **Upper Bound:** If $\forall z \in \mathbb{R}, F_Y(z) - F_X(z) \leq \epsilon$ and $P(X \leq b_X) = 1, P(Y \leq b_Y) = 1$, then
- (a) If $\alpha > \epsilon'$ then $P\left(\text{CVaR}_\alpha(X) \leq \frac{\epsilon'}{\alpha} \max(b_X, b_Y) + (1 - \frac{\epsilon'}{\alpha}) \text{CVaR}_{\alpha-\epsilon'}^{\hat{F}_Y}\right) > 1 - \delta$.
 - (b) If $\alpha \leq \epsilon'$, then $\text{CVaR}_\alpha(X) \leq \max(b_X, b_Y)$
- (2) **Lower Bound:** If $\forall z \in \mathbb{R}, F_X(z) - F_Y(z) \leq \epsilon$ and $P(X \geq a_X) = 1, P(Y \geq a_Y) = 1$, then
- (a) If $\alpha + \epsilon' \leq 1$, then

$$P\left(\text{CVaR}_\alpha(X) \geq (1 + \frac{\epsilon'}{\alpha}) \text{CVaR}_{\alpha+\epsilon'}^{\hat{F}_Y} - \frac{\epsilon'}{\alpha} \text{CVaR}_{\epsilon'}^{\hat{F}_Y}\right) > 1 - \delta. \quad (26)$$

- (b) If $\alpha + \epsilon' > 1$, then

$$P\left(\text{CVaR}_\alpha(X) \geq \frac{1}{\alpha} (\mathbb{E}_{\hat{F}_Y}[Y] - \epsilon' \text{CVaR}_{\epsilon'}^{\hat{F}_Y} + (\alpha + \epsilon' - 1)a_{\min})\right) > 1 - \delta. \quad (27)$$

PROOF. The proof is available in Appendix A.7. \square

The parameter ϵ in Theorem 5.7 captures the distributional discrepancy between X and Y , consistent with its role in Theorem 5.1. Additionally, the theorem introduces ϵ' to represent the discrepancy between F_X and \hat{F}_Y , where \hat{F}_Y denotes the empirical CDF of Y constructed from the sample $\{Y_i\}_{i=1}^n$. The parameter η accounts for the additional distributional discrepancy beyond ϵ , and captures the estimation error in approximating F_Y using the empirical sample $\{Y_i\}_{i=1}^n$. By combining Theorem 5.1 with the DKW inequality Dvoretzky, Kiefer, and Wolfowitz 1956, we obtain probabilistic guarantees for the estimated bounds.

6 Value Function Bounds for Static CVaR Value Function

In this section, we leverage the CVaR bounds from the previous section to establish bounds between the simplified and original value functions as defined in (16), where the simplification is considered in a general form with respect to the belief transition model. We then derive bounds for the specific case in which the simplification applies to the observation model. The implications of these bounds for policy evaluation and open-loop POMDP planning will be examined in the Experiments section.

6.1 Bounds for a General Belief Transition Model Simplification

In this section, we establish bounds on the difference between the CDFs of the returns, computed with respect to the simplified and original belief transition models. These bounds are then used to bound the original value function in terms of the simplified value function.

Theorem 6.1 demonstrates that the difference between the CDFs of the returns, computed with respect to the simplified and original belief transition models, can be characterized in terms of the difference between the simplified and original belief transition models.

THEOREM 6.1. *Let P and P_s denote the probability measures induced by the original and simplified belief-transition models, respectively. Denote by \mathbb{E}^s the expectation taken with respect to the simplified belief-transition model. Then, the following holds:*

$$\sup_{l \in \mathbb{R}} |P(R_{k:T} \leq l | b_k, a_k, \pi) - P_s(R_{k:T} \leq l | b_k, a_k, \pi)| \leq \sum_{t=k}^{T-1} \mathbb{E}^s [\Delta^s(b_t, a_t) | b_k, a_k], \quad (28)$$

where Δ^s is the TV distance that is defined by

$$\Delta^s(b_{t-1}, a_{t-1}) \triangleq \int_{b_t \in B} |P(b_t | b_{t-1}, a_{t-1}) - P_s(b_t | b_{t-1}, a_{t-1})| db_t. \quad (29)$$

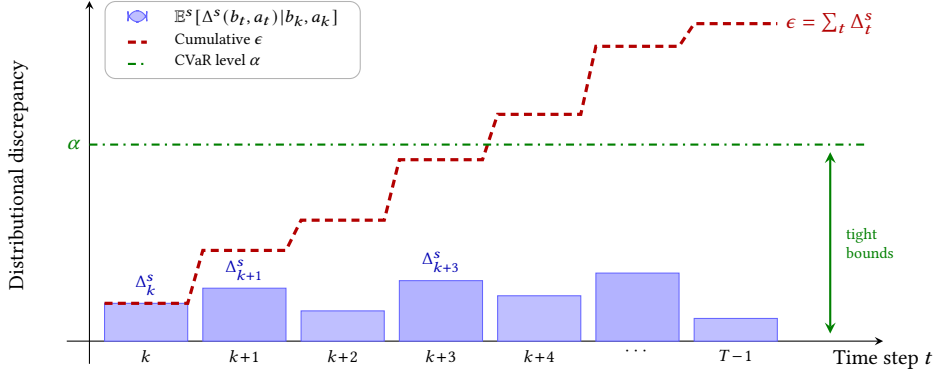


Fig. 5. Accumulation of distributional discrepancy over the planning horizon. Each bar represents the expected one-step TV distance $\mathbb{E}^s[\Delta^s(b_t, a_t) | b_k, a_k]$ at time t . The cumulative sum $\epsilon = \sum_{t=k}^{T-1} \Delta_t^s$ (dashed) governs the bound quality: when $\epsilon < \alpha$ (below the dash-dotted line), the CVaR bounds from Theorem 6.2 remain informative; when $\epsilon \geq \alpha$, the bounds reduce to trivial extrema.

PROOF. The proof is available in Appendix C.1. \square

The expression $\mathbb{E}^s[\Delta^s(b_t, a_t) | b_k, a_k]$ quantifies the expected one-step distributional discrepancy at time t between the transition dynamics of the simplified and original belief-MDPs, conditioned on the planning process being initiated at time k . Summing this quantity over the horizon accumulates the total distributional discrepancy, leading to the bound in (28), which in turn bounds the cumulative distribution function of the return across the horizon. This accumulation mechanism is illustrated in Figure 5.

By leveraging Theorem 5.1 and combining it with the supremum norm bounds for the simplified and original return CDFs in (28), we derive the following bounds on the value functions.

THEOREM 6.2. Let $\delta_{d_{min}} \in [0, 1]$, $\delta_{d_{max}} \in [0, 1]$ and denote

$$\epsilon \triangleq \epsilon(b_k, a_k) \triangleq \min\left(\sum_{i=k}^{T-1} \mathbb{E}^s[\Delta^s(b_i, a_i) | b_k, a_k, \pi], 1\right), \quad (30)$$

- (1) **Upper Bound:** assume that $P(R_{k:T} \leq d_{max}) > 1 - \delta_{d_{max}}$ and $P_s(R_{k:T} \leq d_{max}) > 1 - \delta_{d_{max}}$, then
 - (a) If $\epsilon < \alpha$, then $U_s \triangleq (1 - \frac{\epsilon}{\alpha})Q_{M_s}^\pi(b_k, a_k, \alpha - \epsilon) + \frac{\epsilon}{\alpha}d_{max}$
 - (b) If $\epsilon \geq \alpha$ then $U_s \triangleq d_{max}$
- (2) **Lower Bound:** assume that $P(R_{k:T} \geq d_{min}) > 1 - \delta_{d_{min}}$ and $P_s(R_{k:T} \geq d_{min}) > 1 - \delta_{d_{min}}$, then
 - (a) If $\epsilon + \alpha < 1$ then $L_s \triangleq (1 + \frac{\epsilon}{\alpha})Q_{M_s}^\pi(b_k, a_k, \alpha + \epsilon) - \frac{\epsilon}{\alpha}Q_{M_s}^\pi(b_k, a_k, \epsilon)$
 - (b) If $\epsilon + \alpha \geq 1$ then $L_s \triangleq \frac{1}{\alpha}[-(\alpha + \epsilon - 1)d_{min} + Q_{M_s}^\pi(b_k, a_k) - \epsilon Q_{M_s}^\pi(b_k, a_k, \epsilon)]$

Then $P(L_s \leq Q_M^\pi(b_k, a_k, \alpha)) > 1 - \delta_{d_{min}}$ and $P(Q_M^\pi(b_k, a_k, \alpha) \leq U_s) > 1 - \delta_{d_{max}}$.

PROOF. The proof is available in Appendix C.3. \square

The bounds established in Theorem 6.2 provide upper and lower bounds on the original value function in terms of the simplified value function, evaluated at an adjusted confidence level that accounts for the distributional discrepancy ϵ between the simplified and original belief transition models.

6.2 Bounds for Observation Model Simplification

Simplification of the observation model is a special case of simplification of the belief transition model. Despite that, computation of the belief transition model is still an open question in the field, and therefore the bounds from Theorem 6.2 should be adjusted for this specific simplification setting.

Let q_z denote the simplified observation model associated with the POMDP M_s , and let p_z denote the original observation model associated with the POMDP M . The bounds for observation model simplification are exhibited in Theorem 6.3.

THEOREM 6.3. *In the case where the simplified and original observation models are denoted by q_z and p_z respectively, it holds that*

$$\sup_{l \in \mathbb{R}} |P(R_{k:T} \leq l | b_k, a_k, \pi) - P_s(R_{k:T} \leq l | b_k, a_k, \pi)| \leq \sum_{t=k}^{T-1} \mathbb{E}^s [\Delta^s(x_{t+1}) | b_k, a_k], \quad (31)$$

where Δ^s is the TV distance that is defined by

$$\Delta^s(x_t) \triangleq \int_{z_t \in Z} |p_z(z_t | x_t) - q_z(z_t | x_t)| dz_t. \quad (32)$$

PROOF. The proof is available in Appendix C.2. □

Theorem 6.3 establishes a state-dependent upper bound on the sup-norm difference between the CDFs of the return. This bound is amenable to practical computation. The state x_{t+1} appearing in (31) can be sampled from the distribution $P(\cdot | x_t, \pi_t) \prod_{i=k+1}^{t-1} P(x_{i+1} | x_i, \pi_i) P(x_k | b_k)$, where π_i denotes the action selected by policy π at time i .

By leveraging Theorem 6.2 with Theorem 6.3, we obtain Corollary 6.4, which provides computable CVaR bounds based on state-dependent total variation distance.

COROLLARY 6.4. *The bound from Theorem 6.2 holds for $\epsilon(b_k, a_k) = \sum_{t=k}^{T-1} \mathbb{E}^s [\Delta^s(x_{t+1}) | b_k, a_k]$.*

PROOF. The proof is available in Appendix C.4. □

7 Online Bound Estimation

In this section, we derive practical estimators corresponding to the theoretical bounds presented in Section 6, and describe how these bounds can be efficiently computed within the context of online policy evaluation and open-loop planning. All estimators are constructed from samples generated by particle-based belief estimators drawn under the simplified belief-transition distribution. Specifically, we develop estimators for the action-value function, the distributional discrepancy ϵ appearing in Corollary 6.4, and the minimum and maximum values of the return, thereby enabling computation of the complete bound stated in Corollary 6.4. Moreover, we provide performance guarantees for these estimators, establishing their reliability when computed from a finite number of samples.

7.1 Action-Value Function Estimator

The action-value function is defined as the CVaR of the return $R_{k:T} \triangleq \sum_{t=k}^T c(b_t, a_t)$, and can be estimated in a straightforward manner by generating sample trajectories of the return and computing the empirical CVaR from these samples.

To generate return samples, it is necessary to simulate belief trajectories from time k to time T . This is achieved using a particle-based belief estimator, where the belief is represented by a weighted set of $N_p \in \mathbb{N}$ particles. Given a particle belief \bar{b}_k , provided by the user to represent the agent's belief at time k , the agent generates N_b simulated

particle-belief trajectories $\{\bar{b}_t^i\}$, where $i \in \{1, \dots, N_b\}$ indexes the trajectory and $t \in \{k, \dots, T\}$ denotes the time step. For each simulated trajectory, a return sample is computed as $\bar{R}_{k:T}^i = \sum_{t=k}^T c(\bar{b}_t^i, \pi(\bar{b}_t^i))$, resulting in a collection of return samples $\{\bar{R}_{k:T}^i\}_{i=1}^{N_b}$. Let $\bar{b}_t^i \triangleq \{(x_t^{i,j}, w_t^{i,j})\}_{j=1}^{N_p}$ denote the i -th simulated particle belief at time t , where j indexes the particles. Define the normalized weights by $\tilde{w}_t^{i,j} \triangleq \frac{w_t^{i,j}}{\sum_{j=1}^{N_p} w_t^{i,j}}$. Assuming the cost function is state-dependent, the cost associated with belief \bar{b}_t^i and action a is given by $c(\bar{b}_t^i, a) = \sum_{j=1}^{N_p} \tilde{w}_t^{i,j} c(x_t^{i,j}, a)$. By estimating CVaR according to (13), we get the action-value function estimator

$$\hat{Q}_{M_p}^\pi(\bar{b}_k, a, \alpha) \triangleq \hat{C}(\{R^i\}_{i=1}^{N_b}) = R^{(N_b)} - \frac{1}{\alpha} \sum_{i=1}^{N_b} (R^{(i)} - R^{(i-1)}) \left(\frac{i}{N_b} - (1 - \alpha) \right)^+. \quad (33)$$

Detailed pseudo-code for the estimation of the action-value function is presented in Algorithm 1.

7.2 Online CDF Bound Estimation

The bound on the difference between return simplified and original CDFs, established in Theorem 6.3 and denoted by ϵ in Corollary 6.4, plays a central role in bounding the discrepancy between the simplified and original action-value functions. Notably, it is the only term in the bound that explicitly captures the impact of the difference between the simplified and original observation models. A challenge arises from the fact that the quantity ϵ cannot be directly estimated during planning, as its computation requires access to the full observation model p_z , which is typically too expensive to evaluate online. For the purpose of online computation of the bound, we adopt the methodology proposed in Lev-Yehudi, Barenboim, and Indelman 2024, which enables evaluation without real-time access to the original observation model. This is achieved by decoupling the offline sampling phase—conducted using the original observation model—from the online sampling phase, which relies solely on the simplified observation model. Specifically, the offline-online decoupling strategy and the state-level importance-sampling estimator in (34) were introduced by Lev-Yehudi, Barenboim, and Indelman 2024; the belief-level aggregation, horizon-level accumulation, and the probabilistic guarantees developed in the remainder of this section are novel contributions of the present work. This offline-online decoupling procedure is illustrated in Figure 6.

Let Q_0 be a distribution over the state space, and denote the TV-distance expectation given the previous state and action by m . (34) shows how the one-step distributional discrepancy bound m can be computed using importance sampling.

$$m(x_t, a) \triangleq \mathbb{E}_{x_{t+1} \sim P(\cdot | x_t, a)} [\Delta^s(x_{t+1}) | x_t, a] = \mathbb{E}_{x_{t+1} \sim Q_0} \left[\frac{P(x_{t+1} | x_t, a)}{Q_0(x_{t+1})} \Delta^s(x_{t+1}) | x_t, a \right]. \quad (34)$$

Define the belief-dependent one-step distributional discrepancy m , and the belief-dependent total distributional discrepancy bound of the CDFs difference at time t by ϵ_t .

$$m(b_t, a) \triangleq \mathbb{E}[m(x_t, a) | b_t, a], \quad (35)$$

$$\epsilon_t(b_t, a) \triangleq \sum_{\tau=t}^{T-1} \mathbb{E}[\Delta^s(x_{\tau+1}) | b_t, a] = \sum_{\tau=t}^{T-1} \mathbb{E}[m(b_\tau, a) | b_t, a]. \quad (36)$$

In practice, a set of states $\{x_n^\Delta\}_{n=1}^{N_\Delta} \stackrel{\text{i.i.d.}}{\sim} Q_0$ is drawn from a user-specified distribution Q_0 , and the TV-distance corresponding to each sampled state is computed offline. During online planning, the precomputed TV distance estimates are reweighted via importance sampling, thereby adapting the offline-computed distributional discrepancy to reflect the actual distributional discrepancy encountered by the agent during execution, as described in (37). By utilizing $\{x_n^\Delta\}$,

Algorithm 1 CVaR Value Function Estimation for Policy π **Global Parameters:** N_p, N_b, T, π **Input:** Particle belief \bar{b} , planning horizon T , policy π , action a , risk level α , number of belief trajectories N_b and number of belief particles N_p .**Output:** Estimated value $\hat{V}^\pi(\bar{b})$ or $\hat{Q}^\pi(\bar{b}, a)$

```

1: procedure GENPF( $\bar{b}, a$ )
2:   Sample  $x_0$  from  $\bar{b}$  with prob.  $w_i / \sum_i w_i$ 
3:    $z \leftarrow G(x_0, a)$ 
4:   for  $i = 1$  to  $N_p$  do
5:      $(x'_i, r_i) \leftarrow G(x_i, a)$ 
6:      $w'_i \leftarrow w_i \cdot Z(z \mid a, x'_i)$ 
7:   end for
8:    $\bar{b}' \leftarrow \{(x'_i, w'_i)\}_{i=1}^{N_p}$ 
9:    $\rho \leftarrow \frac{\sum_i w_i r_i}{\sum_i w_i}$ 
10:  return  $\bar{b}', \rho$ 
11: end procedure
12: procedure SAMPLENEXTBELIEFS(beliefs,  $\pi$ )
13:   NextBeliefs  $\leftarrow list()$ 
14:   for  $j = 1$  to  $N_b$  do
15:     NextBelief  $\leftarrow$  GENPF(beliefs[j],
16:        $\pi$ (beliefs[j]))
17:     append NextBelief to NextBeliefs
18:   end for
19:   return NextBeliefs
20: procedure GENBELIEFTRAJECTORIES( $\bar{b}, \pi, T$ )
21:   trajectories  $\leftarrow list()$ 
22:   for  $i = 1$  to  $N_b$  do
23:     append  $\bar{b}$  to trajectories
24:   end for
25:   for  $t = 0$  to  $T - 1$  do
26:     NextBeliefs  $\leftarrow$ 
27:     SampleNextBeliefs(trajectories[t],  $\pi$ )
28:     append NextBeliefs to trajectories
29:   end for
30:   return trajectories

```

```

1: procedure GENERATERETURNSAMPLE( $\bar{b}, a, \pi$ )
2:   trajectories  $\leftarrow$  GenBeliefTrajectories( $\bar{b}, \pi, T$ )
3:   ReturnSample  $\leftarrow list()$ 
4:   for  $i = 1$  to  $N_b$  do
5:     Return  $\leftarrow$  c(trajectories[0][i], a)
6:     for  $t = 1$  to  $T$  do
7:       Return += c(trajectories[t][i],
8:          $\pi$ (trajectories[t][i]))
9:     end for
10:    append Return to ReturnSample
11:  return ReturnSample
12: end procedure
13: procedure CVARESTIMATE(samp,  $\alpha$ )
14:   Sort samp in ascending order as  $z_1, \dots, z_n$  with
15:    $z_0 = 0$ 
16:   return  $z_n - \frac{1}{\alpha} \sum_{i=0}^{n-1} (z_{i+1} - z_i) (\frac{i}{n} - (1 - \alpha))^+$ 
17: end procedure
18: procedure ESTIMATEV $^\pi(\bar{b}, \alpha)$ 
19:   return ESTIMATEQ( $\bar{b}, \pi(\bar{b}), \alpha$ )
20: end procedure
21: procedure ESTIMATEQ( $\bar{b}, a, \alpha$ )
22:   samp  $\leftarrow$  GenerateReturnSample( $\bar{b}, a, \pi$ )
23:   return CVARESTIMATE(samp,  $\alpha$ )
24: end procedure

```

(34) and (35) can be estimated as follows

$$\hat{m}(x_t, a) = \frac{1}{N^\Delta} \sum_{n=1}^{N^\Delta} \frac{P(x_n^\Delta \mid x_t, a)}{Q_0(x_n^\Delta)} \Delta^s(x_n^\Delta), \quad (37)$$

$$\hat{m}(\bar{b}_t, a) = \sum_{i=1}^{N_p} \hat{m}(x_t^i, a) \tilde{w}_t^i, \quad (38)$$

for $\bar{b}_t \triangleq \{(x_t^i, \tilde{w}_t^i)\}$ where \tilde{w}_t^i are the normalized weights. Using the particle-belief trajectories $\{\bar{b}_\tau^i\}_{i=1}^{N_b}$ introduced in Section 7.1, the TV-distance at time $\tau + 1$ is estimated by using $\{\bar{b}_\tau^i\}_{i=1}^{N_b}$ as samples from the conditional distribution of

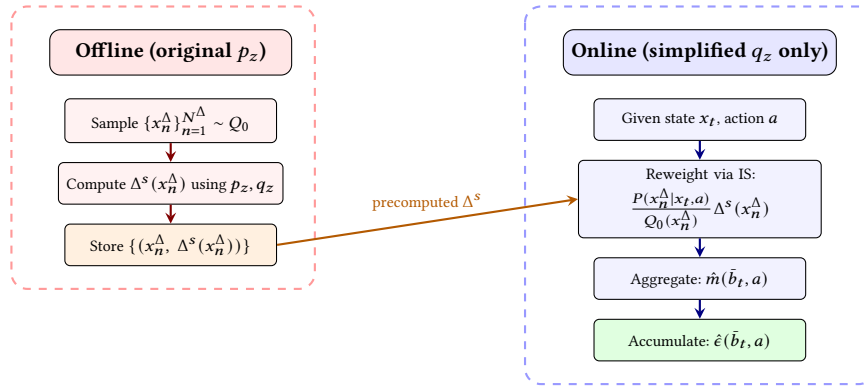


Fig. 6. Offline–online decoupling for distributional discrepancy estimation. In the offline phase, states are sampled from a proposal distribution Q_0 and the TV distances Δ^s are computed using the original observation model p_z . During online planning, the precomputed Δ^s values are reweighted via importance sampling using only the state-transition model, eliminating the need to evaluate p_z in real time.

\bar{b}_τ given \bar{b}_t , as described below.

$$\hat{\mathbb{E}}[m(b_\tau, a)|\bar{b}_t, a] = \frac{1}{N_b} \sum_{i=1}^{N_b} \hat{m}(\bar{b}_\tau^i, \pi(\bar{b}_\tau^i)). \quad (39)$$

The estimate of ϵ is then computed directly by

$$\hat{\epsilon}(\bar{b}_t, a) = \sum_{\tau=t}^{T-1} \hat{\mathbb{E}}[m(\bar{b}_\tau, \pi_\tau)|\bar{b}_t, a]. \quad (40)$$

Theorem 7.1 establishes performance guarantees for the distributional discrepancy estimator defined in (40), and demonstrates that it converges exponentially fast to the true distributional discrepancy as the number of sampled beliefs N_b increases.

THEOREM 7.1. *Let $\eta > 0, \delta \in (0, 1)$. If $\hat{\Delta}$ is unbiased, then*

$$P(|\hat{\epsilon}_t(\bar{b}_t, a) - \epsilon_t(\bar{b}_t, a)| \geq \eta) \leq 2 \exp\left(-\frac{2\eta^2 N_b}{D^2(T-k)^2(R_{\max} - R_{\min})^2}\right) \quad (41)$$

for $D = \max_{i \in \{k+1, \dots, T-1\}} D_i$ where $D_i = \sup_{x_{i+1}} P(x_{i+1}|x_i, a_i)/Q_0(x_{i+1})$.

PROOF. The proof is available in Appendix C.5. □

7.3 Online Return Bound Estimation

The bound in Theorem 6.2 requires knowledge of the upper and lower bounds on the return under both the original and simplified distributions. Formally, we need estimators \hat{d}_{\min} and \hat{d}_{\max} for d_{\min} and d_{\max} in Theorem 6.2. A simple choice is

$$\hat{d}_{\min} = (T - k + 1)R_{\min}, \quad \hat{d}_{\max} = (T - k + 1)R_{\max}, \quad (42)$$

which, however, ignores the dependence of the return on the agent’s belief b_k and policy π . For example, if the belief indicates that the agent is far from any obstacle and the planning horizon is too short for a collision to occur, taking the maximal possible return obscures this contextual information and results in a looser bound than necessary.

To obtain tighter estimates, we define

$$\hat{d}_{\max}^{\pi}(b_k) = \max_{i \in \{1, \dots, N_b\}} R^i, \quad \hat{d}_{\min}^{\pi}(b_k) = \min_{i \in \{1, \dots, N_b\}} R^i, \quad (43)$$

where $\{R^i\}_{i=1}^{N_b} \sim P_s(\cdot | b_k, \pi)$ are the return samples used to estimate the action–value function. Theorem 7.2 provides performance guarantees for these estimators.

THEOREM 7.2. *For the estimators $\hat{d}_{\max}^{\pi}(b_k) = \max_i R^i$ and $\hat{d}_{\min}^{\pi}(b_k) = \min_i R^i$, where $i \in \{1, \dots, N_b\}$, $R^1, \dots, R^{N_b} \sim P_s$, and for ϵ as defined in (30), the following bounds hold.*

$$P_s(R_{k:T} \geq \hat{d}_{\min}^{\pi}(b_k) | b_k, \pi) \geq \frac{N_b}{N_b + 1}, \quad P_s(R_{k:T} \leq \hat{d}_{\max}^{\pi}(b_k) | b_k, \pi) \geq \frac{N_b}{N_b + 1} \quad (44)$$

$$P(R_{k:T} \geq \hat{d}_{\min}^{\pi}(b_k) | b_k, \pi) \geq \frac{N_b}{N_b + 1} - \epsilon, \quad P(R_{k:T} \leq \hat{d}_{\max}^{\pi}(b_k) | b_k, \pi) \geq \frac{N_b}{N_b + 1} - \epsilon. \quad (45)$$

PROOF. The proof is available in Appendix C.6. \square

The bounds for both the simplified and the original returns are computed using return samples generated from the simplified belief–transition model. The uncertainty in the upper bound on the original return, induced by using samples drawn from the simplified return distribution, is quantified by ϵ , which represents the distributional discrepancy between the original and simplified returns.

7.4 Performance Guarantees

In this section we provide performance guarantees for the bounds exhibited in previous sections, making them reliable in practice.

7.4.1 Guarantees with Known Return Bounds. Theorem 7.3 establishes performance guarantees for the original action–value function in terms of the simplified action–value function, under the assumption that the simplification is applied to the belief–transition model. These bounds hold for a general ρ -POMDP, where the cost is belief-dependent.

THEOREM 7.3. *Let $\delta, \delta_{\min}, \delta_{\max} \in [0, 1]$, and let b_k denote the initial belief. Consider samples $R^1, \dots, R^{N_b} \sim P_s(\cdot | b_k, \pi)$ generated using the simplified belief–transition model. Define*

$$\epsilon \triangleq \epsilon(b_k, a_k) \triangleq \min \left(\sum_{i=k}^{T-1} \mathbb{E}^s [\Delta^s(b_i, a_i) | b_k, a_k, \pi], 1 \right), \quad (46)$$

$$\eta = \sqrt{\ln(1/\delta)/(2N_b)}, \quad \epsilon' = \epsilon + \eta. \quad (47)$$

(1) **Upper Bound:** assume that $P(R_{k:T} \leq d_{\max}) > 1 - \delta_{\max}$ and $P_s(R_{k:T} \leq d_{\max}) > 1 - \delta_{\max}$, then

(a) If $\epsilon' < \alpha$, then $U_s \triangleq (1 - \frac{\epsilon'}{\alpha}) \hat{Q}_{M_s}^{\pi}(b_k, a_k, \alpha - \epsilon') + \frac{\epsilon'}{\alpha} d_{\max}$

(b) If $\epsilon' \geq \alpha$ then $U_s \triangleq d_{\max}$

(2) **Lower Bound:** assume that $P(R_{k:T} \geq d_{\min}) > 1 - \delta_{\min}$ and $P_s(R_{k:T} \geq d_{\min}) > 1 - \delta_{\min}$, then

(a) If $\epsilon' + \alpha < 1$ then $L_s \triangleq (1 + \frac{\epsilon'}{\alpha}) \hat{Q}_{M_s}^{\pi}(b_k, a_k, \alpha + \epsilon') - \frac{\epsilon'}{\alpha} \hat{Q}_{M_s}^{\pi}(b_k, a_k, \epsilon')$

(b) If $\epsilon' + \alpha \geq 1$ then $L_s \triangleq \frac{1}{\alpha} [-(\alpha + \epsilon' - 1)d_{\min} + \hat{Q}_{M_s}^{\pi}(b_k, a_k) - \epsilon' \hat{Q}_{M_s}^{\pi}(b_k, a_k, \epsilon')]$

Then $P(L_s \leq Q_M^{\pi}(b_k, a_k, \alpha)) > (1 - \delta)(1 - \delta_{\min})$ and $P(Q_M^{\pi}(b_k, a_k, \alpha) \leq U_s) > (1 - \delta)(1 - \delta_{\max})$.

PROOF. The proof is available in Appendix C.7. \square

Estimation of the belief-transition model remains an open problem in the literature; consequently, the distributional discrepancy ϵ in Theorem 7.3, when defined in terms of the belief-transition model, is currently intractable to estimate. In the special case where only the observation model is simplified, the one-step distributional discrepancy Δ^s is defined with respect to the observation model rather than the belief-transition model (see Section 6.2). In this case, Theorem 7.3 holds when Δ^s is defined using the original and simplified observation models, as characterized in Theorem 6.4, thereby rendering the estimation of ϵ tractable.

To attain standard bounds, one can set trivial bounds to the return $d_{\min} = (T - k + 1)R_{\min}$ and $d_{\max} = (T - k + 1)R_{\max}$. These bounds would produce $\delta_{d_{\min}} = \delta_{d_{\max}} = 0$ and guarantees of $1 - \delta$ for the bounds in Theorem 7.3.

7.4.2 Guarantees with Estimated Return Bounds. In practice, it is preferable to estimate the return bounds d_{\min} and d_{\max} with respect to the current belief and policy in order to obtain tighter bounds (see Section 7.3). Theorem 7.4 establishes guarantees for the resulting simplified bounds, in which d_{\min} and d_{\max} are replaced by their estimators.

THEOREM 7.4. *Let b_k be an initial belief and let $R^1, \dots, R^{N_b} \sim P_s(\cdot | b_k, \pi)$ be a sample that utilizes the simplified belief-transition model. Denote*

$$\epsilon \triangleq \epsilon(b_k, a_k) \triangleq \min\left(\sum_{i=k}^{T-1} \mathbb{E}^s[\Delta^s(b_i, a_i) | b_k, a_k, \pi], 1\right) \quad (48)$$

$$\eta = \sqrt{\ln(1/\delta)/(2N_b)}, \quad \epsilon' = \epsilon + \eta \quad (49)$$

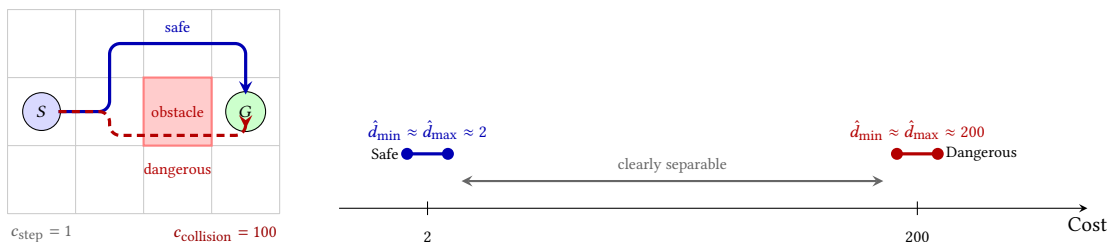
$$\hat{d}_{\max}^\pi(b_k) = \max_{i \in \{1, \dots, N_b\}} R^i, \quad \hat{d}_{\min}^\pi(b_k) = \min_{i \in \{1, \dots, N_b\}} R^i, \quad (50)$$

- (1) **Upper Bound:** Under the following conditions, it holds that $P(Q_M^\pi(\bar{b}_k, a_k, \alpha) \leq U_s | b_k, \pi) \geq (1 - \delta) \left(\frac{N_b}{N_b + 1} - \epsilon \right)$
- (a) If $\epsilon' < \alpha$, then $U_s \triangleq (1 - \frac{\epsilon'}{\alpha}) \hat{Q}_{M_s}^\pi(b_k, a_k, \alpha - \epsilon') + \frac{\epsilon'}{\alpha} \hat{d}_{\max}^\pi(b_k)$
 - (b) If $\epsilon' \geq \alpha$ then $U_s \triangleq \hat{d}_{\max}^\pi(b_k)$
- (2) **Lower Bound:** Under the following conditions, it holds that $P(Q_M^\pi(\bar{b}_k, a_k, \alpha) \geq L_s | b_k, \pi) \geq (1 - \delta) \left(\frac{N_b}{N_b + 1} - \epsilon \right)$
- (a) If $\epsilon' + \alpha < 1$ then $L_s \triangleq (1 + \frac{\epsilon'}{\alpha}) \hat{Q}_{M_s}^\pi(b_k, a_k, \alpha + \epsilon') - \frac{\epsilon'}{\alpha} \hat{Q}_{M_s}^\pi(b_k, a_k, \epsilon')$
 - (b) If $\epsilon' + \alpha \geq 1$ then $L_s \triangleq \frac{1}{\alpha} [-(\alpha + \epsilon' - 1) \hat{d}_{\min}^\pi(b_k) + \hat{Q}_{M_s}^\pi(b_k, a_k) - \epsilon' \hat{Q}_{M_s}^\pi(b_k, a_k, \epsilon')]$

PROOF. The proof is available in Appendix C.8. □

Recall that the theoretical bounds derived in Section 6 impose constraints on the relationship between the distributional discrepancy ϵ and the CVaR confidence level α . When these conditions are violated, the resulting bounds on the action-value function become trivial. Employing estimators for the minimum and maximum return enables the agent to act according to the guarantees in Theorem 7.4, even when these constraints are not satisfied.

As an example (illustrated in Figure 7), consider $\epsilon = \alpha = 0.1$, $N_b = 1000$, and $\delta = 0.01$, with planning horizon $T = 2$. The agent must choose between a dangerous path that passes through an obstacle and a safe path that avoids it. The agent incurs a cost of 1 for remaining in place and a cost of 100 upon colliding with an obstacle. In this setting, even under partial observability, the probability of encountering an obstacle along the safe path, as well as the probability of not encountering an obstacle along the dangerous path, may be small. Consequently, the estimators satisfy $\hat{d}_{\max}^\pi(b_0) = \hat{d}_{\min}^\pi(b_0) \approx 1 \times 2$ for the safe path and $\hat{d}_{\max}^\pi(b_0) = \hat{d}_{\min}^\pi(b_0) \approx 100 \times 2$ for the dangerous path. This allows the agent to distinguish between the two paths, in the sense that the CVaR of the dangerous path is strictly larger than that of the safe path.



(a) An agent at position S must choose between a safe path (blue, cost 1 per step) and a dangerous path (red, passing through an obstacle with collision cost 100). The goal's position is G .

(b) When $\epsilon' \geq \alpha$, the CVaR bounds collapse to $[\hat{d}_{\min}, \hat{d}_{\max}]$. The return estimators for the safe path (≈ 2) and dangerous path (≈ 200) remain well-separated.

Fig. 7. Illustration of bound-based action selection when $\epsilon' \geq \alpha$. (a) The agent chooses between a safe path (cost $\approx 1 \times 2 = 2$) and a dangerous path through an obstacle (cost $\approx 100 \times 2 = 200$). (b) Although the CVaR bounds collapse to $[\hat{d}_{\min}, \hat{d}_{\max}]$, the return estimators remain well-separated, enabling the agent to distinguish between the two paths.

When the constraint $\epsilon' < \alpha$ required for the original bounds is violated—as in this example where $\epsilon = \alpha = 0.1$ and hence $\epsilon' \geq \epsilon \geq \alpha$ —the bounds in Theorem 7.4 reduce to \hat{d}_{\max} and \hat{d}_{\min} , causing the upper and lower bounds to coincide. Nevertheless, decision making remains possible: the estimators for the safe and dangerous paths differ substantially (≈ 2 versus ≈ 200), enabling the agent to distinguish between them.

By Corollary 6.4, the guarantees stated in Theorem 7.4 and Theorem 7.3 also apply to the specific setting in which the observation model is simplified, with the distributional discrepancy ϵ between the original and simplified observation models defined as in Corollary 6.4. As shown in Section 7, this setting can be resolved within the framework of online planning.

8 Limitations

The bounds in Theorem 6.2 depend on the accumulation of one-step distributional discrepancies over the planning horizon, which may limit their effectiveness for long-horizon problems.

Importantly, this accumulation does not necessarily grow linearly with the horizon and is highly problem dependent. For example, in a Light-Dark environment, the agent receives observations only in light regions and relies exclusively on the state-transition model in dark regions. As a result, no distributional discrepancy is accumulated in dark regions, since the observation model is not invoked. Consequently, the effective distributional discrepancy can grow sublinearly with the horizon. This behavior is examined empirically in the experiments section, where we also consider a more challenging variant of the Light-Dark environment in which distributional discrepancy accumulates even in dark regions.

Moreover, even when the distributional discrepancy becomes large relative to α , the agent can still act. In this case, the value function bounds collapse to their extrema; specifically, the upper value function bound reduces to \hat{d}_{\max} (Theorem 7.4), which is expected to be low in safe regions and high in dangerous ones. Analogous considerations hold for the lower bound. Consequently, decision making relies on minimum and maximum return samples conditioned

on the path and policy, while the simplified observation model continues to provide computational acceleration, as it remains necessary for sampling return realizations.

Finally, the proposed simplification framework yields computational gains only when sampling from the state-transition model is cheaper than sampling from the observation model. The bounds in Theorem 6.2 require samples from both the simplified observation model and the state-transition model to compensate for the absence of the original observation model. Consequently, if the state-transition model is computationally more expensive than the original observation model, the simplification approach would increase rather than decrease planning time. This limitation is shared by other observation model simplification frameworks Lev-Yehudi, Barenboim, and Indelman 2024.

9 Experiments

In this section, we evaluate our derived bounds across several standard benchmark environments. We demonstrate the efficacy of our bounds by examining their performance on selected action sequences, illustrating their capacity to distinguish between safe and unsafe trajectories while achieving computational acceleration relative to the baseline model. We subsequently demonstrate the integration of these bounds into open-loop planning frameworks. All simulations were conducted using the POMDPPlanners package Pariante and Indelman 2026. Detailed simulation configurations are provided in Appendix E, and hardware specifications in Appendix G.

9.1 Theoretical CVaR Bounds

Specifically, we compare a truncated Gaussian Mixture Model (GMM) and its corresponding truncated Normal approximation for CVaR estimation under bounded support. Such a setting arises, for example, in POMDP planning, where a computationally expensive model used by the agent during online planning is replaced with a more tractable surrogate model, thereby improving the agent’s decision-making speed Lev-Yehudi, Barenboim, and Indelman 2024. In these settings, the agent’s decisions may rely on bounds for the original value function that are derived from the tractable surrogate model Barenboim and Indelman 2022.

The GMM consists of five components with means $\mu_1 = 0.2$, $\mu_2 = -0.2$, $\mu_3 = -0.5$, $\mu_4 = 0.5$, $\mu_5 = 0.0$, variances $\sigma_1^2 = 0.5$, $\sigma_2^2 = 0.2$, $\sigma_3^2 = 0.1$, $\sigma_4^2 = 0.1$, $\sigma_5^2 = 0.3$, and weights $w_1 = 0.3$, $w_2 = 0.2$, $w_3 = 0.05$, $w_4 = 0.05$, $w_5 = 0.4$. The Normal approximation matches the GMM’s mean and variance but cannot reproduce its multi-modal structure or outlier effects. All samples are truncated to the interval $[-1, 1]$, which reshapes the tails and slightly distorts boundary components. We compute CVaR at the 20% quantile for sample sizes ranging from 100 to 10,000, with 100 independent repetitions per setting to ensure statistical reliability. The distributional discrepancy (ϵ in Theorem 5.7) between the truncated GMM and the truncated Normal distribution is assessed via simulation, by estimating their respective cumulative distribution functions over a common set of bins and computing the maximum difference across all bins. This setup enables a direct assessment of the trade-off between computational efficiency and statistical accuracy when approximating a complex truncated mixture by a single truncated Normal distribution.

Figure 8c presents the sampling time comparison between the truncated GMM and the truncated Normal distribution, with an observed average time ratio of approximately 3.7 in favor of the Normal distribution. Figure 8d reports a total computational speedup of approximately 3.1 when comparing the process of sampling from the truncated GMM and estimating its CVaR to that of sampling from the truncated Normal and computing both upper and lower bounds as given in Theorem 5.7. Figure 8a illustrates the convergence behavior of the CVaR bounds as a function of the number of samples, comparing estimates obtained from the truncated GMM with bounds derived from the truncated Normal surrogate. It is important to note that these bounds are obtained without requiring full knowledge of the underlying

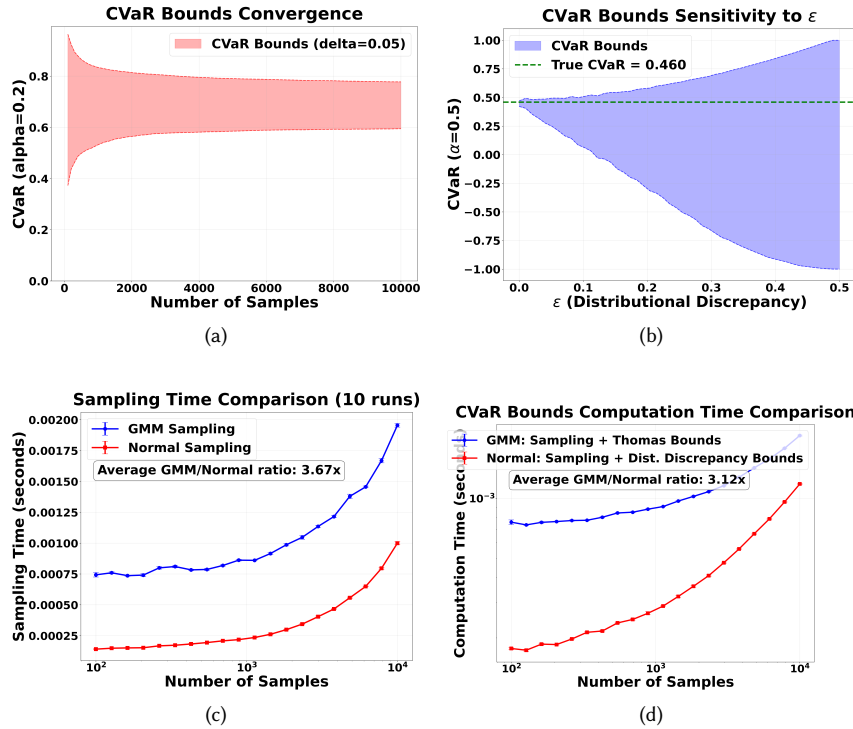


Fig. 8. Figure 8a shows the bounds established in Theorem 5.7, demonstrating how a simple truncated Normal distribution can be employed to bound the CVaR of a truncated GMM. Figure 8b illustrates the sensitivity of the CVaR bounds to the distributional discrepancy ϵ , showing how the bound interval widens as ϵ increases, while the true CVaR remains contained within the bounds. When ϵ exceeds the risk level α , the bounds become trivial, spanning the entire support; this is expected, as a large distributional discrepancy implies that the surrogate random variable Y provides negligible information about the target random variable X . Figure 8c presents a comparison of the sampling times for each distribution, while Figure 8d reports the total computation time required to sample from the truncated GMM and estimate its CVaR, in contrast to sampling from the truncated Normal surrogate and computing the associated concentration bounds. Figures 8a, 8c, and 8d were configured with confidence level $\alpha = 0.2$ and probability of error $\delta = 0.05$. Figure 8b uses $\alpha = 0.5$. Figures 8c and 8d display 95% confidence intervals around the empirical means.

GMM distribution. Instead, they rely solely on the discrepancy between the corresponding CDFs. Figure 8b depicts the sensitivity of the CVaR bounds to the distributional discrepancy ϵ . In this experiment, the base distribution F is a truncated Normal on $[-1, 1]$ with mean 0 and standard deviation 1. For each value of $\epsilon \in [0, 0.5]$, a perturbed distribution G is constructed such that its CDF satisfies $G(x) = \min(F(x) + \epsilon, 1)$, yielding a Kolmogorov–Smirnov distance of exactly ϵ between F and G by construction. Samples from G are obtained via inverse transform sampling. The resulting bounds grow monotonically with ϵ while consistently enclosing the true CVaR of F . When ϵ exceeds the risk level α , the bounds become trivial, spanning the full support; this is expected, since a large distributional discrepancy implies that Y provides negligible information about X .

We evaluated the concentration bounds established by Thomas and Learned-Miller 2019 alongside our proposed bounds from Theorem 5.5 on a set of probability distributions: Beta(2, 2), Beta(0.5, 0.5), Beta(2, 5), Beta(5, 2), Beta(10, 2), Beta(2, 10), and the Laplace(0, 1) distribution. These distributions were selected to match those used in the original study

by Thomas and Learned-Miller 2019, enabling a direct comparison under identical conditions. For each distribution, our bounds precisely coincide with those reported by Thomas and Learned-Miller 2019, resulting in complete overlap between the two sets of bounds. The graphs exhibiting these results are available in Appendix B (Figure 16).

9.2 POMDP Environments

We evaluate our approach on three POMDP domains: 2D Light-Dark Navigation, Laser Tag, and Push. Each environment contains dangerous areas where the likelihood of incurring high penalties is elevated, requiring the agent to balance risk-aware decision-making with task completion. In the 2D Light-Dark POMDP, an agent must navigate from a start position to a goal region while avoiding these dangerous areas. The observation noise is position-dependent, with lower uncertainty near designated beacon locations, requiring the agent to balance information gathering with goal-directed movement. In Laser Tag POMDP, the agent must locate and tag an opponent in a partially observable environment using noisy range-bearing measurements from multiple sensors, resulting in an 8-dimensional observation space, while navigating around dangerous regions. The Push POMDP involves manipulating an object to a target location while managing partial observability about the object’s position through noisy 2-dimensional observations and avoiding dangerous areas. For each domain, we construct two environment variants: an original environment with a complex observation model represented by Gaussian Mixture Models (GMMs) capturing multi-modal observation distributions, and a simplified environment where this complex distribution is approximated using a single Gaussian distribution. This approximation introduces a controlled model mismatch, allowing us to evaluate the robustness of planning algorithms when the true observation dynamics differ from the assumed model. The GMM-based observation models enable realistic representation of sensor fusion, occlusions, and multi-hypothesis tracking, while the Gaussian approximation provides computational tractability at the cost of distributional fidelity. Full environment specifications are provided in Appendix D.

9.3 Online Distributional Discrepancy Estimation

To compute the distributional discrepancy ϵ appearing in Corollary 6.4, we define Q_0 as the uniform distribution over the axis-aligned square whose lower-left corner is x_{start} and upper-right corner is x_{goal} . Samples x_n^Δ are drawn from the mixture distribution $(p_Z + q_Z)/2$; that is, with probability 0.5, a sample is drawn from the original GMM observation model, and with probability 0.5, from the simplified observation model. The estimator $\hat{\Delta}^s(x_n^\Delta)$ is then defined as

$$\hat{\Delta}^s(x_n^\Delta) = \sum_{j=1}^{N_z} 2 \cdot \frac{\left| p_z(z_j^n | x_n^\Delta) - q_z(z_j^n | x_n^\Delta) \right|}{p_z(z_j^n | x_n^\Delta) + q_z(z_j^n | x_n^\Delta)}, \quad (51)$$

and is evaluated over $N^\Delta = 100$ presampled states. Here, $N_z = 2000$ denotes the number of sampled observations used in the estimation procedure. Given equation (51), the belief-dependent one-step distributional discrepancy $\hat{m}(\bar{b}_t, a)$ can be estimated accordingly. Since the state-transition model in (37) assigns exponentially small probability to states that are far from the current state, we employ a K-Nearest Neighbors (KNN) approach with $K = 10$ to select a subset of the samples $\{x_n^\Delta\}$ that lie in the vicinity of a given state x . The estimation is then performed over this localized subset, rather than the entire collection $\{x_n^\Delta\}$.

9.4 Empirical Static CVaR Bound Evaluation: Open-Loop Policies

To evaluate the bounds we define for each environment two action-sequences - one that dictates a safe path and the other that dictates a dangerous path. Figure 9 shows that bounds based on the simplified observation models distinguish between the two action sequences and would eliminate the dangerous path under action elimination. The estimated distributional discrepancies are $\epsilon = 0.38$ and $\epsilon = 0.36$ for the dangerous and safe paths in Light-Dark, $\epsilon = 0.52$ and $\epsilon = 0.53$ in Laser Tag, and $\epsilon = 0.24$ and $\epsilon = 0.20$ in Push. Despite high distributional discrepancies across paths within each environment, the bounds successfully discriminate between the two action sequences. Notably, in the Laser Tag environment, the estimated ϵ exceeds 0.5, which is the value of the risk level α ; nevertheless, the bounds remain sufficiently tight to separate the safe and dangerous action sequences.

Comparing the bounds computation time using the original observation models using the bounds of Thomas and Learned-Miller 2019 to our bounds that use the simplified observation models, we gain approximately 20.89 \times acceleration in Light-Dark POMDP, 8.87 \times in Laser Tag POMDP, and 7.62 \times in Push POMDP. Figure 10 illustrates how the acceleration remains solid when the number of return samples and horizon changes.

Figure 11 presents the evolution of the CVaR bounds as a function of the planning horizon for the same safe and dangerous action sequences depicted in Figure 9, where each action sequence is decomposed into sub-sequences of increasing horizon length. In the Light-Dark environment, the bounds are separated from the earliest horizon, since the agent’s start state is close to the dangerous area and the dangerous path immediately traverses the high-cost region. In Laser Tag and Push, the bounds of both paths are similar at early horizons, before the dangerous path enters the hazardous region, confirming that the bound separation is driven by the actual risk difference rather than by an artifact of the bounding mechanism. In Laser Tag, the separation is most pronounced: both paths have comparable bounds up to horizon 4, after which the dangerous path’s bounds increase sharply as it enters the dangerous area, while the safe path remains at low values throughout. In Push, the two paths overlap closely up to horizon 4, and the bounds diverge around horizon 6 when the dangerous path approaches the hazardous region. These patterns are consistent across both $\alpha = 0.5$ and $\alpha = 0.1$, indicating that the bounds remain discriminative under a more risk-averse setting. The bottom row of Figure 11 further examines the sensitivity of the bounds to the risk level α at a fixed horizon. As α decreases, the CVaR focuses on worse-case outcomes, causing both the bound values and the bound intervals to increase; nevertheless, the bounds maintain a clear separation between the safe and dangerous paths across the full range of α .

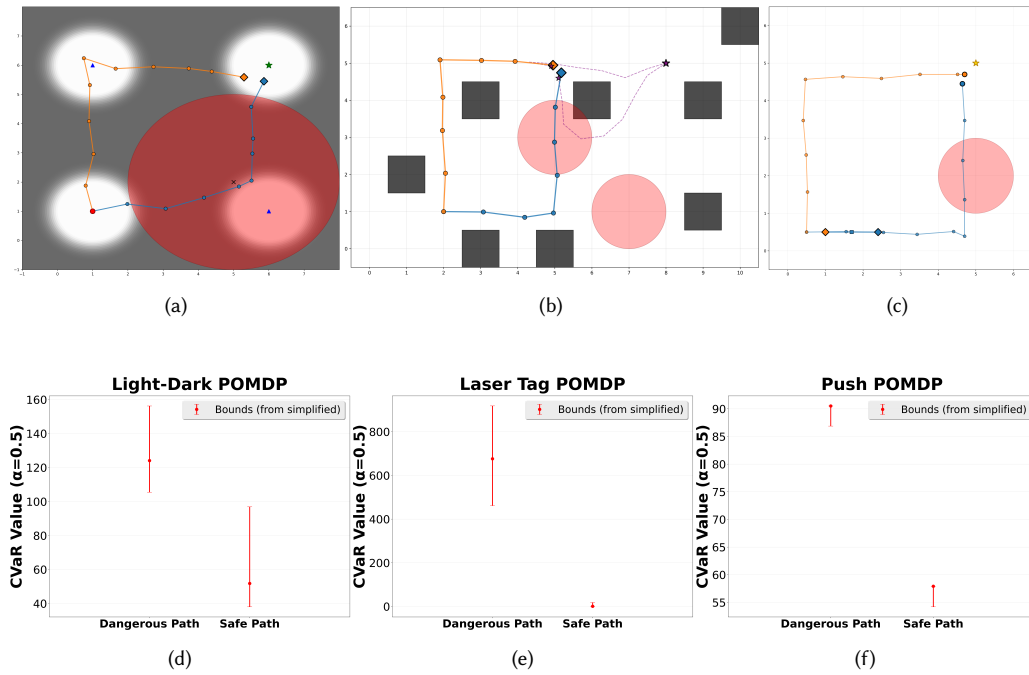


Fig. 9. Figures 9a, 9b, and 9c illustrate pairs of agent trajectories, consisting of a safe (orange) and a dangerous (blue) path. In Figure 9a, the agent moves from the lower-left to the upper-right goal location; the dangerous trajectory incurs higher cost. Figure 9b depicts trajectories in the Laser Tag environment, where the dangerous path traverses a high-cost region indicated in red. Figure 9c shows a similar pair of trajectories, with the dangerous path entering a hazardous region that leads to a terminal state. Across all three environments, the theoretical bounds on the values of the corresponding action sequences successfully discriminate between the safe and dangerous trajectories. Bounds are computed with probability of error $\delta = 0.05$.

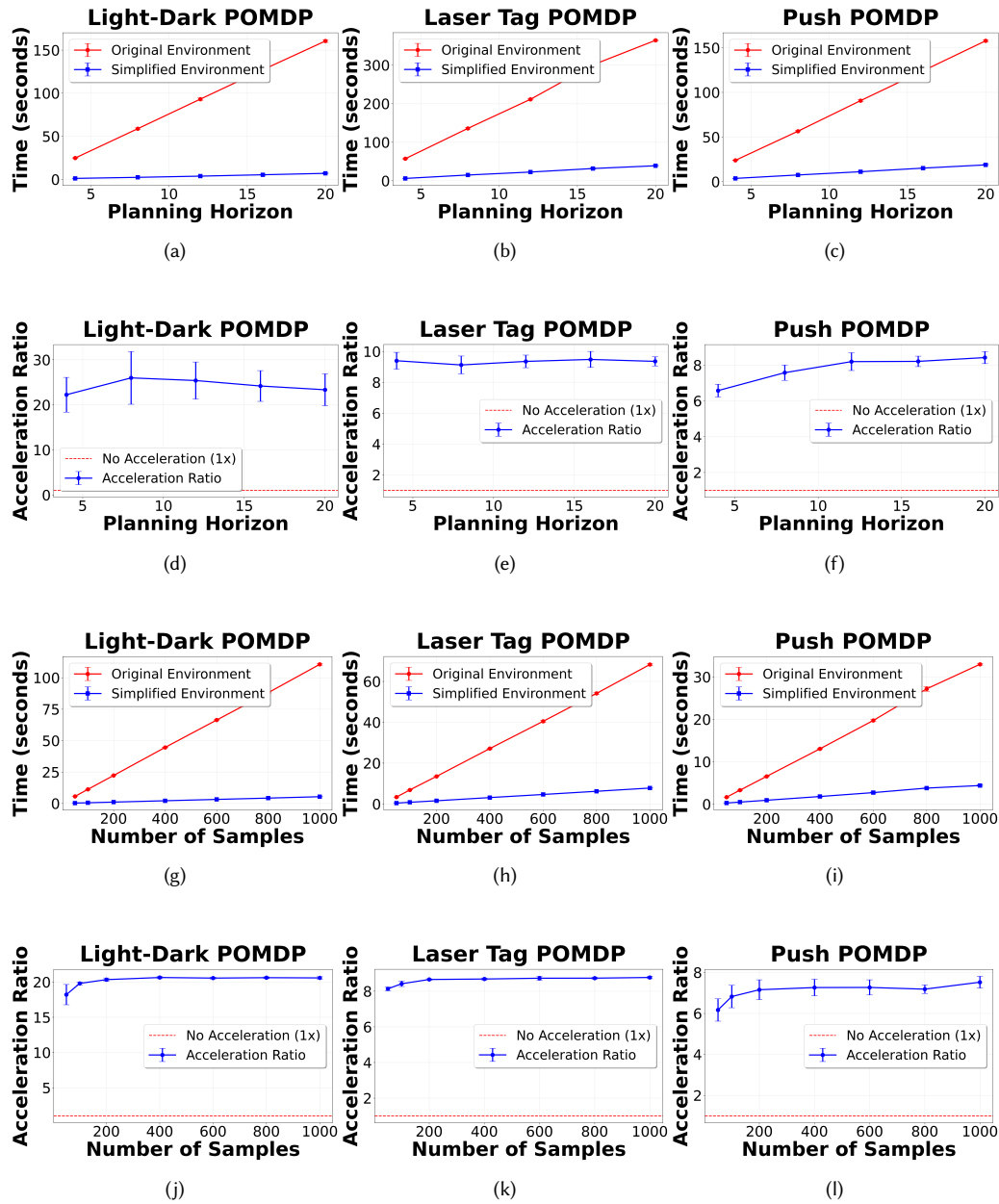


Fig. 10. Sensitivity analysis of the computational acceleration with respect to the planning horizon and number of return samples, for Light-Dark (left), Laser Tag (center), and Push (right), with $\alpha = 0.5$. Rows 1–2: computation time and acceleration ratio as a function of the planning horizon. Rows 3–4: computation time and acceleration ratio as a function of the number of return samples. Error bars indicate 95% confidence intervals.

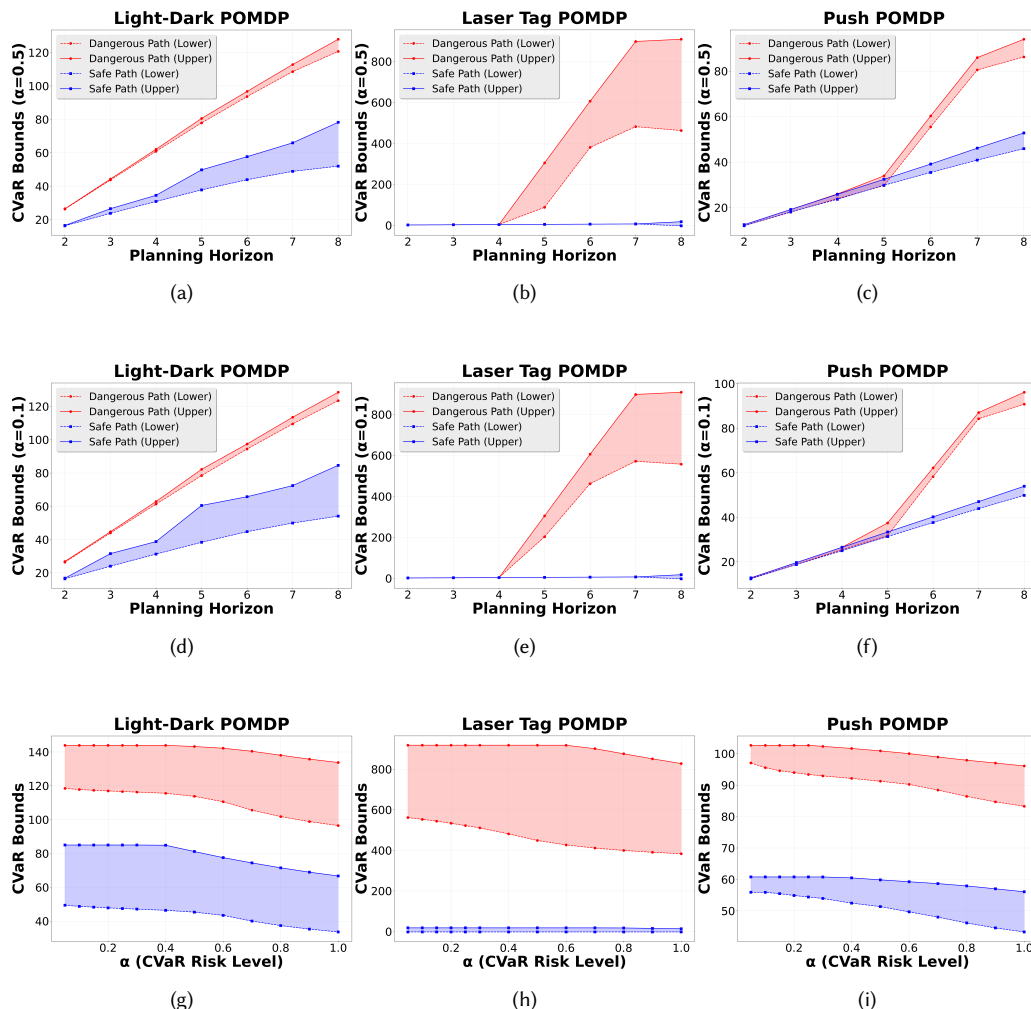


Fig. 11. Sensitivity of the CVaR bounds for the Light-Dark (left), Laser Tag (center), and Push (right) environments, using the complete safe (blue) and dangerous (red) action sequences depicted in Figure 9; solid and dashed lines indicate the upper and lower bounds, respectively. Rows 1–2: bounds as a function of the planning horizon with $\alpha = 0.5$ and $\alpha = 0.1$, respectively. Row 3: bounds as a function of the risk level α at a fixed horizon. As the horizon increases, the accumulated distributional discrepancy grows, causing the bounds to widen. As α decreases (more risk-averse), the bounds increase and the bound intervals widen, yet they remain well separated between the safe and dangerous paths across the full range of α . Bounds are computed with probability of error $\delta = 0.05$.

9.5 Empirical Static CVaR Bound Evaluation: Closed-Loop Policy

The preceding evaluation assessed bounds on fixed open-loop action sequences. We now demonstrate that the framework extends to closed-loop planners, using the Light-Dark POMDP as a test case. Specifically, we use the neural network trained by BetaZero Moss et al. 2024a as a deterministic policy: BetaZero learns offline approximations of the optimal policy and value function for POMDPs and combines them with online Monte Carlo tree search at test time. Here, we

extract a deterministic closed-loop policy from the trained network by selecting at each belief state the action with minimum predicted cost. The BetaZero configuration used in our experiments is detailed in Appendix F.

We evaluate two objectives. First, we test whether the bounds computed under the simplified observation model successfully distinguish between policies of differing risk levels. We compare the BetaZero policy against the same safe and dangerous action sequences from the preceding subsection. As shown in Figures 12 and 13, the bounds clearly separate the dangerous sequence from both the safe sequence and the BetaZero policy, with non-overlapping bound intervals. The trajectory plot confirms this ordering: the dangerous sequence traverses the high-cost region, while the BetaZero policy navigates through the illuminated safe zones. This separation persists across the full range of risk levels α and planning horizons.

Second, we show that evaluating the bounds under the simplified observation model is substantially faster than under the original model. Figure 14 shows a consistent $\approx 5\times$ speedup, stable across planning horizons from 4 to 12 and return sample counts from 100 to 1000.

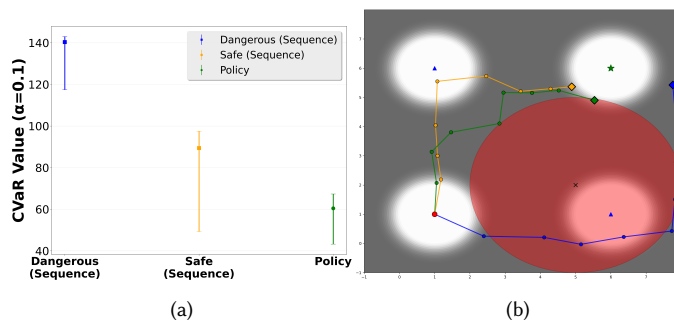


Fig. 12. Evaluation of the BetaZero neural network policy against the safe and dangerous action sequences in the Light-Dark POMDP ($\alpha = 0.1, H = 9$), with bounds computed under the simplified observation model. Figure 12a: CVaR bounds for the dangerous sequence (blue), safe sequence (orange), and BetaZero policy (green). The bound intervals of the policy and dangerous sequence do not overlap, demonstrating that the bounds correctly identify the policy as less risky. Bounds are computed with probability of error $\delta = 0.05$. Figure 12b: agent trajectories; the BetaZero policy (green) and safe sequence (orange) navigate through the illuminated safe zones, while the dangerous sequence (blue) traverses the high-cost region.

10 Conclusions

In this work we introduced a belief-simplification framework for risk-averse policy evaluation in POMDPs under a static CVaR objective, with guaranteed bounds on the resulting action-value function estimators, enabling accelerated online policy evaluation. Our approach establishes bounds on the true action-value function by leveraging an approximate action-value function computed under a simplified belief-transition model. We further derived specialized bounds for the case of a simplified observation model and showed how these bounds can be employed to accelerate online planning. To support these results, we developed the requisite mathematical foundations for bounding the CVaR of a random variable X through an auxiliary random variable Y , under assumptions relating their respective cumulative and density functions. These theoretical results are independent of the POMDP-planning setting and provide a general analytical framework that can facilitate future research on risk-sensitive decision making.

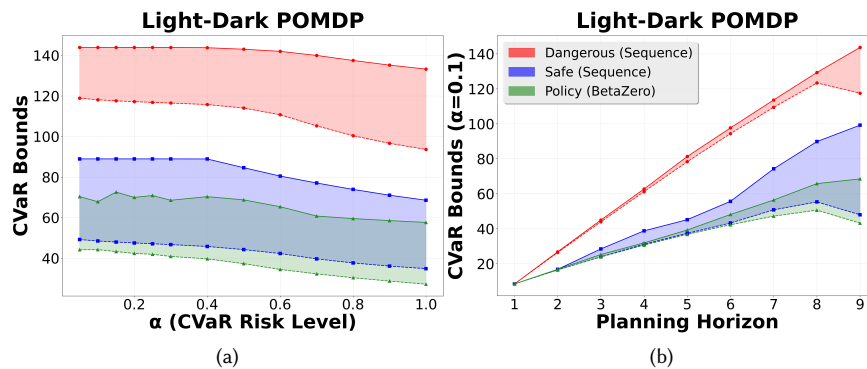


Fig. 13. Sensitivity of the CVaR bounds (computed under the simplified observation model) for the BetaZero policy, safe sequence, and dangerous sequence in the Light-Dark POMDP; solid and dashed lines denote upper and lower bounds, respectively. Figure 13a: bounds as a function of the risk level α at horizon $H = 9$. Figure 13b: bounds as a function of the planning horizon at $\alpha = 0.1$. The dangerous sequence remains clearly separated from the policy and safe sequence across all conditions. Bounds are computed with probability of error $\delta = 0.05$.

Our empirical evaluation, focused on observation model simplification, demonstrates the practical utility of the framework in both open-loop and closed-loop settings. In the open-loop case, the bounds correctly distinguish action sequences of differing risk levels across multiple environments and risk parameters. In the closed-loop case, using a BetaZero neural-network policy, the bounds successfully rank policies by risk level with non-overlapping bound intervals, while achieving a consistent $\approx 5\times$ computational speedup over evaluation under the original model. The theoretical framework accommodates general belief-transition model simplifications, including state-transition models, whose empirical investigation we leave for future work.

References

Acerbi, Carlo and Dirk Tasche (2002). “On the coherence of expected shortfall”. In: *Journal of banking & finance* 26.7, pp. 1487–1503.

Ahmadi, Mohamadreza et al. (2020). “Risk-averse planning under uncertainty”. In: *2020 American Control Conference (ACC)*. IEEE, pp. 3305–3312.

Ahmadi, Mohamadreza et al. (2021a). “Constrained risk-averse Markov decision processes”. In: *Proceedings of the AAAI Conference on Artificial Intelligence*. Vol. 35. 13, pp. 11718–11725.

Ahmadi, Mohamadreza et al. (2021b). “Risk-averse stochastic shortest path planning”. In: *2021 60th IEEE Conference on Decision and Control (CDC)*. IEEE, pp. 5199–5204.

Ahmadi, Mohamadreza et al. (2023). “Risk-averse decision making under uncertainty”. In: *IEEE Transactions on Automatic Control* 69.1, pp. 55–68.

Artzner, Philippe et al. (1999). “Coherent measures of risk”. In: *Mathematical finance* 9.3, pp. 203–228.

Assis Santana, Pedro Rodrigues Quemel e, Sylvie Thiébaux, and Brian Williams (Mar. 2016). “RAO*: An Algorithm for Chance-Constrained POMDP’s”. In: *Proceedings of the AAAI Conference on Artificial Intelligence* 30.1. DOI: [10.1609/aaai.v30i1.10423](https://doi.org/10.1609/aaai.v30i1.10423). URL: <https://ojs.aaai.org/index.php/AAAI/article/view/10423>.

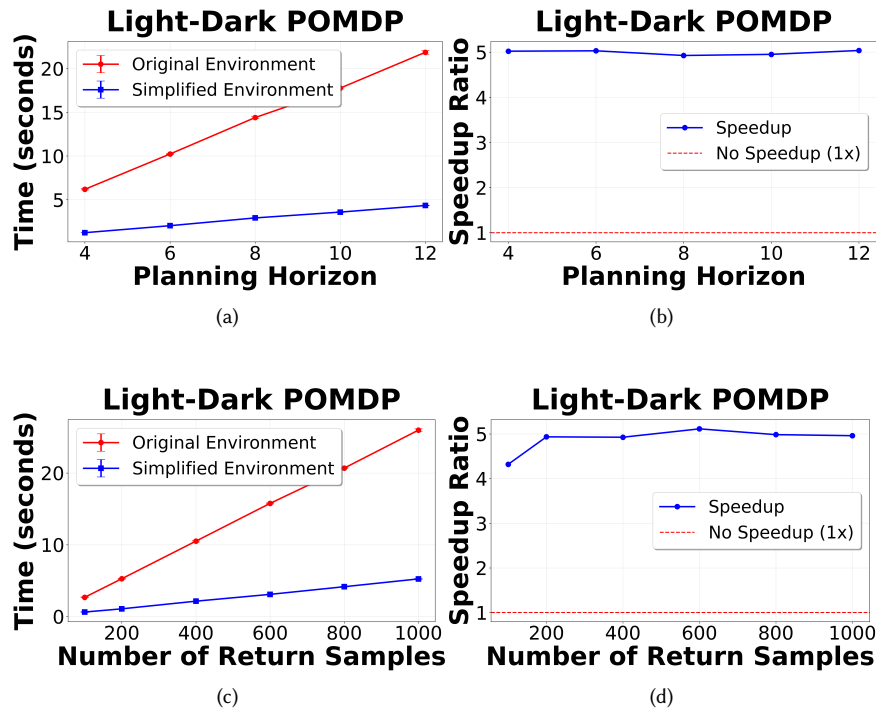


Fig. 14. Computational speedup from evaluating CVaR bounds under the simplified observation model relative to the original model for the BetaZero policy in the Light-Dark POMDP ($\alpha = 0.1$). Row 1: computation time and speedup ratio as a function of the planning horizon. Row 2: computation time and speedup ratio as a function of the number of return samples. The simplified model achieves a consistent $\approx 5\times$ speedup across all conditions. Error bars indicate 95% confidence intervals.

Barenboim, Moran and Vadim Indelman (July 2022). “Adaptive Information Belief Space Planning”. In: *Proceedings of the Thirty-First International Joint Conference on Artificial Intelligence, IJCAI-22*. Ed. by Lud De Raedt. Main Track. International Joint Conferences on Artificial Intelligence Organization, pp. 4588–4596. DOI: [10.24963/ijcai.2022/637](https://doi.org/10.24963/ijcai.2022/637). URL: <https://doi.org/10.24963/ijcai.2022/637>.

– (2023). “Online POMDP Planning with Anytime Deterministic Guarantees”. In: *Advances in Neural Information Processing Systems*. Ed. by A. Oh et al. Vol. 36. Curran Associates, Inc., pp. 79886–79902. URL: https://proceedings.neurips.cc/paper_files/paper/2023/file/fc6bd0eef19459655d5b097af783661d-Paper-Conference.pdf.

– (2026). “Online POMDP planning with anytime deterministic optimality guarantees”. In: *Artificial Intelligence* 350, p. 104442. ISSN: 0004-3702. DOI: <https://doi.org/10.1016/j.artint.2025.104442>. URL: <https://www.sciencedirect.com/science/article/pii/S0004370225001614>.

Brown, David B (2007). “Large deviations bounds for estimating conditional value-at-risk”. In: *Operations Research Letters* 35.6, pp. 722–730.

Chow, Yinlam et al. (2015). “Risk-sensitive and robust decision-making: a cvar optimization approach”. In: *Advances in neural information processing systems* 28.

Cubuktepe, Murat et al. (2021). “Robust finite-state controllers for uncertain POMDPs”. In: *Proceedings of the AAAI Conference on Artificial Intelligence*. Vol. 35. 13, pp. 11792–11800.

- Dabney, Will et al. (2018). “Distributional reinforcement learning with quantile regression”. In: *Proceedings of the AAAI conference on artificial intelligence*. Vol. 32. 1.
- Dixit, Anushri, Mohamadreza Ahmadi, and Joel W Burdick (2023). “Risk-averse receding horizon motion planning for obstacle avoidance using coherent risk measures”. In: *Artificial Intelligence* 325, p. 104018.
- Dvoretzky, A., J. Kiefer, and J. Wolfowitz (1956). “Asymptotic Minimax Character of the Sample Distribution Function and of the Classical Multinomial Estimator”. In: *The Annals of Mathematical Statistics* 27.3, pp. 642–669. DOI: [10.1214/aoms/1177728174](https://doi.org/10.1214/aoms/1177728174). URL: <https://doi.org/10.1214/aoms/1177728174>.
- Hou, Ping, William Yeoh, and Pradeep Varakantham (2016). “Solving risk-sensitive POMDPs with and without cost observations”. In: *Proceedings of the AAAI Conference on Artificial Intelligence*. Vol. 30. 1.
- Koenig, Sven and Reid G Simmons (1994). “Risk-sensitive planning with probabilistic decision graphs”. In: *Principles of Knowledge Representation and Reasoning*. Elsevier, pp. 363–373.
- Lev-Yehudi, Idan, Moran Barenboim, and Vadim Indelman (Mar. 2024). “Simplifying Complex Observation Models in Continuous POMDP Planning with Probabilistic Guarantees and Practice”. In: vol. 38. 18, pp. 20176–20184. DOI: [10.1609/aaai.v38i18.29997](https://ojs.aaai.org/index.php/AAAI/article/view/29997). URL: <https://ojs.aaai.org/index.php/AAAI/article/view/29997>.
- Lim, Michael H et al. (2023). “Optimality guarantees for particle belief approximation of POMDPs”. In: *Journal of Artificial Intelligence Research* 77, pp. 1591–1636.
- Majumdar, Anirudha and Marco Pavone (2020). “How should a robot assess risk? towards an axiomatic theory of risk in robotics”. In: *Robotics Research: The 18th International Symposium ISRR*. Springer, pp. 75–84.
- Marecki, Janusz and Pradeep Varakantham (2010). “Risk-sensitive planning in partially observable environments”. In: *AAMAS*, pp. 1357–1368.
- Moss, Robert J. et al. (2024a). “BetaZero: Belief-State Planning for Long-Horizon POMDPs using Learned Approximations”. In: *Reinforcement Learning Conference (RLC)*.
- Moss, Robert J. et al. (2024b). “ConstrainedZero: Chance-Constrained POMDP Planning Using Learned Probabilistic Failure Surrogates and Adaptive Safety Constraints”. In: *International Joint Conference on Artificial Intelligence (IJCAI)*.
- Ono, Masahiro et al. (2015). “Chance-constrained dynamic programming with application to risk-aware robotic space exploration”. In: *Autonomous Robots* 39, pp. 555–571.
- Osogami, Takayuki (2015). “Robust partially observable Markov decision process”. In: *International Conference on Machine Learning*. PMLR, pp. 106–115.
- Papadimitriou, Christos H. and John N. Tsitsiklis (Aug. 1987a). “The Complexity of Markov Decision Processes”. In: *Math. Oper. Res.* 12.3, 441–450. ISSN: 0364-765X.
- (1987b). “The Complexity of Markov Decision Processes”. In: *Math. Oper. Res.* 12, pp. 441–450. URL: <https://api.semanticscholar.org/CorpusID:29322444>.
- Pariante, Yaacov and Vadim Indelman (2026). *POMDPPlanners: Open-Source Package for POMDP Planning*. arXiv: [2602.20810](https://arxiv.org/abs/2602.20810) (cs.AI). URL: <https://arxiv.org/abs/2602.20810>.
- Pflug, Georg Ch (2000). “Some remarks on the value-at-risk and the conditional value-at-risk”. In: *Probabilistic constrained optimization: Methodology and applications*, pp. 272–281.
- Rockafellar, R Tyrrell, Stanislav Uryasev, et al. (2000). “Optimization of conditional value-at-risk”. In: *Journal of risk* 2, pp. 21–42.
- Silver, David and Joel Veness (2010). “Monte-Carlo planning in large POMDPs”. In: *Advances in neural information processing systems* 23.

- Sunberg, Zachary and Mykel Kochenderfer (2018). “Online algorithms for POMDPs with continuous state, action, and observation spaces”. In: *Proceedings of the International Conference on Automated Planning and Scheduling*. Vol. 28, pp. 259–263.
- Thomas, Philip and Erik Learned-Miller (June 2019). “Concentration Inequalities for Conditional Value at Risk”. In: *Proceedings of the 36th International Conference on Machine Learning*. Ed. by Kamalika Chaudhuri and Ruslan Salakhutdinov. Vol. 97. Proceedings of Machine Learning Research. PMLR, pp. 6225–6233. URL: <https://proceedings.mlr.press/v97/thomas19a.html>.
- Xu, Huan and Shie Mannor (2010). “Distributionally robust Markov decision processes”. In: *Advances in Neural Information Processing Systems* 23.
- Zhitnikov, A. and V. Indelman (2022). “Simplified Risk Aware Decision Making with Belief Dependent Rewards in Partially Observable Domains”. In: *Artificial Intelligence, Special Issue on “Risk-Aware Autonomous Systems: Theory and Practice”*.
- Zhitnikov, Andrey, Ori Sztyglic, and Vadim Indelman (2025). “No compromise in solution quality: Speeding up belief-dependent continuous partially observable Markov decision processes via adaptive multilevel simplification”. In: *The International Journal of Robotics Research* 44.2, pp. 157–195. DOI: [10.1177/02783649241261398](https://doi.org/10.1177/02783649241261398). eprint: <https://doi.org/10.1177/02783649241261398>. URL: <https://doi.org/10.1177/02783649241261398>.

A CVaR Bounds Proofs

THEOREM A.1. Let X and Y be random variables and $\epsilon \in [0, 1]$.

(1) **Upper Bound:** assume that $P(X \leq b_X) = 1, P(Y \leq b_Y) = 1$ and $\forall z \in \mathbb{R}, F_Y(z) - F_X(z) \leq \epsilon$, then

(a) If $\alpha > \epsilon$,

$$\text{CVaR}_\alpha(X) \leq \frac{\epsilon}{\alpha} \max(b_X, b_Y) + (1 - \frac{\epsilon}{\alpha}) \text{CVaR}_{\alpha-\epsilon}(Y). \quad (52)$$

(b) If $\alpha \leq \epsilon$, then $\text{CVaR}_\alpha(X) \leq \max(b_X, b_Y)$.

(2) **Lower Bound:** If $P(X \geq a_X) = 1, P(Y \geq a_Y) = 1$ and $\forall z \in \mathbb{R}, F_X(z) - F_Y(z) \leq \epsilon$, then

(a) If $\alpha + \epsilon \leq 1$,

$$\text{CVaR}_\alpha(X) \geq (1 + \frac{\epsilon}{\alpha}) \text{CVaR}_{\alpha+\epsilon}(Y) - \frac{\epsilon}{\alpha} \text{CVaR}_\epsilon(Y) \quad (53)$$

(b) If $\alpha + \epsilon > 1$ and $a_{\min} = \min(a_X, a_Y)$,

$$\text{CVaR}_\alpha(X) \geq \frac{1}{\alpha} (\mathbb{E}[Y] - \epsilon \text{CVaR}_\epsilon(Y) + (\alpha + \epsilon - 1)a_{\min}) \quad (54)$$

PROOF. The strategy of the proof is to construct two distributions derived from F_Y , denoted F_Y^L and F_Y^U , such that F_X is stochastically bounded between them; that is, $F_Y^L \leq F_X \leq F_Y^U$. Consequently, since CVaR is a coherent risk measure, it follows that

$$\text{CVaR}_\alpha^{F_Y^L} \leq \text{CVaR}_\alpha^{F_X} \leq \text{CVaR}_\alpha^{F_Y^U}, \quad (55)$$

where $\text{CVaR}_\alpha^{F_Y^L}$, $\text{CVaR}_\alpha^{F_X}$, and $\text{CVaR}_\alpha^{F_Y^U}$ denote the CVaR at level α corresponding to the distributions F_Y^L , F_X , and F_Y^U , respectively.

Let $a_{\min} = \min(a_X, a_Y)$ and $b_{\min} = \min(b_X, b_Y)$. Define the interval $[b_{\min}, b_X)$ to be \emptyset if $b_{\min} = b_X$, and equal to $[b_Y, b_X)$ otherwise. Analogously, define $[a_{\min}, a_X)$ in the same manner. We then define upper and lower bounds for F_Y as follows (see Figure 15):

$$F_Y^U(y) = \begin{cases} 0 & y < \max(a_X, q_{1-\epsilon}^Y) \\ \min(F_Y(y) - \epsilon, 1 - \epsilon) & y \in [\max(a_X, q_{1-\epsilon}^Y), b_{\min}) \\ 1 - \epsilon & y \in [b_{\min}, b_X) \\ 1 & y \geq \max(b_X, b_Y), \end{cases} \quad (56)$$

$$F_Y^L(y) = \begin{cases} 0 & y < a_{\min} \\ \epsilon & y \in [a_{\min}, a_Y) \\ \min(F_Y(y) + \epsilon, 1) & y \in [a_Y, \min(q_\epsilon^Y, b_X)) \\ 1 & y \geq \min(q_\epsilon^Y, b_X). \end{cases} \quad (57)$$

As a first step, we verify that F_Y^L and F_Y^U are valid CDFs and that they satisfy $F_Y^L \leq F_X \leq F_Y^U$. To establish that F is a CDF, it suffices to verify the following properties:

- (1) F is non-decreasing;
- (2) $F : \mathbb{R} \rightarrow [0, 1]$ with $\lim_{x \rightarrow \infty} F(x) = 1$ and $\lim_{x \rightarrow -\infty} F(x) = 0$;
- (3) F is right-continuous.

Proof that F_Y^L is a CDF:

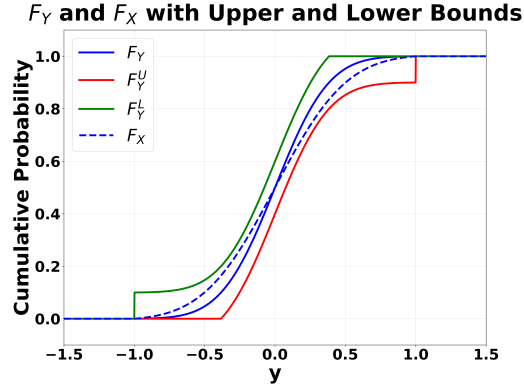


Fig. 15. Illustration of the upper and lower bounds F_Y^U and F_Y^L on the cumulative distribution function F_X .

- (1) On the interval $[a_Y, \min(q_{1-\epsilon}^Y, b_X))$, the function F_Y^L is monotone increasing, since F_Y is monotone increasing by virtue of being a CDF. Outside this interval, F_Y^L is constant and consequently preserves monotonicity.
- (2) By definition, $\lim_{y \rightarrow \infty} F_Y^L(y) = 1$ and $\lim_{y \rightarrow -\infty} F_Y^L(y) = 0$. We need to show that F_Y^L is bounded between 0 and 1. By its definition, F_Y^L is bounded between 0 and 1.
- (3) Within the interval $[a_Y, \min(q_{1-\epsilon}^Y, b_X))$, F_Y^L is right-continuous since F_Y is right-continuous as a CDF. Outside this interval, F_Y^L is constant and hence also right-continuous.

Proof that F_Y^U is a CDF:

- (1) On the interval $[\max(a_X, q_{1-\epsilon}^Y), b_{min})$, the function F_Y^U is monotone increasing, since F_Y is monotonically increasing by virtue of being a CDF. Outside this interval, F_Y^U is constant and consequently preserves monotonicity.
- (2) By definition, $\lim_{y \rightarrow \infty} F_Y^U(y) = 1$ and $\lim_{y \rightarrow -\infty} F_Y^U(y) = 0$. By its definition, F_Y^U is bounded between 0 and 1.
- (3) Within the interval $[\max(a_X, q_{1-\epsilon}^Y), b_{min})$, F_Y^U is right-continuous since F_Y is right-continuous as a CDF. Outside this interval, F_Y^U is constant and hence also right-continuous.

Proof that $F_Y^L \leq F_X \leq F_Y^U$: To establish that $F_Y^L \leq F_X \leq F_Y^U$, we need to show that for all $z \in \mathbb{R}$, $F_Y^L(z) \geq F_X(z) \geq F_Y^U(z)$. Let $z \in \mathbb{R}$.

- If $z < a_{min}$ then $F_Y^L(z) = 0 = F_X(z)$.
- If $z \in [a_{min}, a_Y)$ then $F_X(z) = F_X(z) - F_Y(z) + F_Y(z) \leq |F_X(z) - F_Y(z)| + F_Y(z) \leq \epsilon + F_Y(z) = \epsilon = F_Y^L(z)$.
- If $z \in [a_Y, \min(q_{1-\epsilon}^Y, b_X))$ we assume that $F_Y(z) + \epsilon \leq 1$ because otherwise $F_Y^L(z) = 1$ and the inequality holds. $F_Y^L(z) = F_Y(z) + \epsilon = F_Y(z) - F_X(z) + F_X(z) + \epsilon \geq F_X(z) - |F_Y(z) - F_X(z)| + \epsilon \geq F_X(z)$.
- If $z \geq \min(q_{1-\epsilon}^Y, b_X)$ then $F_Y^L(z) = 1 \geq F_X(z)$.

and therefore $F_Y^L \leq F_X$. Note that the last proof holds when $b_X = \infty$, making F_Y^L a valid CDF when the support of X is not bounded from above.

- If $z < \max(a_X, q_{1-\epsilon}^Y)$ then $F_Y^U(z) = 0 \leq F_X(z)$.
- If $z \in [\max(a_X, q_{1-\epsilon}^Y), b_{min})$ then $F_Y^U(z) \leq F_Y(z) - \epsilon = F_Y(z) - F_X(z) + F_X(z) - \epsilon \leq |F_Y(z) - F_X(z)| + F_X(z) - \epsilon \leq \epsilon + F_X(z) - \epsilon = F_X(z)$.
- If $z \in [b_{min}, b_X)$ then $F_Y^U(z) = 1 - \epsilon = F_Y(z) - \epsilon = F_Y(z) - \epsilon + F_X(z) - F_X(z) \leq F_X(z) - \epsilon + |F_Y(z) - F_X(z)| \leq F_X(z)$.

and therefore $F_X \leq F_Y^U$. Note that the last proof holds when $a_X = -\infty$, making F_Y^U a valid CDF when the support of X is not bounded from below.

Next, we derive bounds for the CVaR associated with F_Y^U and F_Y^L .

Upper bound for $\text{CVaR}_\alpha^{F_Y^U}$: From Acerbi and Tasche 2002, CVaR is equal to an integral of the VaR

$$\text{CVaR}_\alpha^{F_Y^U} = \frac{1}{\alpha} \int_{1-\alpha}^1 \inf\{y \in \mathbb{R} : F_Y^U(y) \geq \tau\} d\tau = \frac{1}{\alpha} \int_{1-\alpha+\epsilon}^{1+\epsilon} \inf\{y \in \mathbb{R} : F_Y^U(y) \geq \tau - \epsilon\} d\tau \quad (58)$$

If $\alpha \leq \epsilon$, then $1 - \alpha + \epsilon \geq 1$, rendering the bound in the preceding equation trivial, as it attains the maximum value of the support of both X and Y .

$$\frac{1}{\alpha} \int_{1-\alpha+\epsilon}^{1+\epsilon} \inf\{y \in \mathbb{R} : F_Y^U(y) \geq \tau - \epsilon\} \leq \frac{1}{\alpha} \int_{1-\alpha+\epsilon}^{1+\epsilon} \max(b_X, b_Y) d\tau = \max(b_X, b_Y). \quad (59)$$

That is, $\text{CVaR}_\alpha(X) \leq \max(b_X, b_Y)$.

If $\alpha > \epsilon$, then $1 - \alpha + \epsilon < 1$, and the integral may be decomposed into one term that is trivially bounded by the maximum of the support and another term that can be computed explicitly

$$\begin{aligned} \text{CVaR}_\alpha^{F_Y^U} &= \frac{1}{\alpha} \int_{1-\alpha+\epsilon}^{1+\epsilon} \inf\{y \in \mathbb{R} : F_Y^U(y) \geq \tau - \epsilon\} d\tau = \frac{1}{\alpha} \underbrace{\left[\int_1^{1+\epsilon} \inf\{y \in \mathbb{R} : F_Y^U(y) \geq \tau - \epsilon\} d\tau \right]}_{\triangleq A_1} \\ &\quad + \underbrace{\left[\int_{1-\alpha+\epsilon}^1 \inf\{y \in \mathbb{R} : F_Y^U(y) \geq \tau - \epsilon\} d\tau \right]}_{\triangleq A_2} \end{aligned} \quad (60)$$

The term A_1 is bounded, in a manner analogous to (59), by $\epsilon \max(b_X, b_Y)$, which is essentially the tightest bound attainable given the definition of F_Y^U . The term A_2 can be expressed in terms of the CVaR of Y , evaluated at a shifted confidence level. Specifically, the variable $\tau - \epsilon$ in A_2 lies within the interval $[1 - \alpha, 1 - \epsilon]$. Over this range, for all $y \in [\max(a_X, q_{1-\epsilon}^Y), b_{\min}]$, the inequality $F_Y^U(y) \leq F_Y(y) - \epsilon$ holds. This follows because if $q_{1-\epsilon}^Y \geq a_X$, then by definition $F_Y^U(y) = \min(F_Y(y) - \epsilon, 1 - \epsilon)$, and if $a_X > q_{1-\epsilon}^Y$, then $F_Y^U(y) = 0 \leq F_Y(y) - \epsilon$ for $y \in [q_{1-\epsilon}^Y, a_X]$ and again $F_Y^U(y) = \min(F_Y(y) - \epsilon, 1 - \epsilon)$ for $y \in [a_X, b_{\min}]$.

$$A_2 \leq \int_{1-\alpha+\epsilon}^1 \inf\{y \in \mathbb{R} : F_Y(y) - \epsilon \geq \tau - \epsilon\} d\tau = \int_{1-(\alpha-\epsilon)}^1 \inf\{y \in \mathbb{R} : F_Y(y) \geq \tau\} d\tau = (\alpha - \epsilon) \text{CVaR}_{\alpha-\epsilon}(Y). \quad (61)$$

Note that the confidence level is valid, as $\alpha, \epsilon \in (0, 1)$ and $\alpha > \epsilon$ imply $\alpha - \epsilon \in (0, 1)$. By combining the previous two expressions, we obtain a single bound:

$$\text{CVaR}_\alpha^{F_Y^U} \leq \epsilon \frac{\max(b_X, b_Y)}{\alpha} + (1 - \frac{\epsilon}{\alpha}) \text{CVaR}_{\alpha-\epsilon}(Y). \quad (62)$$

In the case where $a_X = -\infty$, we have $\max(a_X, q_{1-\epsilon}^Y) = q_{1-\epsilon}^Y$, and the definition of F_Y^U no longer involves a_X . Therefore, the inequality remains valid in the case of $a_X = -\infty$.

Lower bound for $\text{CVaR}_\alpha^{F_Y^L}$: From Acerbi and Tasche 2002, CVaR is equal to an integral of the VaR

$$\text{CVaR}_\alpha^{F_Y^L} = \frac{1}{\alpha} \int_{1-\alpha}^1 \inf\{y \in \mathbb{R} : F_Y^L(y) \geq \tau\} d\tau = \frac{1}{\alpha} \int_{1-(\epsilon+\alpha)}^{1-\epsilon} \inf\{y \in \mathbb{R} : F_Y^L(y) \geq \tau + \epsilon\} d\tau. \quad (63)$$

It holds that $F_Y^L(y) \leq F_Y(y) + \epsilon$ and therefore

$$\begin{aligned} \text{CVaR}_\alpha^{F_Y^L} &\geq \frac{1}{\alpha} \int_{1-(\epsilon+\alpha)}^{1-\epsilon} \inf\{y \in \mathbb{R} : F_Y(y) + \epsilon \geq \tau + \epsilon\} d\tau = \frac{1}{\alpha} \int_{1-(\epsilon+\alpha)}^{1-\epsilon} \inf\{y \in \mathbb{R} : F_Y(y) \geq \tau\} d\tau \\ &= \frac{1}{\alpha} \left[\int_{1-(\epsilon+\alpha)}^1 \inf\{y \in \mathbb{R} : F_Y(y) \geq \tau\} d\tau - \int_{1-\epsilon}^1 \inf\{y \in \mathbb{R} : F_Y(y) \geq \tau\} d\tau \right] \\ &= \frac{1}{\alpha} [(\alpha + \epsilon) \text{CVaR}_{\alpha+\epsilon}(Y) - \epsilon \text{CVaR}_\epsilon(Y)]. \end{aligned} \quad (64)$$

In the case where $\epsilon + \alpha > 1$,

$$\begin{aligned} \text{CVaR}_\alpha^{F_Y^L} &= \frac{1}{\alpha} \int_{1-(\epsilon+\alpha)}^{1-\epsilon} \inf\{y \in \mathbb{R} : F_Y^L(y) \geq \tau + \epsilon\} d\tau \\ &= \frac{1}{\alpha} \underbrace{\left[\int_0^{1-\epsilon} \inf\{y \in \mathbb{R} : F_Y^L(y) \geq \tau + \epsilon\} d\tau \right]}_{\triangleq A_3} + \underbrace{\left[\int_{1-(\epsilon+\alpha)}^0 \inf\{y \in \mathbb{R} : F_Y^L(y) \geq \tau + \epsilon\} d\tau \right]}_{\triangleq A_4}. \end{aligned} \quad (65)$$

$$\begin{aligned} A_3 &\geq \int_0^{1-\epsilon} \inf\{y \in \mathbb{R} : F_Y(y) \geq \tau\} d\tau = \int_0^1 \inf\{y \in \mathbb{R} : F_Y(y) \geq \tau\} d\tau - \int_{1-\epsilon}^1 \inf\{y \in \mathbb{R} : F_Y(y) \geq \tau\} d\tau \\ &= \mathbb{E}[Y] - \epsilon \text{CVaR}_\epsilon(Y) \end{aligned} \quad (66)$$

In the case of A_4 , after the change of variable, τ ranges from $1 - \alpha$ to ϵ , and therefore

$$A_4 = \int_{1-\alpha}^\epsilon \inf\{y \in \mathbb{R} : F_Y^L(y) \geq \tau\} d\tau \geq (\alpha + \epsilon - 1) a_{\min} \quad (67)$$

By combining the last equations to one bound we get

$$\text{CVaR}_\alpha(X) \geq \text{CVaR}_\alpha^{F_Y^L} \geq \frac{1}{\alpha} (\mathbb{E}[Y] - \epsilon \text{CVaR}_\epsilon(Y) + (\alpha + \epsilon - 1) a_{\min}). \quad (68)$$

□

THEOREM A.2. *Given the definition of X, Y, ϵ and α as in Theorem 5.1, the lower and upper bounds of Theorem 5.1 converge to $\text{CVaR}_\alpha(X)$ as $\epsilon \rightarrow 0$.*

PROOF. Let f and g be continuous functions such that $f(0)$ and $g(0)$ are finite. Then $\lim_{x \rightarrow 0} f(x)g(x) = (\lim_{x \rightarrow 0} f(x))(\lim_{x \rightarrow 0} g(x))$. This property will be used throughout the proof.

Assume that $F_Y(z) - F_X(z) \leq \epsilon$ for all $z \in \mathbb{R}$. Since we consider the limit as $\epsilon \rightarrow 0$, we further assume that $\alpha > \epsilon$ when computing the bound. Noting that CVaR is continuous with respect to the confidence level, it follows that $\lim_{\epsilon \rightarrow 0} \text{CVaR}_{\alpha-\epsilon}(Y) = \text{CVaR}_\alpha(Y)$.

$$\lim_{\epsilon \rightarrow 0} \frac{\epsilon}{\alpha} \max(b_X, b_Y) + (1 - \frac{\epsilon}{\alpha}) \text{CVaR}_{\alpha-\epsilon}(Y) = \lim_{\epsilon \rightarrow 0} (1 - \frac{\epsilon}{\alpha}) \text{CVaR}_{\alpha-\epsilon}(Y) = \lim_{\epsilon \rightarrow 0} 1 - \frac{\epsilon}{\alpha} \lim_{\epsilon \rightarrow 0} \text{CVaR}_{\alpha-\epsilon}(Y) = \text{CVaR}_\alpha(Y) \quad (69)$$

If $F_X(z) - F_Y(z) \leq \epsilon$ for all $z \in \mathbb{R}$, then, since we consider the limit as $\epsilon \rightarrow 0$, we assume in the derivation of the bound that $\alpha + \epsilon \leq 1$.

$$\lim_{\epsilon \rightarrow 0} (1 + \frac{\epsilon}{\alpha}) \text{CVaR}_{\alpha+\epsilon}(Y) - \frac{\epsilon}{\alpha} \text{CVaR}_\epsilon(Y) = \lim_{\epsilon \rightarrow 0} 1 + \frac{\epsilon}{\alpha} \lim_{\epsilon \rightarrow 0} \text{CVaR}_{\alpha+\epsilon}(Y) - \lim_{\epsilon \rightarrow 0} \frac{\epsilon}{\alpha} \lim_{\epsilon \rightarrow 0} \text{CVaR}_\epsilon(Y) = \text{CVaR}_\alpha(Y). \quad (70)$$

□

THEOREM A.3. Let X be a random variable, $\alpha \in (0, 1]$, $\delta \in (0, 0.5)$, $\epsilon = \sqrt{\ln(1/\delta)/(2n)}$. Let $X_1, \dots, X_n \stackrel{iid}{\sim} F_X$ be random variables that define the ECDF \hat{F}_X .

- (1) **Upper Bound:** If $P(X \leq b) = 1$, then
 - (a) If $\alpha > \epsilon$ then $P(\text{CVaR}_\alpha(X) \leq (1 - \frac{\epsilon}{\alpha})C_{\alpha-\epsilon}^{\hat{F}_X} + \frac{\epsilon}{\alpha}b) > 1 - \delta$.
 - (b) If $\alpha \leq \epsilon$ then $\text{CVaR}_\alpha(X) \leq b$
- (2) **Lower Bound:** If $P(X \geq a) = 1$, then
 - (a) If $\alpha + \epsilon < 1$, then $P(\text{CVaR}_\alpha(X) \geq (1 + \frac{\epsilon}{\alpha})C_{\alpha+\epsilon}^{\hat{F}_X} - \frac{\epsilon}{\alpha}C_\epsilon^{\hat{F}_X}) > 1 - \delta$.
 - (b) If $\alpha + \epsilon \geq 1$, then $P(\text{CVaR}_\alpha(X) \geq \frac{1}{\alpha}[(\alpha + \epsilon - 1)a + E_{\hat{F}_X}[X] - \epsilon C_\epsilon^{\hat{F}_X}]) > 1 - \delta$.

PROOF. From DKW inequality the following inequalities can be derived Thomas and Learned-Miller 2019

$$\Pr\left(\sup_{x \in \mathbb{R}} (\hat{F}(x) - F(x)) \leq \sqrt{\frac{\ln(1/\delta)}{2n}}\right) \geq 1 - \delta, \Pr\left(\sup_{x \in \mathbb{R}} (\hat{F}(x) - F(x)) \geq \sqrt{\frac{\ln(1/\delta)}{2n}}\right) \geq 1 - \delta. \quad (71)$$

Let $\epsilon = \sqrt{\frac{\ln(1/\delta)}{2n}}$. By using Theorem 5.1 we get the following.

If $\alpha > \epsilon$ then

$$\begin{aligned} P(\text{CVaR}_\alpha(X) \leq \frac{\alpha - \epsilon}{\alpha}C_{\alpha-\epsilon}^{\hat{F}_X} + \frac{\epsilon}{\alpha}b) &= P(C_\alpha(X) \leq \frac{\alpha - \epsilon}{\alpha}C_{\alpha-\epsilon}^{\hat{F}_X} + \frac{\epsilon}{\alpha}b \mid \underbrace{\sup_{z \in \mathbb{R}} (\hat{F}_X - F_X) \leq \epsilon}_{=1}) P(\underbrace{\sup_{z \in \mathbb{R}} (\hat{F}_X - F_X) \leq \epsilon}_{>1-\delta}) \\ &+ P(C_\alpha(X) \leq \frac{\alpha - \epsilon}{\alpha}C_{\alpha-\epsilon}^{\hat{F}_X} + \frac{\epsilon}{\alpha}b \mid \underbrace{\sup_{z \in \mathbb{R}} (\hat{F}_X - F_X) > \epsilon}_{\geq 0}) P(\underbrace{\sup_{z \in \mathbb{R}} (\hat{F}_X - F_X) > \epsilon}_{\geq 0}) \quad (72) \\ &> 1 - \delta. \end{aligned}$$

Observe that, conditional on the event

$$\sup_{z \in \mathbb{R}} (\hat{F}_X(z) - F_X(z)) \leq \epsilon,$$

the bound in Theorem 5.1 holds deterministically. Consequently, the probability that

$$C_\alpha(X) \leq \frac{\alpha - \epsilon}{\alpha}C_{\alpha-\epsilon}^{\hat{F}_X} + \frac{\epsilon}{\alpha}b$$

holds, given

$$\sup_{z \in \mathbb{R}} (\hat{F}_X(z) - F_X(z)) \leq \epsilon,$$

is equal to one. The same observation is necessary through the rest of the proof in a similar manner. If $\alpha + \epsilon < 1$, then

$$\begin{aligned} P(C_\alpha(X) \geq (1 + \frac{\epsilon}{\alpha})C_{\alpha+\epsilon}^{\hat{F}_X} - \frac{\epsilon}{\alpha}C_\epsilon^{\hat{F}_X}) &= P(C_\alpha(X) \geq (1 + \frac{\epsilon}{\alpha})C_{\alpha+\epsilon}^{\hat{F}_X} - \frac{\epsilon}{\alpha}C_\epsilon^{\hat{F}_X} \mid \underbrace{\sup_{z \in \mathbb{R}} (F_X - \hat{F}_X) \leq \epsilon}_{=1}) P(\underbrace{\sup_{z \in \mathbb{R}} (F_X - \hat{F}_X) \leq \epsilon}_{>1-\delta}) \\ &+ P(C_\alpha(X) \geq (1 + \frac{\epsilon}{\alpha})C_{\alpha+\epsilon}^{\hat{F}_X} - \frac{\epsilon}{\alpha}C_\epsilon^{\hat{F}_X} \mid \underbrace{\sup_{z \in \mathbb{R}} (F_X - \hat{F}_X) > \epsilon}_{\geq 0}) P(\underbrace{\sup_{z \in \mathbb{R}} (F_X - \hat{F}_X) > \epsilon}_{\geq 0}) \quad (73) \\ &> 1 - \delta \end{aligned}$$

If $\alpha + \epsilon \geq 1$, then

$$\begin{aligned}
 & P(C_\alpha(X) \geq \frac{1}{\alpha} [(\alpha + \epsilon - 1)a + E_{\hat{F}_X}[X] - \epsilon C_\epsilon^{\hat{F}_X}]) \\
 &= P(C_\alpha(X) \geq \frac{1}{\alpha} [(\alpha + \epsilon - 1)a + E_{\hat{F}_X}[X] - \epsilon C_\epsilon^{\hat{F}_X}] \mid \sup_{z \in \mathbb{R}} (F_X - \hat{F}_X) \leq \epsilon) P(\sup_{z \in \mathbb{R}} (F_X - \hat{F}_X) \leq \epsilon) \\
 &\quad \underbrace{\hspace{10em}}_{=1} \underbrace{\hspace{10em}}_{>1-\delta} \\
 &+ P(C_\alpha(X) \geq \frac{1}{\alpha} [(\alpha + \epsilon - 1)a + E_{\hat{F}_X}[X] - \epsilon C_\epsilon^{\hat{F}_X}] \mid \sup_{z \in \mathbb{R}} (F_X - \hat{F}_X) > \epsilon) P(\sup_{z \in \mathbb{R}} (F_X - \hat{F}_X) > \epsilon) \\
 &\quad \underbrace{\hspace{10em}}_{\geq 0} \underbrace{\hspace{10em}}_{\geq 0} \\
 &> 1 - \delta
 \end{aligned} \tag{74}$$

□

THEOREM A.4. (Tighter CVaR Lower Bound) Let $\alpha \in (0, 1)$, X and Y be random variables. Define a random variable Y^L such that $F_{Y^L}(y) \triangleq \min(1, F_Y(y) + g(y))$ for $g : \mathbb{R} \rightarrow [0, \infty)$. Assume $\lim_{x \rightarrow -\infty} g(x) = 0$, g is continuous from the right and monotonic increasing. If $\forall x \in \mathbb{R}, F_X(x) \leq F_Y(x) + g(x)$, then F_{Y^L} is a CDF and $\text{CVaR}_\alpha(Y^L) \leq \text{CVaR}_\alpha(X)$.

PROOF. In order to prove that F_{Y^L} is a CDF we need to prove that F_{Y^L} is:

- (1) Monotonic increasing
- (2) $F : \mathbb{R} \rightarrow [0, 1]$, $\lim_{x \rightarrow \infty} F_{Y^L}(x) = 1$, $\lim_{x \rightarrow -\infty} F_{Y^L}(x) = 0$
- (3) Continuous from the right

Monotonic increasing: Note that for every $f_i : \mathbb{R} \rightarrow \mathbb{R}, i = 1, 2$ that are monotonic increasing, $f_1(f_2(x))$ is also monotonic increasing in x . Denote $f(x) := \min(x, 1)$ and $f_2(x) := F_Y(x) + g(x)$. $F_Y(x)$ is a CDF and therefore monotonic increasing, so $f_2(x)$ is monotonic increasing as a sum of monotonic increasing functions. f_1 is also monotonic increasing, and $F_{Y^L}(x) = f_1(f_2(x))$. Therefore $F_{Y^L}(x)$ is monotonic increasing.

Limits:

$$1 \geq \lim_{x \rightarrow \infty} F_{Y^L}(x) = \lim_{x \rightarrow \infty} \min(1, F_Y(x) + g(x)) \geq \lim_{x \rightarrow \infty} \min(1, F_Y(x)) = \lim_{x \rightarrow \infty} F_Y(x) = 1 \tag{75}$$

and therefore $\lim_{x \rightarrow \infty} F_{Y^L}(x) = 1$.

$$0 \leq \lim_{x \rightarrow -\infty} F_{Y^L}(x) = \lim_{x \rightarrow -\infty} \min(1, F_Y(x) + g(x)) \leq \lim_{x \rightarrow -\infty} F_Y(x) + g(x) = \lim_{x \rightarrow -\infty} F_Y(x) + \lim_{x \rightarrow -\infty} g(x) = 0$$

and therefore $\lim_{x \rightarrow -\infty} F_{Y^L}(x) = 0$. By definition $\forall x \in \mathbb{R}, F_{Y^L}(x) \leq 1$, and $\forall x \in \mathbb{R}, F_{Y^L}(x) \geq 0$ because both g and F_{Y^L} are non negative functions.

Continuity from the right: F_Y is continuous from the right because it is a CDF, and g is continuous from the right by assumption. Their sum $F_Y + g$ is therefore continuous from the right, and since the constant function 1 is continuous, $F_{Y^L} = \min(1, F_Y + g)$ is continuous from the right as the minimum of two right-continuous functions. Thus, F_{Y^L} is a CDF.

Bound proof: If $Y^L \leq X$, then $\text{CVaR}_\alpha(Y^L) \leq \text{CVaR}_\alpha(X)$ because CVaR is a coherent risk measure. Note that if $F_Y(x) + g(x) < 1$ then

$$F_X(x) \leq F_Y(x) + g(x) = F_{Y^L}(x),$$

and if $F_Y(x) + g(x) \geq 1$, $1 = F_{Y^L}(x) \geq F_X(x)$. Therefore $Y^L \leq X$. \square

THEOREM A.5. *Let $\alpha \in (0, 1)$, X and Y be random variables. Define $h : \mathbb{R} \rightarrow [0, \infty)$ to be a continuous function, $g(z) := \int_{-\infty}^z h(x)dx$ and Y^L to be a random variable such that $F_{Y^L}(y) := \min(1, F_Y(y) + g(y))$. If $\lim_{z \rightarrow -\infty} g(z) = 0$ and $\forall x \in \mathbb{R}, f_x(x) \leq f_y(x) + h(x)$, then F_{Y^L} is a CDF and $\text{CVaR}_\alpha(Y^L) \leq \text{CVaR}_\alpha(X)$.*

PROOF. We will show the g satisfies the properties of Theorem 5.3, and therefore this theorem holds. We need to prove that

- (1) $\lim_{z \rightarrow -\infty} g(z) = 0$
- (2) g is continuous from the right.
- (3) g is monotonic increasing.
- (4) $F_X(y) \leq F_Y(y) + g(y)$

It is given in the theorem's assumptions that $\lim_{z \rightarrow -\infty} g(z) = 0$, so (1) holds. h is non negative and therefore g is monotonic increasing, so (3) holds. g is continuous if its derivative exists for all $z \in \mathbb{R}$. Let $z \in \mathbb{R}$ and $a < z$.

$$\frac{d}{dz}g(z) = \frac{d}{dz} \int_{-\infty}^z h(x)dx = \frac{d}{dz} \left[\int_{-\infty}^a h(x)dx + \int_a^z h(x)dx \right] = \frac{d}{dz} \int_a^z h(x)dx = h(z) \quad (76)$$

where the third equality holds because $\int_{-\infty}^a h(x)dx = g(a)$ is a constant that does not depend on z . The last equality holds from the fundamental theorem of calculus because h is continuous. Finally, (4) holds because

$$F_X(y) \triangleq \int_{-\infty}^y f_x(x)dx \leq \int_{-\infty}^y f_y(x) + h(x)dx \triangleq F_Y(y) + g(y). \quad (77)$$

\square

COROLLARY A.6. *Let X be a random variable, $\alpha \in (0, 1]$, $\delta \in (0, 1)$, $\epsilon = \sqrt{\ln(1/\delta)/(2n)}$, $a \in \mathbb{R}$, $b \in \mathbb{R}$. Let $X_1, \dots, X_n \stackrel{iid}{\sim} F_X$ be random variables that define the ECDF \hat{F}_X . Denote by $U(n)$ and $L(n)$ the upper and lower bounds respectively from Theorem 5.5, where n is the number of samples, then*

- (1) *If $P(X \leq b) = 1$, then $\lim_{n \rightarrow \infty} U(n) \stackrel{a.s.}{=} \text{CVaR}_\alpha(X)$.*
- (2) *If $P(X \geq a) = 1$, then $\lim_{n \rightarrow \infty} L(n) \stackrel{a.s.}{=} \text{CVaR}_\alpha(X)$.*

where *a.s.* denotes almost sure convergence.

PROOF.

$$\lim_{n \rightarrow \infty} U(n) \stackrel{a.s.}{=} \lim_{n \rightarrow \infty} \left(1 - \frac{\epsilon}{\alpha} \right) C_{\alpha-\epsilon}^{\hat{F}_X} + \frac{\epsilon}{\alpha} b \stackrel{a.s.}{=} \lim_{n \rightarrow \infty} C_{\alpha-\epsilon}^{\hat{F}_X} = \lim_{n \rightarrow \infty} C_\alpha^{\hat{F}_X} = C_\alpha^{F_X} \quad (78)$$

where the first and second equalities follow from the fact that $\epsilon \rightarrow 0$ as $n \rightarrow \infty$; the third equality holds by the continuity of CVaR with respect to α ; and the fourth equality holds by the almost sure convergence of the empirical CVaR of i.i.d. samples to the true CVaR. For the same reason,

$$\lim_{n \rightarrow \infty} L(n) \stackrel{a.s.}{=} \lim_{n \rightarrow \infty} \left(1 + \frac{\epsilon}{\alpha} \right) C_{\alpha+\epsilon}^{\hat{F}_X} - \frac{\epsilon}{\alpha} C_\epsilon^{\hat{F}_X} \stackrel{a.s.}{=} \lim_{n \rightarrow \infty} C_{\alpha+\epsilon}^{\hat{F}_X} \stackrel{a.s.}{=} \lim_{n \rightarrow \infty} C_\alpha^{\hat{F}_X} \stackrel{a.s.}{=} \lim_{n \rightarrow \infty} C_\alpha^{F_X}. \quad (79)$$

\square

THEOREM A.7. *Let X and Y be random variables, $\epsilon \in [0, 1]$, and $\eta = \sqrt{\ln(1/\delta)/(2n)}$, $\epsilon' = \min(\epsilon + \eta, 1)$. Let Y_1, \dots, Y_n be independent and identically distributed samples from F_Y , and denote by \hat{F}_Y the associated empirical cumulative distribution function.*

- (1) **Upper Bound:** *If $\forall z \in \mathbb{R}, F_Y(z) - F_X(z) \leq \epsilon$ and $P(X \leq b_X) = 1, P(Y \leq b_Y) = 1$, then*

(a) If $\alpha > \epsilon'$ then

$$P\left(\text{CVaR}_\alpha(X) \leq \frac{\epsilon'}{\alpha} \max(b_X, b_Y) + \left(1 - \frac{\epsilon'}{\alpha}\right) \text{CVaR}_{\alpha-\epsilon'}^{\hat{F}_Y}\right) > 1 - \delta. \quad (80)$$

(b) If $\alpha \leq \epsilon'$, then $\text{CVaR}_\alpha(X) \leq \max(b_X, b_Y)$

(2) **Lower Bound:** If $\forall z \in \mathbb{R}, F_X(z) - F_Y(z) \leq \epsilon$ and $P(X \geq a_X) = 1, P(Y \geq a_Y) = 1$, then

(a) If $\alpha + \epsilon' \leq 1$, then

$$P\left(\text{CVaR}_\alpha(X) \geq \left(1 + \frac{\epsilon'}{\alpha}\right) \text{CVaR}_{\alpha+\epsilon'}^{\hat{F}_Y} - \frac{\epsilon'}{\alpha} \text{CVaR}_{\epsilon'}^{\hat{F}_Y}\right) > 1 - \delta. \quad (81)$$

(b) If $\alpha + \epsilon' > 1$, then

$$P\left(\text{CVaR}_\alpha(X) \geq \frac{1}{\alpha} \left(\mathbb{E}_{\hat{F}_Y}[Y] - \epsilon' \text{CVaR}_{\epsilon'}^{\hat{F}_Y} + (\alpha + \epsilon' - 1)a_{\min}\right)\right) > 1 - \delta. \quad (82)$$

PROOF. We begin by establishing that ϵ' bounds the distributional discrepancy between \hat{F}_Y and F_X , under the assumption that $\sup_x (\hat{F}_Y(x) - F_Y(x)) \leq \eta$. Let $x \in \mathbb{R}$,

$$\begin{aligned} \hat{F}_Y(x) - F_X(x) &= \hat{F}_Y(x) - F_Y(x) + F_Y(x) - F_X(x) \\ &\leq |\hat{F}_Y(x) - F_Y(x)| + |F_Y(x) - F_X(x)| \leq \eta + \epsilon = \epsilon'. \end{aligned} \quad (83)$$

Assume that $\alpha > \epsilon'$. Note that, conditional on the event $\sup_{z \in \mathbb{R}} (\hat{F}_Y(z) - F_X(z)) \leq \epsilon'$, the upper bound in Theorem 5.1 holds deterministically. Consequently, the probability that

$$\text{CVaR}_\alpha(X) \leq \frac{\epsilon'}{\alpha} \max(b_X, b_Y) + \left(1 - \frac{\epsilon'}{\alpha}\right) \text{CVaR}_{\alpha-\epsilon'}^{\hat{F}_Y} \quad (84)$$

holds is equal to one. From the law of total probability,

$$\begin{aligned} &P\left(\text{CVaR}_\alpha(X) \leq \frac{\epsilon'}{\alpha} \max(b_X, b_Y) + \left(1 - \frac{\epsilon'}{\alpha}\right) \text{CVaR}_{\alpha-\epsilon'}^{\hat{F}_Y}\right) \\ &= P\left(\text{CVaR}_\alpha(X) \leq \frac{\epsilon'}{\alpha} \max(b_X, b_Y) + \left(1 - \frac{\epsilon'}{\alpha}\right) \text{CVaR}_{\alpha-\epsilon'}^{\hat{F}_Y} \mid \sup_{z \in \mathbb{R}} (\hat{F}_Y(z) - F_X(z)) \leq \epsilon'\right) P\left(\sup_{z \in \mathbb{R}} (\hat{F}_Y(z) - F_X(z)) \leq \epsilon'\right) \\ &+ P\left(\text{CVaR}_\alpha(X) \leq \frac{\epsilon'}{\alpha} \max(b_X, b_Y) + \left(1 - \frac{\epsilon'}{\alpha}\right) \text{CVaR}_{\alpha-\epsilon'}^{\hat{F}_Y} \mid \sup_{z \in \mathbb{R}} (\hat{F}_Y(z) - F_X(z)) > \epsilon'\right) P\left(\sup_{z \in \mathbb{R}} (\hat{F}_Y(z) - F_X(z)) > \epsilon'\right) \\ &= P\left(\sup_{z \in \mathbb{R}} (\hat{F}_Y(z) - F_X(z)) \leq \epsilon'\right) \\ &+ P\left(\text{CVaR}_\alpha(X) \leq \frac{\epsilon'}{\alpha} \max(b_X, b_Y) + \left(1 - \frac{\epsilon'}{\alpha}\right) \text{CVaR}_{\alpha-\epsilon'}^{\hat{F}_Y} \mid \sup_{z \in \mathbb{R}} (\hat{F}_Y(z) - F_X(z)) > \epsilon'\right) P\left(\sup_{z \in \mathbb{R}} (\hat{F}_Y(z) - F_X(z)) > \epsilon'\right) \\ &\geq P\left(\sup_{z \in \mathbb{R}} (\hat{F}_Y(z) - F_X(z)) \leq \epsilon'\right) \end{aligned} \quad (85)$$

From DKW Dvoretzky, Kiefer, and Wolfowitz 1956 inequality the following inequalities can be derived Thomas and Learned-Miller 2019

$$\Pr\left(\sup_{x \in \mathbb{R}} (\hat{F}(x) - F(x)) \leq \sqrt{\frac{\ln(1/\delta)}{2n}}\right) \geq 1 - \delta, \quad \Pr\left(\sup_{x \in \mathbb{R}} (\hat{F}(x) - F(x)) \geq \sqrt{\frac{\ln(1/\delta)}{2n}}\right) \geq 1 - \delta. \quad (86)$$

$$\begin{aligned}
 P(\sup_{z \in \mathbb{R}} (\hat{F}_Y(z) - F_X(z)) \leq \epsilon') &\geq P(\sup_{z \in \mathbb{R}} (\hat{F}_Y(z) - F_Y(z)) + \sup_{z \in \mathbb{R}} (F_Y(z) - F_X(z)) \leq \epsilon') \\
 &\geq P(\sup_{z \in \mathbb{R}} (\hat{F}_Y(z) - F_Y(z)) + \epsilon \leq \epsilon + \eta) \\
 &= P(\sup_{z \in \mathbb{R}} (\hat{F}_Y(z) - F_Y(z)) \leq \eta) > 1 - \delta.
 \end{aligned} \tag{87}$$

The first inequality follows from the triangle inequality; the second holds since ϵ bounds the distributional discrepancy between X and Y ; and the third follows from (86).

As with the preceding equations, all bounds in Theorem 5.1 hold deterministically for a given distributional discrepancy, where the discrepancy between \hat{F}_Y and F_X is ϵ' . Consequently, the remaining probabilistic guarantees hold with probability at least $1 - \delta$. \square

B Comparison with the Concentration Bounds of Thomas et al. Thomas and Learned-Miller 2019

See Figure 16.

C Static CVaR Simplification Proofs

THEOREM C.1.

$$\sup_{l \in \mathbb{R}} |P(R_{k:T} \leq l | b_k, a_k, \pi) - P_s(R_{k:T} \leq l | b_k, a_k, \pi)| \leq \sum_{t=k}^{T-1} \mathbb{E}^s [\Delta^s(b_t, a_t) | b_k, a_k], \tag{88}$$

where Δ^s is the TV distance that is defined by

$$\Delta^s(b_{t-1}, a_{t-1}) \triangleq \int_{b_t \in B} |P(b_t | b_{t-1}, a_{t-1}) - P_s(b_t | b_{t-1}, a_{t-1})| db_t. \tag{89}$$

PROOF. By expanding the belief path from time $k + 1$ to time T we get

$$\begin{aligned}
 P(\sum_{t=k}^T c(b_t, a_t) \leq l | b_k, \pi) &= \int_{b_{k+1:T} \in B^{T-k}} P(R_{k:T} \leq l | b_{k:T}, \pi) \prod_{i=k+1}^T P(b_i | b_{i-1}, \pi, a_i) db_{k+1:T} \\
 &= \int_{b_{k+1:T} \in B^{T-k}} 1_{R_{k:T} \leq l} \prod_{i=k+1}^T P(b_i | b_{i-1}, \pi, a_i) db_{k+1:T},
 \end{aligned} \tag{90}$$

where the second equality holds because $R_{k:T}$ is constant given π and $b_{k:T}$. Hence, the subtraction between the simplified and original return CDFs can be exhibited using the difference between the multiplication of the belief transition models.

$$P(R_{k:T} \leq l | b_k, \pi) - P_s(R_{k:T} \leq l | b_k, \pi) = \int_{b_{k+1:T} \in B^{T-k}} 1_{R_{k:T} \leq l} \left[\prod_{i=k+1}^T P(b_i | b_{i-1}, \pi, a_i) - \prod_{i=k+1}^T P_s(b_i | b_{i-1}, \pi, a_i) \right] db_{k+1:T} \tag{91}$$

By applying the triangle inequality we get the following bound

$$\begin{aligned}
 |P(R_{k:T} \leq l | b_k, \pi) - P_s(R_{k:T} \leq l | b_k, \pi)| &\leq \int_{b_{k+1:T} \in B^{T-k}} 1_{R_{k:T} \leq l} \left| \prod_{i=k+1}^T P(b_i | b_{i-1}, \pi, a_i) - \prod_{i=k+1}^T P_s(b_i | b_{i-1}, \pi, a_i) \right| db_{k+1:T} \\
 &\leq \int_{b_{k+1:T} \in B^{T-k}} \left| \prod_{i=k+1}^T P(b_i | b_{i-1}, \pi, a_i) - \prod_{i=k+1}^T P_s(b_i | b_{i-1}, \pi, a_i) \right| db_{k+1:T} = g(T),
 \end{aligned} \tag{92}$$

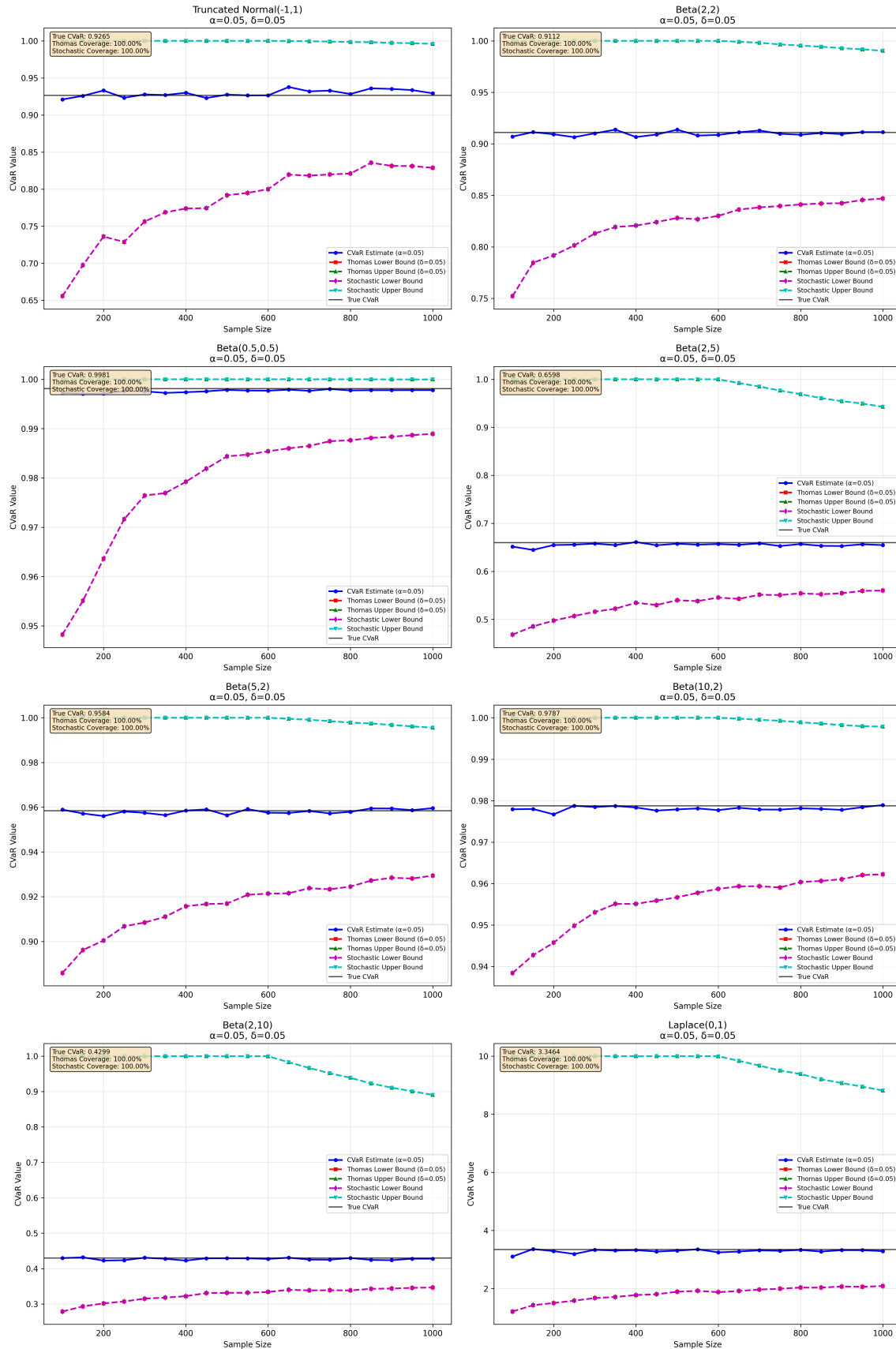


Fig. 16. Comparison of concentration inequalities for $\text{CVaR}_\alpha(X)$ established by Theorem 5.5 (this work) and by Thomas and Learned-Miller 2019, evaluated on Beta(2, 2), Beta(0.5, 0.5), Beta(2, 5), Beta(5, 2), Beta(10, 2), Beta(2, 10), and Laplace(0, 1) distributions. The two sets of bounds coincide for all tested distributions.

where

$$g(t) \triangleq \int_{b_{k+1:t} \in B^{t-k+1}} \left| \prod_{i=k+1}^t P(b_i | b_{i-1}, \pi, a_i) - \prod_{i=k+1}^t P_s(b_i | b_{i-1}, \pi, a_i) \right| db_{k+1:t}. \quad (93)$$

We will prove that

$$g(t+1) \leq g(t) + \mathbb{E}^s[\Delta^s(b_t, a_t) | b_k, a_k] = \epsilon_t \quad (94)$$

for $t \in \{k+1, \dots, T\}$, where $\epsilon_k = 0$, and therefore

$$|P(R_{k:t} \leq l | b_k, \pi) - P_s(R_{k:t} \leq l | b_k, \pi)| \leq \epsilon_t. \quad (95)$$

For the case where $t = k$, b_t is constant, and therefore the $c(b_t, a_t)$ does not depend on the belief transition model. Hence, $P_s(c(b_t, a_t) \leq l | b_t, a_t) = P(c(b_t, a_t) \leq l | b_t, a_t)$. Therefore we get

$$P(c(b_k, a_k) \leq l | b_k, a_k) - P_s(c(b_k, a_k) \leq l | b_k, a_k) = 0 = \epsilon_k. \quad (96)$$

The rest of the proof will use induction over $t \in \{k+1, \dots, T\}$.

Base case, $t = k+1$:

$$\begin{aligned} g(k+1) &= \int_{b_{k+1} \in B} \left| \prod_{i=k+1}^{k+1} P(b_i | b_{i-1}, \pi, a_i) - \prod_{i=k+1}^{k+1} P_s(b_i | b_{i-1}, \pi, a_i) \right| db_{k+1:k+1} \\ &= \int_{b_{k+1} \in B} |P(b_{k+1} | b_k, \pi, a_k) - P_s(b_{k+1} | b_k, \pi, a_k)| db_{k+1} = \Delta^s(b_k, a_k) = \mathbb{E}^s[\Delta^s(b_k, a_k) | b_k, a_k] \\ &= \epsilon_{k+1} \end{aligned} \quad (97)$$

Induction step: Assume that the claim is true for $t \in \{k+1, \dots, T-1\}$ and prove for $t+1$.

Our proof's strategy is to express $g(t+1)$ recursively, using $g(t)$, and separate the bound at time $t+1$ into 2 components - one at time t and one at time $t+1$. We then bound the term at time $t+1$, and use the induction step to bound the recursive part of g at time t .

For all $x_i, y_i \in \mathbb{R}$,

$$\prod_{i=k+1}^{t+1} x_i - \prod_{i=k+1}^{t+1} y_i = \prod_{i=k+1}^{t+1} x_i - x_{t+1} \prod_{i=k+1}^t y_i + x_{t+1} \prod_{i=k+1}^t y_i - \prod_{i=k+1}^{t+1} y_i = x_{t+1} \left(\prod_{i=k+1}^t x_i - \prod_{i=k+1}^t y_i \right) + (x_{t+1} - y_{t+1}) \prod_{i=k+1}^t y_i. \quad (98)$$

By denoting $x_i = P(b_i | b_{i-1}, a_{i-1})$ and $y_i = P_s(b_i | b_{i-1}, a_{i-1})$ we get

$$\begin{aligned} &\prod_{i=k+1}^{t+1} P(b_i | b_{i-1}, \pi, a_i) - \prod_{i=k+1}^{t+1} P_s(b_i | b_{i-1}, \pi, a_i) \\ &= [P(b_{t+1} | b_t, a_t) - P_s(b_{t+1} | b_t, a_t)] \prod_{i=k+1}^t P_s(b_i | b_{i-1}, a_{i-1}) + P(b_{t+1} | b_t, a_t) \left[\prod_{i=k+1}^t P(b_i | b_{i-1}, \pi, a_i) - \prod_{i=k+1}^t P_s(b_i | b_{i-1}, \pi, a_i) \right]. \end{aligned} \quad (99)$$

By combining the equation above with the triangle inequality, we get

$$g(t+1) \leq A_1 + A_2 \quad (100)$$

for

$$A_1 \triangleq \int_{b_{k+1:t+1} \in B^{t-k}} |P(b_{t+1} | b_t, a_t) - P_s(b_{t+1} | b_t, a_t)| \prod_{i=k+1}^t P_s(b_i | b_{i-1}, a_{i-1}) b_{k+1:t}, \quad (101)$$

$$A_2 \triangleq \int_{b_{k+1:t+1} \in B^{t-k}} P(b_{t+1}|b_t, a_t) \left| \prod_{i=k+1}^t P(b_i|b_{i-1}, \pi, a_i) - \prod_{i=k+1}^t P_s(b_i|b_{i-1}, \pi, a_i) \right| db_{k+1:t} \quad (102)$$

A_1 is the expectation over the TV-distance of the belief at time t .

$$A_1 = \mathbb{E}^s [\Delta^s(b_t, a_t) | b_k, a_k]. \quad (103)$$

As we see below, A_2 does not depend on the belief integration at time $t + 1$, and therefore equals to $g(t)$. From the induction assumption, we get that $g(t) \leq \epsilon_t$.

$$\begin{aligned} A_2 &= \int_{b_{k+1:t} \in B^{t-k}} P(b_{t+1}|b_t, a_t) \left| \prod_{i=k+1}^t P(b_i|b_{i-1}, \pi, a_i) - \prod_{i=k+1}^t P_s(b_i|b_{i-1}, \pi, a_i) \right| db_{k:t+1} \\ &= \int_{b_{k+1:t} \in B^{t-k}} \left| \prod_{i=k+1}^t P(b_i|b_{i-1}, \pi, a_i) - \prod_{i=k+1}^t P_s(b_i|b_{i-1}, \pi, a_i) \right| \underbrace{\int_{b_{t+1}} P(b_{t+1}|b_t, a_t) db_{t+1}}_{=1} db_{k+1:t} \\ &= g(t) \leq \epsilon_t \end{aligned} \quad (104)$$

By combining the computations of A_1 and A_2 ,

$$g(t+1) \leq A_1 + A_2 = g(t) + \mathbb{E}^s [\Delta^s(b_t, a_t) | b_k, a_k]. \quad (105)$$

The last equation completes the induction proof. Utilizing the recursive relation of ϵ_t , we get the bound we want to prove.

$$|P(R_{k:T} \leq l | b_k, \pi) - P_s(R_{k:T} \leq l | b_k, \pi)| \leq g(T) \leq g(T-1) + \mathbb{E}^s [\Delta^s(b_{T-1}, a_{T-1}) | b_k, a_k] \leq \sum_{t=k}^{T-1} \mathbb{E}^s [\Delta^s(b_t, a_t) | b_k, a_k]. \quad (106)$$

□

THEOREM C.2. *In the case where the simplified and original observation models are denoted by q_z and p_z respectively, it holds that*

$$\sup_{l \in \mathbb{R}} |P(R_{k:T} \leq l | b_k, \pi) - P_s(R_{k:T} \leq l | b_k, \pi)| \leq \sum_{t=k}^{T-1} \mathbb{E}^s [\Delta^s(x_{t+1}) | b_k, a_k], \quad (107)$$

where Δ^s is the TV distance that is defined by

$$\Delta^s(x_t) \triangleq \int_{z_t \in Z} |p(z_t | x_t) - q(z_t | x_t)| dz_t. \quad (108)$$

PROOF. We show that for each $t \in \{k, \dots, T-1\}$,

$$\mathbb{E}^s [\Delta^s(b_t, a_t) | b_k, a_k] \leq \mathbb{E}^s [\Delta^s(x_{t+1}) | b_k, a_k], \quad (109)$$

and therefore

$$\sup_{l \in \mathbb{R}} |P(R_{k:T} \leq l | b_k, \pi) - P_s(R_{k:T} \leq l | b_k, \pi)| \leq \sum_{t=k}^{T-1} \mathbb{E}^s [\Delta^s(b_t, a_t) | b_k, a_k] \leq \sum_{t=k}^{T-1} \mathbb{E}^s [\Delta^s(x_{t+1}) | b_k, a_k]. \quad (110)$$

We start by expressing the belief transition model using the observation and state-transition models. Here we assume that b_t is known. That is, $b_t = \{(x_i, w_i)\}_{i=1}^n$, where x_i and w_i are constants.

$$\begin{aligned} P(b_{t+1}|b_t, a_t) &= \int_{x_t \in X, x_{t+1} \in X, z_{t+1} \in Z} P(b_{t+1}|b_t, a_t, z_{t+1}, x_t, x_{t+1}) P(z_{t+1}, x_t, x_{t+1}|b_t, a_t) dz_{t+1} dx_{t+1} dx_t \\ &= \int_{x_t \in X, x_{t+1} \in X, z_{t+1} \in Z} P(b_{t+1}|b_t, a_t, z_{t+1}, x_t, x_{t+1}) p(z_{t+1}|x_{t+1}) \times P(x_{t+1}|x_t, a_t) b(x_t) dz_{t+1} dx_{t+1} dx_t. \end{aligned} \quad (111)$$

Similarly,

$$P_s(b_{t+1}|b_t, a_t) = \int_{x_t \in X, x_{t+1} \in X, z_{t+1} \in Z} P_s(b_{t+1}|b_t, a_t, z_{t+1}, x_t, x_{t+1}) q(z_{t+1}|x_{t+1}) P(x_{t+1}|x_t, a_t) b(x_t) dz_{t+1} dx_{t+1} dx_t. \quad (112)$$

Note that $P(b_{t+1}|b_t, a_t, z_{t+1}, x_t, x_{t+1}) = P_s(b_{t+1}|b_t, a_t, z_{t+1}, x_t, x_{t+1})$, as both terms do not depend on the observation model. By subtracting the simplified and original belief transition models, we can separate the simplified and original observation models.

$$\begin{aligned} &|P(b_{t+1}|b_t, a_t) - P_s(b_{t+1}|b_t, a_t)| \\ &= \left| \int_{x_t \in X, x_{t+1} \in X, z_{t+1} \in Z} P_s(b_{t+1}|b_t, a_t, z_{t+1}, x_t, x_{t+1}) P(x_{t+1}|x_t, a_t) b(x_t) (p(z_{t+1}|x_{t+1}) - q(z_{t+1}|x_{t+1})) dz_{t+1} dx_{t+1} dx_t \right| \\ &\leq \int_{x_t \in X, x_{t+1} \in X, z_{t+1} \in Z} P_s(b_{t+1}|b_t, a_t, z_{t+1}, x_t, x_{t+1}) P(x_{t+1}|x_t, a_t) b(x_t) |p(z_{t+1}|x_{t+1}) - q(z_{t+1}|x_{t+1})| dz_{t+1} dx_{t+1} dx_t. \end{aligned} \quad (113)$$

where the inequality holds from the triangle inequality. It holds that

$$\begin{aligned} \Delta^s(b_t, a_t) &= \int_{b_{t+1} \in B} |P(b_{t+1}|b_t, a_t) - P_s(b_{t+1}|b_t, a_t)| db_{t+1} \\ &\leq \int_{b_{t+1} \in B} \int_{x_t \in X, x_{t+1} \in X, z_{t+1} \in Z} P_s(b_{t+1}|b_t, a_t, z_{t+1}, x_t, x_{t+1}) P(x_{t+1}|x_t, a_t) b(x_t) |p(z_{t+1}|x_{t+1}) - q(z_{t+1}|x_{t+1})| dz_{t+1} dx_{t+1} dx_t db_{t+1} \\ &= \int_{x_t \in X, x_{t+1} \in X} P(x_{t+1}|x_t, a_t) b(x_t) \int_{z_{t+1} \in Z} |p(z_{t+1}|x_{t+1}) - q(z_{t+1}|x_{t+1})| \underbrace{\int_{b_{t+1} \in B} P_s(b_{t+1}|b_t, a_t, z_{t+1}, x_t, x_{t+1}) db_{t+1}}_{=1} dz_{t+1} dx_{t+1} dx_t \\ &= \int_{b_{t+1} \in B} \int_{x_t \in X, x_{t+1} \in X} P(x_{t+1}|x_t, a_t) b(x_t) \Delta^s(x_{t+1}) dx_{t+1} dx_t \\ &= \mathbb{E}^s[\Delta^s(x_{t+1})|b_t, a_t] \end{aligned} \quad (114)$$

where the first inequality holds from (113). From the last equation and expectation monotonicity, we get that $\mathbb{E}^s[\Delta(b_t, a_t)] \leq \mathbb{E}^s[\Delta^s(x_{t+1})|b_t, a_t]$, and therefore the claim holds for each t . Summing over t and applying the tower property yields the result.

$$\mathbb{E}^s[\Delta^s(b_t, a_t)|b_k, a_k] = \mathbb{E}^s[\mathbb{E}^s[\Delta^s(b_t, a_t)|b_t, a_t]|b_k, a_k] \leq \mathbb{E}^s[\mathbb{E}^s[\Delta^s(x_{t+1})|b_t, a_t]|b_k, a_k] = \mathbb{E}^s[\Delta^s(x_{t+1})|b_k, a_k]. \quad (115)$$

□

THEOREM C.3. Let $\delta_{d_{min}} \in [0, 1]$, $\delta_{d_{max}} \in [0, 1]$ and denote

$$\epsilon \triangleq \epsilon(b_k, a_k) \triangleq \min \left(\sum_{i=k}^{T-1} \mathbb{E}^s[\Delta^s(b_i, a_i)|b_k, a_k, \pi], 1 \right), \quad (116)$$

(1) **Upper Bound:** assume that $P(R_{k:T} \leq d_{max}) > 1 - \delta_{d_{max}}$ and $P_s(R_{k:T} \leq d_{max}) > 1 - \delta_{d_{max}}$, then

- (a) If $\epsilon < \alpha$, then $U_s \triangleq (1 - \frac{\epsilon}{\alpha})Q_{M_s}^\pi(b_k, a_k, \alpha - \epsilon) + \frac{\epsilon}{\alpha}d_{max}$
- (b) If $\epsilon \geq \alpha$ then $U_s \triangleq d_{max}$

(2) **Lower Bound:** assume that $P(R_{k:T} \geq d_{min}) > 1 - \delta_{d_{min}}$ and $P_s(R_{k:T} \geq d_{min}) > 1 - \delta_{d_{min}}$, then

- (a) If $\epsilon + \alpha < 1$ then $L_s \triangleq (1 + \frac{\epsilon}{\alpha})Q_{M_s}^\pi(b_k, a_k, \alpha + \epsilon) - \frac{\epsilon}{\alpha}Q_{M_s}^\pi(b_k, a_k, \epsilon)$
- (b) If $\epsilon + \alpha \geq 1$ then $L_s \triangleq \frac{1}{\alpha}[-(\alpha + \epsilon - 1)d_{min} + Q_{M_s}^\pi(b_k, a_k) - \epsilon Q_{M_s}^\pi(b_k, a_k, \epsilon)]$

Then $P(L_s \leq Q_M^\pi(b_k, a_k, \alpha)) > 1 - \delta_{d_{min}}$ and $P(Q_M^\pi(b_k, a_k, \alpha) \leq U_s) > 1 - \delta_{d_{max}}$.

PROOF. From the law of total probability,

$$\begin{aligned} P(Q_M^\pi(b_k, a_k, \alpha) \leq U_s) &= P(Q_M^\pi(b_k, a_k, \alpha) \leq U_s | R_{k:T} \leq d_{max})P(R_{k:T} \leq d_{max}) \\ &\quad + P(Q_M^\pi(b_k, a_k, \alpha) \leq U_s | R_{k:T} > d_{max})P(R_{k:T} > d_{max}) \\ &\geq P(Q_M^\pi(b_k, a_k, \alpha) \leq U_s | R_{k:T} \leq d_{max})P(R_{k:T} \leq d_{max}) \\ &> P(Q_M^\pi(b_k, a_k, \alpha) \leq U_s | R_{k:T} \leq d_{max})(1 - \delta_{d_{max}}). \end{aligned} \tag{117}$$

Similarly,

$$P(Q_M^\pi(b_k, a_k, \alpha) \geq L_s) > P(Q_M^\pi(b_k, a_k, \alpha) \geq L_s | R_{k:T} \geq d_{min})(1 - \delta_{d_{min}}). \tag{118}$$

From Theorem C.1, for all $l \in \mathbb{R}$

$$|P(R_{k:T} \leq l | b_k, \pi) - P_s(R_{k:T} \leq l | b_k, \pi)| \leq \sum_{i=k+1}^{T-1} \mathbb{E}_{b_{k+1:i}} [\Delta^s(b_i, a_i) | b_k, \pi] = \epsilon, \tag{119}$$

The action-value function is defined as the CVaR of the return. Let X and Y be random variables distributed according to the original and simplified models P and P_s , respectively. Theorem 5.1 establishes bounds on $\text{CVaR}_\alpha(X)$ in terms of CVaR of Y , under a known discrepancy between the cumulative distribution functions of X and Y . In our setting, this distributional discrepancy is bounded by ϵ , and thus the result applies directly. \square

COROLLARY C.4. *The bound from Theorem 6.2 holds for $\epsilon(b_k, a_k) = \sum_{t=k}^{T-1} \mathbb{E}^s[\Delta^s(x_{t+1}) | b_k, a_k]$.*

PROOF. Theorem 6.2 establishes bounds on the value and action-value functions under a quantified distributional discrepancy ϵ between the original and simplified return distributions. As long as this discrepancy between their CDFs remains bounded by ϵ , the result remains valid. Consequently, by bounding the belief-based discrepancy ϵ in Theorem 6.2 via the state-based discrepancy bound established in Theorem C.2, we recover the same form of the bound for the newly defined ϵ . \square

THEOREM C.5. *Let $\eta > 0, \delta \in (0, 1)$. If $\hat{\Delta}$ is unbiased, then*

$$P(|\hat{\epsilon}_t(\bar{b}_t, a) - \epsilon_t(\bar{b}_t, a)| \geq \eta) \leq 2 \exp\left(-\frac{2\eta^2 N_b}{D^2(T-k)^2(R_{max} - R_{min})^2}\right) \tag{120}$$

for $D = \max_{i \in \{k+1, \dots, T-1\}} D_i$ where $D_i = \sup_{x_{i+1}} P(x_{i+1} | x_i, a_i) / Q_0(x_{i+1})$.

PROOF. We start by proving that $\hat{m}(\bar{b}_t, a)$ is an unbiased estimator for $m(\bar{b}_t, a)$.

$$\begin{aligned} \mathbb{E}[\hat{m}(\bar{b}_t, a)] &= \sum_{i=1}^{N_p} \mathbb{E}[\hat{m}(x_t^i, a)] \tilde{w}_t^i = \sum_{i=1}^{N_p} \mathbb{E}\left[\frac{P(x_n^\Delta | x_t^i, a)}{Q_0(x_n^\Delta)} \Delta(x_n^\Delta)\right] \tilde{w}_t^i = \sum_{i=1}^{N_p} m(x_t^i, a) \tilde{w}_t^i \\ &= m(\bar{b}_t, a). \end{aligned} \tag{121}$$

It follows that the estimator $\hat{\epsilon}(\bar{b}_t, a)$ of the total distributional discrepancy is an unbiased estimator of $\epsilon(\bar{b}_t, a)$.

$$\begin{aligned} \mathbb{E}[\hat{\epsilon}(\bar{b}_t, a)] &= \sum_{\tau=t}^{T-1} \mathbb{E}[\mathbb{E}[m(\bar{b}_\tau, \pi_\tau) | \bar{b}_\tau, a] | \bar{b}_t, a] = \sum_{\tau=t}^{T-1} \mathbb{E}[\hat{m}(\bar{b}_\tau^1, \pi(\bar{b}_\tau^1)) | \bar{b}_t, a] = \sum_{\tau=t}^{T-1} \mathbb{E}[\mathbb{E}[\hat{m}(\bar{b}_\tau^1, \pi(\bar{b}_\tau^1)) | \bar{b}_\tau^1] | \bar{b}_t, a] \\ &= \sum_{\tau=t}^{T-1} \mathbb{E}[m(\bar{b}_\tau^1, \pi(\bar{b}_\tau^1)) | \bar{b}_t, a] = \epsilon(\bar{b}_t, a) \end{aligned} \quad (122)$$

Define

$$X_i \triangleq \frac{1}{N_b} \sum_{\tau=t}^{T-1} \hat{m}(\bar{b}_\tau^i, \pi(\bar{b}_\tau^i)), \quad (123)$$

and note that

$$\sum_{i=1}^{N_b} X_i = \hat{\epsilon}(\bar{b}_t, a). \quad (124)$$

Since the total variation distance is bounded by 2, each X_i satisfies the bound

$$\frac{2D(T-t)R_{\min}}{N_b} \leq X_i \leq \frac{2D(T-t)R_{\max}}{N_b}. \quad (125)$$

Moreover, the X_i are independent and identically distributed, and thus Hoeffding's inequality applies.

$$\begin{aligned} P(|\hat{\epsilon}(\bar{b}_t, a) - \epsilon(\bar{b}_t, a)| \geq \eta) &= P\left(\left|\sum_{i=1}^{N_b} X_i - \epsilon(\bar{b}_t, a)\right| \geq \eta\right) \leq 2 \exp\left(-\frac{2\eta^2}{D^2(T-k)^2(R_{\max} - R_{\min})^2/N_b^2 \times N_b}\right) \\ &\leq 2 \exp\left(-\frac{2\eta^2 N_b}{D^2(T-k)^2(R_{\max} - R_{\min})^2}\right). \end{aligned} \quad (126)$$

□

THEOREM C.6. For the estimators $\hat{d}_{\max}^\pi(b_k) = \max_{i \in \{1, \dots, N_b\}} R^i$ and $\hat{d}_{\min}^\pi(b_k) = \min_{i \in \{1, \dots, N_b\}} R^i$, where $R^1, \dots, R^{N_b} \sim P_s(\cdot | b_k, \pi)$, and for ϵ as defined in (30), the following bounds hold.

$$P_s(R_{k:T} \geq \hat{d}_{\min}^\pi(b_k)) \geq \frac{N_b}{N_b + 1}, \quad P_s(R_{k:T} \leq \hat{d}_{\max}^\pi(b_k)) \geq \frac{N_b}{N_b + 1} \quad (127)$$

$$P\left(R_{k:T} \geq \hat{d}_{\min}^\pi(b_k) \mid b_k, \pi\right) \geq \frac{N_b}{N_b + 1} - \epsilon, \quad P\left(R_{k:T} \leq \hat{d}_{\max}^\pi(b_k) \mid b_k, \pi\right) \geq \frac{N_b}{N_b + 1} - \epsilon. \quad (128)$$

PROOF. Note that $\{R^i\}_{i=1}^{N_b} \sim P_s(\cdot | b_k, \pi)$ are sampled from the simplified distribution. Observe that $R_{k:T}, R^1, \dots, R^{N_b}$ constitute an i.i.d. sample of size $N_b + 1$ from the simplified distribution. For each $j \in \{0, 1, \dots, N_b\}$, define the event $A_j = \{X_j \text{ is strictly the largest among all } N_b + 1 \text{ samples}\}$, where $X_0 = R_{k:T}$ and $X_i = R^i$ for $i \geq 1$. These events are mutually exclusive, and by the i.i.d. assumption $P_s(A_j)$ is the same for all j . Since $\sum_{j=0}^{N_b} P_s(A_j) \leq 1$, it follows that

$$P_s\left(R_{k:T} > \max_{i \in \{1, \dots, N_b\}} R^i \mid b_k, \pi\right) = P_s(A_0) \leq \frac{1}{N_b + 1}. \quad (129)$$

Similarly, $P_s(R_{k:T} < \min_{i \in \{1, \dots, N_b\}} R^i | b_k, \pi) \leq \frac{1}{N_b + 1}$. Therefore,

$$P_s(R_{k:T} \leq \max_{i \in \{1, \dots, N_b\}} R^i | b_k, \pi) \geq \frac{N_b}{N_b + 1}, \quad P_s(R_{k:T} \geq \min_{i \in \{1, \dots, N_b\}} R^i | b_k, \pi) \geq \frac{N_b}{N_b + 1}. \quad (130)$$

When bounding $P(R_{k:T} \leq \max_{i \in \{1, \dots, N_b\}} R^i)$, observe that $R_{k:T}$ is drawn from the original distribution P , whereas the samples $\{R^i\}_{i=1}^{N_b}$ are drawn from the simplified distribution P_s . Consequently, the symmetry argument used in the previous bound does not apply. To address this mismatch, we employ the bound from Theorem 6.1 to bound the CDF of

the return computed with the original model, using the CDF computed using the simplified belief-transition model.

$$\begin{aligned}
P\left(R_{k:T} \leq \max_{i \in \{1, \dots, N_b\}} R^i \middle| b_k, \pi\right) &= \int_{R^1, \dots, R^{N_b}} P\left(R_{k:T} \leq \max_{i \in \{1, \dots, N_b\}} R^i \middle| R^1, \dots, R^{N_b}, b_k, \pi\right) P_s(R^1, \dots, R^{N_b} | b_k, \pi) dR^1 \dots dR^{N_b} \\
&\geq \int_{R^1, \dots, R^{N_b}} \left(P_s\left(R_{k:T} \leq \max_{i \in \{1, \dots, N_b\}} R^i \middle| R^1, \dots, R^{N_b}, b_k, \pi\right) - \epsilon\right) P_s(R^1, \dots, R^{N_b} | b_k, \pi) dR^1, \dots, dR^{N_b} \\
&= \mathbb{E}_s \left[P_s\left(R_{k:T} \leq \max_{i \in \{1, \dots, N_b\}} R^i \middle| R^1, \dots, R^{N_b}\right) - \epsilon \middle| b_k, \pi \right] \\
&= P_s\left(R_{k:T} \leq \max_{i \in \{1, \dots, N_b\}} R^i\right) - \epsilon \\
&\geq \frac{N_b}{N_b + 1} - \epsilon.
\end{aligned} \tag{131}$$

The first inequality follows directly from Theorem 6.1, and the last inequality holds from the symmetry argument used above.

Similarly,

$$P\left(R_{k:T} \leq \min_{i \in \{1, \dots, N_b\}} R^i \middle| b_k, \pi\right) \geq \frac{N_b}{N_b + 1} - \epsilon. \tag{132}$$

□

THEOREM C.7. Let $\delta, \delta_{d_{\min}}, \delta_{d_{\max}} \in [0, 1]$, and let b_k denote the initial belief. Consider samples $R^1, \dots, R^{N_b} \sim P_s(\cdot | b_k, \pi)$ generated using the simplified belief-transition model. Define

$$\epsilon \triangleq \epsilon(b_k, a_k) \triangleq \min\left(\sum_{i=k}^{T-1} \mathbb{E}^s[\Delta^s(b_i, a_i) | b_k, a_k, \pi], 1\right), \tag{133}$$

$$\eta = \sqrt{\ln(1/\delta)/(2N_b)}, \quad \epsilon' = \epsilon + \eta. \tag{134}$$

(1) **Upper Bound:** assume that $P(R_{k:T} \leq d_{\max}) > 1 - \delta_{d_{\max}}$ and $P_s(R_{k:T} \leq d_{\max}) > 1 - \delta_{d_{\max}}$, then

- (a) If $\epsilon' < \alpha$, then $U_s \triangleq (1 - \frac{\epsilon'}{\alpha}) \hat{Q}_{M_s}^\pi(b_k, a_k, \alpha - \epsilon') + \frac{\epsilon'}{\alpha} d_{\max}$
- (b) If $\epsilon' \geq \alpha$ then $U_s \triangleq d_{\max}$

(2) **Lower Bound:** assume that $P(R_{k:T} \geq d_{\min}) > 1 - \delta_{d_{\min}}$ and $P_s(R_{k:T} \geq d_{\min}) > 1 - \delta_{d_{\min}}$, then

- (a) If $\epsilon' + \alpha < 1$ then $L_s \triangleq (1 + \frac{\epsilon'}{\alpha}) \hat{Q}_{M_s}^\pi(b_k, a_k, \alpha + \epsilon') - \frac{\epsilon'}{\alpha} \hat{Q}_{M_s}^\pi(b_k, a_k, \epsilon')$
- (b) If $\epsilon' + \alpha \geq 1$ then $L_s \triangleq \frac{1}{\alpha} [-(\alpha + \epsilon' - 1)d_{\min} + \hat{Q}_{M_s}^\pi(b_k, a_k) - \epsilon' \hat{Q}_{M_s}^\pi(b_k, a_k, \epsilon')]$

Then $P(L_s \leq Q_M^\pi(b_k, a_k, \alpha)) > (1 - \delta)(1 - \delta_{d_{\min}})$ and $P(Q_M^\pi(b_k, a_k, \alpha) \leq U_s) > (1 - \delta)(1 - \delta_{d_{\max}})$.

PROOF. From the law of total probability,

$$\begin{aligned}
P(Q_M^\pi(b_k, a_k, \alpha) \leq U_s) &= P(Q_M^\pi(b_k, a_k, \alpha) \leq U_s | R_{k:T} \leq d_{\max}) P(R_{k:T} \leq d_{\max}) \\
&\quad + P(Q_M^\pi(b_k, a_k, \alpha) \leq U_s | R_{k:T} > d_{\max}) P(R_{k:T} > d_{\max}) \\
&\geq P(Q_M^\pi(b_k, a_k, \alpha) \leq U_s | R_{k:T} \leq d_{\max}) P(R_{k:T} \leq d_{\max}) \\
&> P(Q_M^\pi(b_k, a_k, \alpha) \leq U_s | R_{k:T} \leq d_{\max}) (1 - \delta_{d_{\max}}).
\end{aligned} \tag{135}$$

Similarly,

$$P(Q_M^\pi(b_k, a_k, \alpha) \geq L_s) > P(Q_M^\pi(b_k, a_k, \alpha) \geq L_s | R_{k:T} \geq d_{\min}) (1 - \delta_{d_{\min}}). \tag{136}$$

From Theorem C.1, for all $l \in \mathbb{R}$

$$|P(R_{k:T} \leq l | b_k, \pi) - P_s(R_{k:T} \leq l | b_k, \pi)| \leq \sum_{i=k+1}^{T-1} \mathbb{E}_{b_{k+1:i}} [\Delta^s(b_i, a_i) | b_k, \pi] = \epsilon, \quad (137)$$

The action-value function is defined as the CVaR of the return. Let X and Y be random variables distributed according to the original and simplified models P and P_s , respectively. Theorem 5.7 establishes bounds on $\text{CVaR}_\alpha(X)$ in terms of CVaR of a sample of Y , under a known discrepancy between the cumulative distribution functions of X and Y . In our setting, this distributional discrepancy is bounded by ϵ , and thus the result applies directly. \square

THEOREM C.8. (Bound Guarantees) Let $\delta \in (0, 0.5)$, and let b_k denote the initial belief. Consider samples $R^1, \dots, R^{N_b} \sim P_s(\cdot | b_k, \pi)$ generated using the simplified belief-transition model. Define

$$\epsilon \triangleq \epsilon(b_k, a_k) \triangleq \min\left(\sum_{i=k}^{T-1} \mathbb{E}^s[\Delta^s(b_i, a_i) | b_k, a_k, \pi], 1\right), \quad (138)$$

$$\eta = \sqrt{\ln(1/\delta)/(2N_b)}, \quad \epsilon' = \epsilon + \eta, \quad (139)$$

$$\hat{d}_{\max}^\pi(b_k) = \max_{i \in \{1, \dots, N_b\}} R^i, \quad \hat{d}_{\min}^\pi(b_k) = \min_{i \in \{1, \dots, N_b\}} R^i. \quad (140)$$

(1) **Upper Bound:**

(a) If $\epsilon' < \alpha$, then $U_s \triangleq (1 - \frac{\epsilon'}{\alpha}) \hat{Q}_{M_s}^\pi(b_k, a_k, \alpha - \epsilon') + \frac{\epsilon'}{\alpha} \hat{d}_{\max}^\pi(b_k)$

(b) If $\epsilon' \geq \alpha$ then $U_s \triangleq \hat{d}_{\max}^\pi(b_k)$

(2) **Lower Bound:**

(a) If $\epsilon' + \alpha < 1$ then $L_s \triangleq (1 + \frac{\epsilon'}{\alpha}) \hat{Q}_{M_s}^\pi(b_k, a_k, \alpha + \epsilon') - \frac{\epsilon'}{\alpha} \hat{Q}_{M_s}^\pi(b_k, a_k, \epsilon')$

(b) If $\epsilon' + \alpha \geq 1$ then $L_s \triangleq \frac{1}{\alpha} [-(\alpha + \epsilon' - 1) \hat{d}_{\min}^\pi(b_k) + \hat{Q}_{M_s}^\pi(b_k, a_k) - \epsilon' \hat{Q}_{M_s}^\pi(b_k, a_k, \epsilon')]$

Then $P(L_s \leq Q_M^\pi(b_k, a_k, \alpha)) > (1 - \delta) \left(\frac{N_b}{N_b+1} - \epsilon\right)$ and $P(Q_M^\pi(b_k, a_k, \alpha) \leq U_s) > (1 - \delta) \left(\frac{N_b}{N_b+1} - \epsilon\right)$.

PROOF. We prove the upper bound; the lower bound follows by an analogous argument applied to $\hat{d}_{\min}^\pi(b_k)$. By Theorem 7.2,

$$P_s(R_{k:T} \leq \hat{d}_{\max}^\pi(b_k) | b_k, \pi) \geq \frac{N_b}{N_b + 1}, \quad P(R_{k:T} \leq \hat{d}_{\max}^\pi(b_k) | b_k, \pi) \geq \frac{N_b}{N_b + 1} - \epsilon. \quad (141)$$

Setting $d_{\max} = \hat{d}_{\max}^\pi(b_k)$ and $\delta_{d_{\max}} = \frac{1}{N_b+1} + \epsilon$ in Theorem 7.3, both of its conditions are satisfied, and we obtain

$$P(Q_M^\pi(b_k, a_k, \alpha) \leq U_s) > (1 - \delta)(1 - \delta_{d_{\max}}) = (1 - \delta) \left(\frac{N_b}{N_b + 1} - \epsilon\right). \quad (142)$$

An analogous argument with $d_{\min} = \hat{d}_{\min}^\pi(b_k)$ and $\delta_{d_{\min}} = \frac{1}{N_b+1} + \epsilon$ yields the lower bound guarantee. \square

D Environment Configurations

The following subsections describe the three POMDP environments used throughout the experiments, including the action elimination experiments of Figure 9. Each domain provides an *original* environment (used for sampling rollouts) and a *simplified* surrogate (used for belief updates and CVaR bound computation). The two models differ only in their observation and reward models, as summarised in Table 1.

Aspect	Original	Simplified
Observation noise	Gaussian Mixture Model (GMM)	Isotropic Gaussian
Reward noise	Stochastic (Push, Laser Tag)	Deterministic

Table 1. Architectural differences between the original and simplified models across all domains.

D.1 Light-Dark

State space: $\mathbf{s} = (x, y) \in \mathbb{R}^2$ (2D continuous position). **Action space:** Discrete – {up, down, left, right}, mapped to unit vectors in \mathbb{R}^2 . **Observation space:** $\mathbf{o} \in \mathbb{R}^2$ – noisy 2D position.

Parameter	Value
Grid size	7×7
Start state	(1, 1)
Goal state	(6, 6); radius 1.5
State transition covariance	$0.06 \cdot I_2$
Obs. noise (far from beacon)	$\mathcal{N}(0, 0.06 \cdot I_2) / \text{GMM}(K=2500)$
Obs. noise (near beacon)	$\mathcal{N}(0, 0.03 \cdot I_2) / \text{GMM}(K=2500, \text{scaled})$
Beacons	(1, 1), (1, 6), (6, 1), (6, 6); radius 1.0
Obstacle	(5, 2); radius 3.0; hit prob 1.0
Goal reward	+10
Obstacle penalty	-10
Step cost (fuel)	-2
Discount factor γ	0.95
Planning horizon H	9 steps

Table 2. Configuration for the 2D Light-Dark POMDP.

Original: Two independent 1D GMMs (one per axis), $K = 2500$ components, approximating the target Normal distribution. **Simplified:** Standard Gaussian $\mathcal{N}(0, \sigma^2 I_2)$ with the same σ .

D.2 Continuous Push

State space: $\mathbf{s} = (r_x, r_y, o_x, o_y, t_x, t_y) \in \mathbb{R}^6$ – robot, object, and target positions. **Action space:** Discrete – {up, down, left, right}, mapped to unit vectors. **Observation space:** $\mathbf{o} \in \mathbb{R}^6$ – robot and target positions observed exactly; object position is noisy: $\hat{o} = o + \epsilon$, $\epsilon \sim \mathcal{N}(0, \sigma^2 I_2)$.

Original: One 1D GMM ($K = 7000$ components) applied independently to each object-position axis; additionally adds stochastic reward noise $\mathcal{N}(0, 25)$. **Simplified:** Gaussian noise $\mathcal{N}(0, 0.01 \cdot I_2)$ on object position; deterministic reward.

D.3 Continuous Laser Tag

State space: $\mathbf{s} = (r_x, r_y, o_x, o_y, \text{term}) \in \mathbb{R}^4 \times \{0, 1\}$ – robot and opponent positions plus terminal flag. **Action space:** Discrete – {up, down, left, right, tag}. **Observation space:** $\mathbf{o} \in \mathbb{R}^8$ – 8-directional laser range measurements with additive noise; terminal states return $\mathbf{o} = -1$.

Original: One 1D GMM with $K = 290$ components ($\sigma_{\text{comp}} = 0.097$), applied independently to all 8 laser measurements; additionally adds stochastic reward noise $\mathcal{N}(0, 0.25)$. **Simplified:** Gaussian noise $\mathcal{N}(0, 1.0)$ per laser measurement; deterministic reward.

Parameter	Value
Grid size	6×6
Initial state	(0.5, 0.5, 1.0, 0.5, 5.0, 5.0)
Robot transition covariance	diag(0.005, 0.005)
Observation noise σ	0.1 (on object position)
Push threshold	1.0
Friction coefficient	0.3
Max push force	2.0
Robot radius	0.3
Dangerous area	(5.0, 2.0); radius 1.0; penalty -20
Discount factor γ	0.95
Planning horizon H	9 steps

Table 3. Configuration for the Continuous Push POMDP.

Parameter	Value
Arena	11×7 continuous grid
Walls	8 axis-aligned wall cells
Initial state	(2.0, 1.0, 8.0, 5.0, 0)
Robot transition covariance	$0.0125 \cdot I_2$
Opponent transition covariance	$0.00625 \cdot I_2$
Opponent pursuit speed	0.6
Laser noise σ	1.0 (per measurement)
Robot / opponent radius	0.3
Tag radius	0.5
Tag reward	+10
Failed-tag penalty	-10
Step cost	-1
Dangerous areas	(5.0, 3.0), (7.0, 1.0); radius 1.0; penalty -300
Discount factor γ	0.95
Planning horizon H	8 steps (7 moves + tag)

Table 4. Configuration for the Continuous Laser Tag POMDP.

D.4 Shared Planner Parameters

Parameter	Value
CVaR level α	0.1
Belief particles N_p	10
Return samples N_r	600
Δ -estimation states	100
Samples per state (for Δ)	2000
k -NN neighbours	10
Discount factor γ	0.95
Confidence parameter δ	0.05
Random seed	42

Table 5. Planner parameters shared across all three environments.

These parameters are used in the open-loop bound evaluation experiments (Figures 9, 10, and 11) and in the closed-loop policy evaluation experiments (Figures 12, 13, and 14).

E Simulations

The planning configurations below correspond to the open-loop experiments in Figures 9, 10, and 11.

Figure 9 presents the estimated bounds and CVaR values for pairs of action sequences across all three environments, computed using 600 sampled belief trajectories and a confidence parameter of $\delta = 0.05$.

The simplified planner samples $N^\Delta = 100$ states offline from the square region defined by the corners $(0, 0)$ and $(7, 7)$. For each sampled state, the distributional discrepancy Δ between the simplified and original observation models is estimated using $N_z = 2000$ samples. CVaR is computed at confidence level $\alpha = 0.5$, and the probabilistic bounds are constructed with confidence level $\delta = 0.05$. We set the number of sampled belief trajectories to $N_b = 600$.

Parameter	Value
Number of Episodes	300
Steps per Episode	30 (max)
Planning Depth	2
Return Samples (N_b)	600
CVaR α	0.5
Number of Particles (N_p)	10
Discount Factor (γ)	0.95
GMM Components	290

Table 6. Planning configuration for the Continuous Laser Tag experiments.

E.0.1 Continuous Laser Tag – Planning Configuration.

Parameter	Value
Number of Episodes	300
Steps per Episode	30 (max)
Planning Depth	2
Return Samples (N_b)	600
CVaR α	0.5
Number of Particles (N_p)	10
Discount Factor (γ)	0.95
GMM Components	7000

Table 7. Planning configuration for the Light-Dark experiments.

E.0.2 Light-Dark – Planning Configuration.

E.0.3 Continuous Push – Planning Configuration. The planning parameters used for Continuous Push experiments are summarized in Table 8; see Figure 9c for representative agent trajectories.

F BetaZero Policy Configuration (Light-Dark)

The closed-loop policy evaluation uses BetaZero Moss et al. 2024a, an AlphaZero-style algorithm for POMDPs. A neural network maps a belief summary vector $\phi(b)$ to a scalar value estimate $V(b)$ and a policy prior $\pi(a | b)$, which guide MCTS over particle beliefs.

Parameter	Value
Number of Episodes	300
Steps per Episode	30 (max)
Planning Depth	2
Return Samples (N_b)	600
CVaR α	0.5
Number of Particles (N_p)	10
Discount Factor (γ)	0.95
GMM Components	7000

Table 8. Planning configuration for the Continuous Push experiments.

F.1 Belief Representation

Particles are summarised into a fixed-size feature vector using the mean-and-standard-deviation representation:

$$\phi(b) = [\bar{\mu}_x, \bar{\mu}_y, \bar{\sigma}_x, \bar{\sigma}_y] \in \mathbb{R}^4, \tag{143}$$

where $\bar{\mu}$ and $\bar{\sigma}$ are the weighted mean and standard deviation of the particle set.

Parameter	Value
State dimension	2
Belief feature dimension	4 (= 2 × state dim)
Particles per belief N_p	500

Table 9. Belief representation parameters for BetaZero on Light-Dark.

Input normalisation is applied using online statistics collected during training:

Feature	Mean	Std
$\bar{\mu}_x$	3.56	1.91
$\bar{\mu}_y$	4.12	1.91
$\bar{\sigma}_x$	0.302	0.407
$\bar{\sigma}_y$	0.303	0.408
Value output	-24.34	36.64

Table 10. Input normalisation statistics for the BetaZero network.

F.2 Network Architecture

Two-headed MLP with a shared trunk and separate value and policy heads:

Layer	Size
Input	4
Hidden 1	128
Hidden 2	128
Value head output	1 (scalar)
Policy head output	4 (one logit per action)

Table 11. BetaZero network architecture.

F.3 MCTS Parameters

Parameter	Value
Search depth	10
Simulations per step (training)	100
Simulations per step (inference)	1000
Exploration constant c	219.13 (tuned)
Temperature τ	0.319 (tuned)
Value weight z_q	1.0
Visit count weight z_n	1.0
DPW action widening k_a, α_a	1.0, 0.5
DPW observation widening k_o, α_o	1.0, 0.5
Discount factor γ	0.95

Table 12. MCTS parameters for BetaZero on Light-Dark.

F.4 Training Loop

Parameter	Value
Outer iterations	50
Episodes per iteration	50
Total training episodes	2500
Episode length	20 steps
Data collection	Full MCTS rollouts
Replay buffer	5 iterations

Table 13. BetaZero training loop parameters.

At each episode, a fresh initial belief is sampled: mean $\sim \mathcal{U}([-1, 8]^2)$, std $\sim \mathcal{U}(0.01, 2.0)$, then $N_p = 500$ particles are drawn from $\mathcal{N}(\text{mean}, \text{std}^2 I)$. This diversity prevents the training distribution from collapsing to a uniform loop.

F.5 Optimizer and Loss

Parameter	Value
Optimizer	Adam
Learning rate	10^{-4}
Batch size	1024
Training epochs per iteration	50
Weight decay	10^{-5}
Loss	Cross-entropy (policy) + MSE (value)

Table 14. Optimizer and loss configuration for BetaZero training.

F.6 Hyperparameter Search

The exploration constant c and temperature τ were selected via Optuna (TPE sampler, 20 trials) with $n_{\text{sim}} = 100$ during search:

Hyperparameter	Search range	Best value
c (exploration constant)	$[1.0, 10 \times \Delta r] \approx [1, 220]$	219.13
τ (temperature)	$[0.05, 0.5]$	0.319
z_q, z_n	fixed	1.0, 1.0

Table 15. Hyperparameter search results for BetaZero on Light-Dark.

Search used a MedianPruner (3 startup trials, 5 warmup steps) and a TPE sampler with seed 42. The objective minimised the final policy loss (cross-entropy vs. MCTS visit counts); the baseline uniform policy corresponds to $\ln 4 \approx 1.386$. The best trial was retrained at $n_{\text{sim}} = 1000$ for the final model used in all experiments.

G Hardware Specifications

All simulations were conducted on a machine equipped with an 11th Gen Intel® Core™ i9-11900K CPU running at 3.50 GHz and 64 GB of RAM.